Small proteins maintain the fidelity of spore envelope assembly through regulated cell death during sporulation in *Bacillus subtilis*

By Irene S. Tan

A dissertation submitted to Johns Hopkins University in conformity with the requirements for the degree of Doctor of Philosophy

Baltimore, Maryland
May, 2015

ABSTRACT

Under conditions of nutrient deprivation, the bacterium *Bacillus subtilis* undergoes a relatively simple, alternative developmental pathway called sporulation that results in the production of a largely metabolically dormant cell type called a spore. The spore is encased in two concentric shells, the coat and the cortex, which are important for maintaining the spore's dormancy and protecting it from various environmental insults. Despite being spatially separated by a membrane layer, the assembly of these two structures, which form the spore envelope, is linked and orchestrated by two coat proteins, SpoVM and SpoIVA. SpoVM and SpoIVA are the only coat proteins known to be involved in cortex assembly indicating that they play a unique role in coordinating the assembly of the coat and cortex. While the roles of SpoVM and SpoIVA in coat assembly are well-understood, their roles in cortex assembly and the mechanisms that regulate the coordinated assembly of coat and cortex remain a mystery.

Using classical genetics to select for spontaneous suppressors of cortex-deficient mutants, we discovered a sporulation checkpoint where a previously un-annotated gene encodes a small 37-amino-acid protein, CmpA. We found that CmpA is degraded in wild type cells, but persists in a cortex-deficient mutant and propose a model in which the degradation of CmpA signals proper initiation of coat assembly. However, when a cell is unable to properly initiate coat assembly, CmpA persists and functions as an adaptor to deliver the morphogenetic protein SpoIVA to the AAA+ protease ClpXP for degradation. Mutations affecting complex formation between CmpA, SpoIVA and ClpX prevented degradation of SpoIVA indicating that they were sufficient to bypass the checkpoint and sporulation was able to proceed. The degradation of SpoIVA initiates an apoptotic-like event which leads to cell lysis. We believe this to be a mechanism to selectively remove unfit cells that are unable to properly assemble the spore envelope. Left unchecked, mutations in sporulating genes accumulate readily and ultimately lead to loss of the sporulation program. Thus, the CmpA-dependent regulated cell

death pathway actively selects against defective cells in order to maintain the integrity of the sporulation program.

Advisor:

Dr. Kumaran S. Ramamurthi, Laboratory of Molecular Biology, NCI, NIH, Bethesda, MD

Readers

Dr. Kumaran S. Ramamurthi, Laboratory of Molecular Biology, NCI, NIH, Bethesda, MD

Dr. Young-Sam Lee, Department of Biology, Johns Hopkins University, Baltimore, MD

TABLE OF CONTENTS

LIST OF TABLES

LIST OF FIGURES

Chapter 1

Introduction to sporulation in *Bacillus subtilis*

A version of this chapter has been published and appears in:

Tan IS, Ramamurthi KS (2014). Spore formation in *Bacillus subtilis*. *Environmental Microbiology Reports.*

INTRODUCTION

Understanding the mechanisms that drive cell differentiation and morphogenesis is essential in answering the question of how organisms develop. However, elucidating these mechanisms can be difficult due to the complex and intertwined processes that occur during development (Hartwell & Weinert, 1989; Sasai, 2013). One approach to this problem has been to study the relatively simple developmental program of endospore formation ("sporulation") in the bacterium *Bacillus subtilis*. During sporulation a single rod-shaped cell divides asymmetrically, resulting in two genetically identical daughter cells that undergo different cell fates (Errington, 2003; Piggot & Hilbert, 2004; Stragier & Losick, 1996). Sporulation in *B. subtilis* is a particularly attractive system to look at cell differentiation and morphogenesis not only because of the relative simplicity of the sporulation developmental program, but also because of the genetic tractability of the system. *B. subtilis* is naturally competent and genes necessary for sporulation are often non-essential for normal growth, both of which facilitate the identification of novel factors that participate in this developmental process. As a result, sporulation studies have provided significant insights into basic biological processes such as differential gene expression, membrane remodeling, intercellular communication, subcellular protein localization, and morphogenesis.

B. subtilis is ubiquitous in nature and can successfully adapt to various changes in the environment. Under stressful conditions *B. subtilis* is able to initiate many survival mechanisms such as motility, uptake of exogenous DNA, biofilm formation and sporulation (B. Burton & Dubnau, 2010; Rao, Glekas, & Ordal, 2008; Vlamakis, Chai, Beauregard, Losick, & Kolter, 2013). The purpose of sporulation is to produce a largely metabolically inactive dormant cell type called an "endospore" (hereafter, referred to simply as a "spore") that is able to survive harsh environmental conditions until favorable growth conditions are restored (Paredes-Sabja, Setlow, & Sarker, 2011). Bacterial spores are one of nature's most resilient cell types and are able to survive under controlled laboratory conditions for several decades, and perhaps even

longer in the environment (Cano & Borucki, 1995; Jacotot & Virat, 1954; P. Setlow, 2007; Vreeland, Rosenzweig, & Powers, 2000). When the spore senses environmental conditions are conducive to growth, it is able to germinate and resume its vegetative cell cycle.

Sporulation initiates when the rod-shaped *B. subtilis* divides asymmetrically, elaborating a "polar septum" that results in two genetically identical but morphologically distinct compartments: a larger "mother cell" and a smaller "forespore", each of which will ultimately experience different cell fates (Fig. 1.1). Both compartments briefly remain side-by-side, held together by the external cell wall. The initially flat polar septum then begins to curve as the mother cell swallows the forespore (a process called "engulfment"), producing a forespore that resides as a double membrane-bound, roughly spherical, organelle inside the mother cell cytosol. The forespore eventually matures into a partially dehydrated, dormant cell that is released into the environment when the mother cell undergoes programmed cell lysis.

Here, we will provide a brief overview of the molecular mechanisms underlying the sporulation process from the decision of a cell to enter the sporulation program to how the cell undergoes the significant morphological changes in order to become a distinct cell type that is resistant to various environmental insults, with an attempt to highlight primary literature that has been published recently. As a roadmap, we will present the sporulation program in separate sections in which so-called "stages" of sporulation are numbered "0" to "V", reflecting a classical nomenclature that was based on various morphological landmarks as viewed by electron microscopy (Piggot & Coote, 1976; Schaeffer, Ionesco, Ryter, & Balassa, 1963). It is important to note, though, that as techniques have advanced, it has become clear that sporulation is not composed of distinct stages that occur sequentially. Instead, these stages actually lie along a continuum in which there may be significant overlap in terms of when a "stage" begins and ends.

Figure 1.1. Schematic representation of morphological changes that occur during sporulation in *Bacillus subtilis*. Distinct stages of sporulation are denoted with a Roman numeral, according to the numbering scheme proposed by Ryter (Ryter, 1965). Peptidoglycan is depicted in gray, membranes are depicted in yellow, DNA is depicted in black, the position of the origin of replication of the chromosomes is shown as a red dot at stage 0 and I, and the spore coat is depicted in green. At stage 0, chromosomes are replicated, but no obvious morphological landmarks of sporulation are yet present. Stage I is defined by chromosome condensation and the anchoring of the origins of replication to the extreme poles of the cell. In stage II, the polar septum is elaborated, followed by engulfment of the forespore in stage III. Stage IV and V represent cortex and coat assembly, respectively. Stage VI refers to "spore maturation"; a particularly obvious morphological feature elaborated at this stage is the tightly condensed, toroidal structure of the forespore chromosome. In stage VII, the mother cell lyses, releasing the mature, largely dormant spore into the environment.

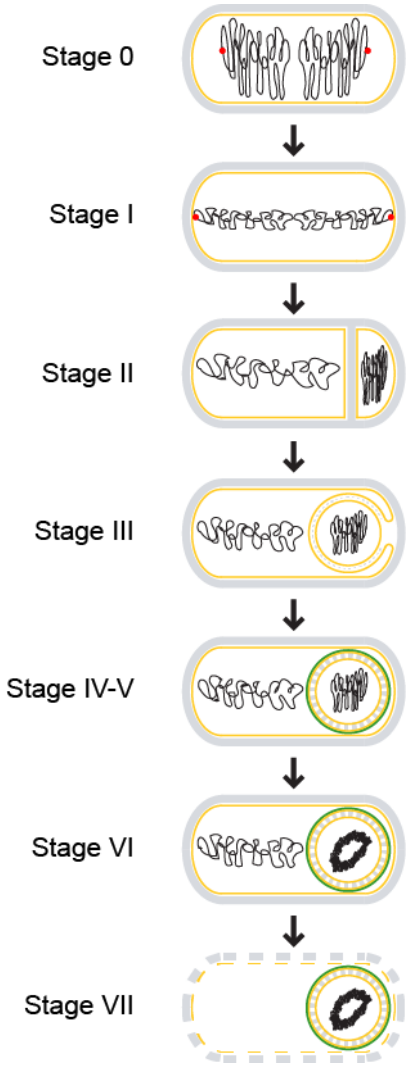
Stage 0
Stage I
Stage II
Stage III
Stage IV-V
Stage VI
Stage VII

Stage 0: The decision to sporulate

As with many other developmental programs, the entry into sporulation is closely regulated and relies on a series of feedback and feed-forward loops. In the bacterial population sporulation does not occur homogenously, but rather occurs in subpopulations. Presumably, this is a bet-hedging strategy that allows the cell to absolutely confirm the need to sporulate prior to engaging in this highly energy-consuming and, once committed, irreversible developmental program (Veening et al., 2008).

The first bet-hedging strategy to delay entry into sporulation is the "cannibalistic" behavior displayed by a subpopulation of cells that are the first to detect the onset of starvation conditions. During cannibalism, this subpopulation of cells kills neighboring isogenic siblings that have not yet detected the onset of such conditions (Gonzalez-Pastor, Hobbs, & Losick, 2003). Cannibalism is reliant on two secreted killing factors, Skf and Sdp (W. T. Liu et al., 2010; Perez Morales, Ho, Liu, Dorrestein, & Ellermeier, 2013), which are produced by cells in a biofilm that produce the biofilm matrix (Lopez, Vlamakis, Losick, & Kolter, 2009). The death of surrounding cells releases nutrients into the environment to support the growth of the subpopulation that produced the toxins. The toxin producing subpopulation is protected through the concurrent production of a protective factor (Ellermeier, Hobbs, Gonzalez-Pastor, & Losick, 2006). In this way, cannibalism is thought to be a mechanism to delay sporulation and to eliminate cells that are no longer beneficial to the population as it moves toward biofilm formation (Mitri, Xavier, & Foster, 2011). Consistent with this model, deletion of genes required for cannibalism result in a faster and more homogeneous entry of cells into the sporulation program (Gonzalez-Pastor et al., 2003).

The transition of *B. subtilis* from vegetative growth to sporulation is largely governed by the transcriptional master regulator Spo0A, which also regulates biofilm formation (Hamon & Lazazzera, 2001). Spo0A transcriptional activity is activated by a 'phosphorelay' system that is governed by five autophosphorylating histidine kinases (KinA-KinE) that respond to different

environmental stresses. While “limited nutrient availability” is broadly defined as the signal for entry into sporulation, the identification of specific molecular ligands that activate the histidine kinases has remained elusive. This difficulty is largely due to the wide array of environmental inputs sensed by the bacterium and the somewhat redundant functions of the sensor kinases (LeDeaux, Yu, & Grossman, 1995). A recent strategy to approach the identification of molecular ligands through co-crystallization successfully identified pyruvate as a potential ligand of KinD (R. Wu et al., 2013). Pyruvate is involved in numerous metabolic pathways and it seems reasonable that its levels in the extracellular environment may serve as an indicator of growth conditions. However, it is still unclear whether pyruvate is the physiological ligand of KinD and what effects this interaction may have on sporulation.

Upon activation and autophosphorylation, the phosphoryl group from the histidine kinases is transferred to Spo0A via the phosphotransferases Spo0F and Spo0B which results in an active phosphorylated Spo0A (referred to as “Spo0A~P”) (Burbulys, Trach, & Hoch, 1991). Spo0A~P then goes on to directly regulate the expression of approximately 121 genes (Molle et al., 2003) including activation of genes necessary for sporulation. Counter-balancing the production of Spo0A~P are several phosphatases including members of the Rap family of phosphatases (Rap A, B, E and H) and the Spo0E phosphatase (Perego et al., 1994). Regulation of the activity of the kinases and phosphatases determines the levels of Spo0A~P and ultimately whether or not sporulation is initiated. The activity of the Rap phosphatases is regulated by small peptides encoded by *phr* genes, which are often found in operons with the *rap* genes (Mueller & Sonenshein, 1992). X-ray analyses have indicated that Phr peptides bind and regulate Rap activity by inducing a conformational change (M. D. Baker & Neiditch, 2011; Gallego del Sol & Marina, 2013; Parashar, Jeffrey, & Neiditch, 2013).

The levels of Spo0A~P are responsible for determining the bacterium’s developmental choices. Lower levels of Spo0A~P result in biofilm formation through promotion of matrix production while higher levels of Spo0A~P promote sporulation (Fig. 1.2). The mechanism through which

Spo0A~P is able to regulate these two distinct cell fates is dependent on its regulation of the levels of the matrix gene repressor SinR and its antirepressor SinI (Chai, Kolter, & Losick, 2011). The *sinI* regulatory region has numerous Spo0A~P operator sites that differ in affinity, which allows its expression to be regulated directly by the levels of Spo0A~P. At lower levels of Spo0A~P the high affinity Spo0A~P operator is bound (Fujita & Losick, 2005) and promotes expression of *sinI*, leading to matrix production and biofilm formation (Fujita, Gonzalez-Pastor, & Losick, 2005). At higher levels of Spo0A~P the lower affinity operators are then able to bind Spo0A~P, which hinders the expression of *sinI* and promotes expression of sporulation genes that also have low affinity Spo0A~P operators (Chai et al., 2011; Kearns, Chu, Branda, Kolter, & Losick, 2005). While high levels of Spo0A~P are important for regulating entry into sporulation, the dynamics through which it achieves high levels of Spo0A~P is also important. The gradual accumulation of Spo0A~P appears to exert a temporal control over the Spo0A regulon, which is necessary for robust sporulation (Vishnoi et al., 2013).

Previous studies proposed a model in which there is a threshold level of Spo0A~P, in addition to the phosphorelay components, that must be crossed in order for sporulation initiation to occur (Eswaramoorthy, Dinh, Duan, Igoshin, & Fujita, 2010; Eswaramoorthy, Duan, et al., 2010; Fujita & Losick, 2005). However, recent studies have found significant overlap in Spo0A~P levels in sporulating and non-sporulating cells (Levine, Fontes, Dworkin, & Elowitz, 2012) indicating there may also be other downstream events that are responsible for the decision to enter sporulation. Consistent with this idea is the observation that entry into sporulation may still be reversible after activation of several Spo0A-regulated *spo* genes and only becomes irreversible upon activation of σ^F in the forespore and σ^E in the mother cell (Dworkin & Losick, 2005). The decision to commit to sporulation instead seems to rely on the ultrasensitive activation of σ^E (Narula, Devi, Fujita, & Igoshin, 2012), which occurs after asymmetric septation and σ^F activation in the forespore.

Figure 1.2. Genetic circuitry that governs the entry into sporulation. Arrows indicate activation; repression is denoted by a bar. Developmental events are depicted in the color corresponding to Spo0A levels or phosphorylation states that govern that event. Thus, unphosphorylated Spo0A corresponds to active DNA replication; low levels of phosphorylated Spo0A (SpoA~P) leads to biofilm formation and cannibalistic behavior; and high levels of phosphorylated Spo0A drives the entry into sporulation. Proteins other than Spo0A that participate in each activation or repression step are depicted in gray.

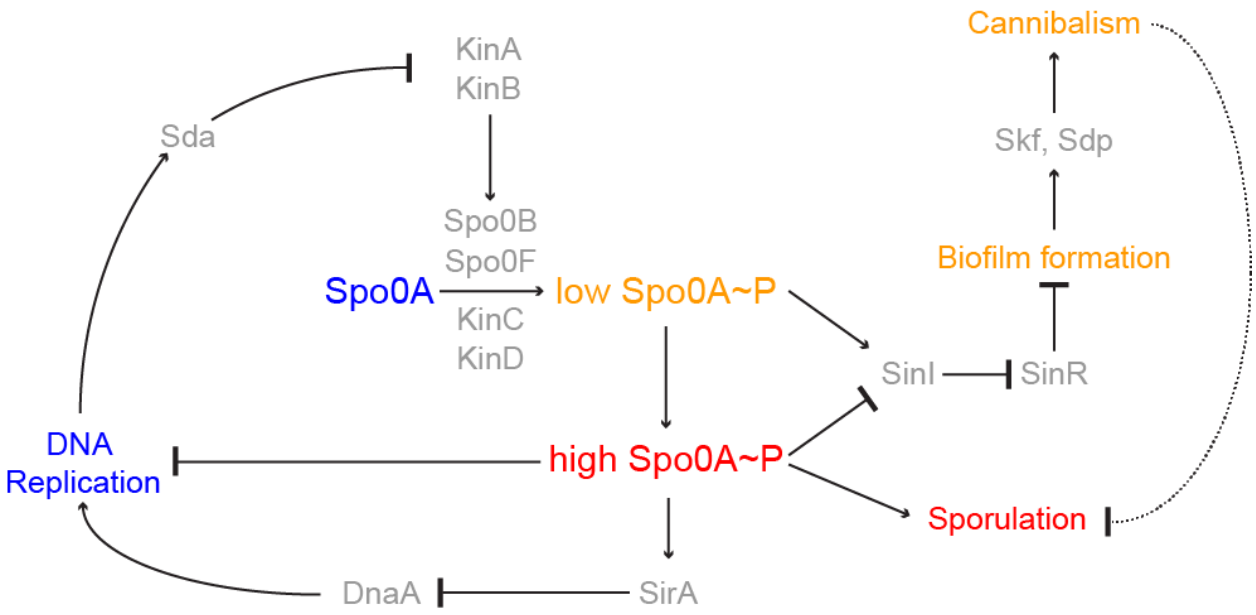

Stage I: Axial filamentation and ensuring correct chromosome copy number

At the onset of sporulation, the cell harbors two chromosomes: one for the mother cell and one for the forespore. The duplicated chromosomes form a condensed serpentine-like structure called the axial filament (Ryter, Schaeffer, & Ionesco, 1966) that stretches from one pole of the cell to the other. The RacA protein is necessary for anchoring the two chromosomes to the cell poles to promote proper chromosome segregation (Ben-Yehuda, Rudner, & Losick, 2003). RacA binds to GC-rich inverted repeats located around the origin of replication (Ben-Yehuda et al., 2005) and localizes to the cell poles through its interaction with DivIVA, which in turn localizes to the two poles of the cell through the recognition of highly negatively curved membranes (Lenarcic et al., 2009; Ramamurthi & Losick, 2009). In this way, RacA ensures that each daughter cell receives one origin of replication (and, by extension, one chromosome). As such, RacA chromosomal binding sites are functionally analogous to eukaryotic centromeres, and RacA itself, while not physically driving chromosome movement, provides a function analogous to that of the eukaryotic mitotic spindle in maintaining chromosome integrity during eukaryotic cell division.

In addition to proper chromosome segregation, proper chromosome number is also necessary for robust sporulation and has been found to be tightly regulated via at least three proteins: SirA (sporulation inhibitor of replication A), Sda (suppressor of *dnaA1*) and Spo0A~P. Transcription of *sirA* is under the control of Spo0A~P and occurs upon entry into sporulation. SirA interacts directly with DnaA to inhibit its binding to the origin of replication, which prevents the initiation of additional rounds of DNA replication during sporulation (Rahn-Lee, Merrikh, Grossman, & Losick, 2011). Sda, on the other hand, inhibits entry into sporulation by binding to the major sporulation histidine kinase KinA during active DNA replication and in response to DNA damage and replication defects (Cunningham & Burkholder, 2009). As a result, entry into sporulation is restricted to the period between rounds of DNA replication (Burkholder, Kurtser, & Grossman, 2001; Veening, Murray, & Errington, 2009). While Spo0A~P plays an indirect role in

regulating chromosome number through its transcriptional regulation of *sirA*, it has also been found to play a more direct role through its ability to bind to sites around the origin of replication. Removal of Spo0A~P binding sites near the origin of replication resulted in an increase in chromosome copy number indicating that Spo0A~P binding to these sites acts as an additional mechanism to inhibit active DNA replication during sporulation (Boonstra et al., 2013).

Stage II: Asymmetric septation

The sporulation program is driven by a cascade of compartment-specific sigma factors that is initiated by asymmetric division of the cell. Understanding the activation of compartment-specific sigma factors during sporulation has revealed conserved mechanisms underlying intercellular signaling and the coupling of transcription with morphological changes in the cell. The transition from a medial septum to an asymmetric septum, which divides the cell into a mother cell and forespore, is a morphological hallmark of sporulation. This switch to a polar septum is dependent on two factors: an increase in levels of the cell division protein FtsZ and the production of the SpoIIE protein, which performs a poorly understood function in deploying FtsZ to polar sites (Carniol, Ben-Yehuda, King, & Losick, 2005). After asymmetric division, the first sporulation-specific sigma factor, forespore-specific σ^F, is activated. Prior to asymmetric division, σ^F is produced under the regulation of Spo0A~P, but held in an inactive state by the anti-sigma factor SpoIIAB. After completion of asymmetric division, SpoIIE (which localizes to the polar septum) performs a second function, wherein it dephosphorylates SpoIIAA, which binds and sequesters SpoIIAB, thereby relieving the inhibition of σ^F (Duncan, Alper, Arigoni, Losick, & Stragier, 1995). Curiously, although SpoIIE is initially produced in both the mother cell and the forespore, activation of σ^F only occurs in the forespore. Although the biochemical mechanism of σ^F activation is well understood, the cell biological mechanism that explains the forespore-specific activation of σ^F is not well known. Part of the answer may be dependent on a preferential localization of SpoIIE on the forespore side of the polar septum (Guberman, Fay,

Dworkin, Wingreen, & Gitai, 2008) and also the temporary genetic asymmetry between the forespore and mother cell that leads to a decrease in the levels of the SpoIIAB anti-sigma factor in the forespore (Dworkin & Losick, 2001).

The temporary genetic asymmetry arises because, at the time of asymmetric septation, the polar septum bisects the axial filament and results in only about a third of the chromosome being harbored in the forespore (L. J. Wu & Errington, 1998). The DNA translocase SpoIIIE then pumps the remaining 70% of the chromosome residing in the mother cell into the forespore (Becker & Pogliano, 2007; B. M. Burton, Marquis, Sullivan, Rapoport, & Rudner, 2007; Fiche et al., 2013; Ptacin et al., 2008; Sharp & Pogliano, 2002; L. J. Wu & Errington, 1994). Prior to translocation of the remaining 70%, the forespore can only express the genes residing on the 30% of the chromosome it harbors initially. This genetic asymmetry has been proposed to play a part in orchestrating the compartment specific activities that occur throughout sporulation (Frandsen, Barak, Karmazyn-Campelli, & Stragier, 1999). Another example of this is the mother cell compartment specific re-activation of *de novo* fatty acid synthesis. Many genes necessary for *de novo* lipid synthesis are located in the portion of the chromosome initially excluded from the forespore, resulting in the forespore's inability to re-activate lipid synthesis (Pedrido et al., 2013). Re-activation of *de novo* lipid synthesis is dependent on Spo0A~P and is required for the mother cell-specific activation of σ^E, the second sporulation-specific sigma factor (Pedrido et al., 2013).

Similar to σ^F, σ^E is produced prior to asymmetric division under the control of Spo0A~P and is found in both compartments after septation (Fujita & Losick, 2002). However, σ^E is produced initially as an inactive pro-σ^E precursor and is specifically activated only in the mother cell. While it was previously established that *spoIIGA* is required for processing of pro-σ^E to its mature form (Jonas, Weaver, Kenney, Moran, & Haldenwang, 1988; Stragier, Bonamy, & Karmazyn-Campelli, 1988), it was only more recently that its product SpoIIGA was identified as a novel type of aspartic protease (Imamura, Zhou, Feig, & Kroos, 2008). Modeling and

mutational evidence suggest that SpoIIGA forms dimers similar to the HIV-1 protease and support a model in which SpoIIGA exists in an inactive state that is then activated through a conformational change induced by association with SpoIIR (Hofmeister, Londono-Vallejo, Harry, Stragier, & Losick, 1995; Imamura et al., 2008). SpoIIR is produced in the forespore under σ^F control and is then secreted into the intermembrane space of the septum that separates the mother cell and forespore, where it activates SpoIIGA. SpoIIR's ability to activate SpoIIGA is dependent on the acylation of its threonine residue (T27) and requires *de novo* fatty acid synthesis (Diez, Schujman, Gueiros-Filho, & de Mendoza, 2012). It is hypothesized that because *de novo* fatty acid synthesis only occurs in the mother cell, only SpoIIR molecules localized to the mother cell side of the septum would be able to be acylated and thus, only SpoIIGA molecules at the mother cell membrane are activated leading to the mother cell specific activation of σ^E (Pedrido et al., 2013). The activation of σ^E then allows transcription of the σ^E regulon, which includes genes necessary for engulfment.

Stage III: Engulfment

After asymmetric division, the polar septum curves around the forespore as the mother cell "swallows" the forespore in a process called engulfment. The result is a double-membrane bound forespore in the mother cell cytosol. Although the dramatic membrane remodeling that occurs during engulfment superficially resembles that of phagocytosis in eukaryotes, the two processes utilize distinct proteins and cytoskeletal elements to achieve this goal. During engulfment, a peptidoglycan degradation machinery composed of SpoIID, SpoIIM and SpoIIP is initially needed for septal wall thinning and subsequently for movement of the engulfing membranes (Abanes-De Mello, Sun, Aung, & Pogliano, 2002). Interestingly, cryo-electron micrographs have revealed that a thin layer of peptidoglycan remains during the engulfment process indicating the peptidoglycan is not completely removed by the degradation machinery (Tocheva et al., 2013). The residual peptidoglycan may be necessary to serve as a template for

subsequent peptidoglycan remodeling events during engulfment and cortex assembly. Recent evidence has indicated that in addition to peptidoglycan degradation, membrane movement during engulfment also relies on active peptidoglycan synthesis (Meyer, Gutierrez, Pogliano, & Dworkin, 2010). This raises the possibility that stiff, newly synthesized, polymers of peptidoglycan may be providing a cytoskeletal role, analogous to that of eukaryotic actin during phagocytosis, to provide the force required for directed membrane movement (Meyer et al., 2010). However, when peptidoglycan is altogether removed by lysozyme treatment, cells are still able to undergo engulfment, albeit at reduced levels. This redundant engulfment mechanism is dependent on a forespore protein, called SpoIIQ, and a mother cell protein, called SpoIIIAH, which reach across the intermembrane space that divides the mother cell and forespore and directly interact, resulting in a "zippering" of both compartments (Blaylock, Jiang, Rubio, Moran, & Pogliano, 2004; Doan, Marquis, & Rudner, 2005). In what has been described as a "ratchet-like" mechanism, the engulfing membrane is able to move forward through random thermal motion of the membrane, but reverse movement is restricted, as the engulfing membrane is stapled to the inner forespore by the tight interaction of SpoIIIAH and SpoIIQ (Broder & Pogliano, 2006).

At the end of engulfment the engulfing membranes must undergo membrane fission to pinch off and release the forespore. The identification of specific factors responsible for membrane fission and fusion in prokaryotes has been historically difficult due to the complexity of the often essential processes that occur concurrently. Unlike most other membrane remodeling events, the membrane fission event that occurs at the end of engulfment is not essential for viability. A recent screen for mutants that were unable to undergo membrane fission at the end of engulfment led to the identification of a mother cell protein called FisB that was enriched at the site of membrane fission during engulfment and was necessary for robust membrane fission. FisB does not resemble or behave like well-studied eukaryotic membrane remodeling proteins like dynamin or the SNARE proteins. Rather, FisB appears to utilize a

novel mechanism to promote membrane remodeling through a preferential association with the phospholipid cardiolipin, which is thought to be enriched along negatively curved leaflets of membranes. The current model is that FisB interacts *in trans* with cardiolipin-enriched membranes at the leading edge of the engulfing membrane to cause a destabilization of both membranes, which in turn could lead to membrane scission (Doan et al., 2013).

At the end of engulfment, the forespore is a free floating cell in the mother cell cytosol. At this time the SpoIIIAA-SpoIIIAH proteins produced under the control of σ^E and the SpoIIQ protein under the control of σ^F are required for the activation of the forespore-specific σ^G (as noted above, SpoIIIAH and SpoIIQ interact directly with one another to "zipper" the mother cell and forespore together during engulfment). The gene encoding the forespore-specific σ^G is under the transcriptional control of σ^F, which ensures that it is only expressed in the forespore. Interestingly, despite being under σ^F transcriptional control, which occurs after asymmetric septation, activation of σ^G occurs only after engulfment has finished. How does σ^G activation occur to coincide with the completion of engulfment? After engulfment, when the forespore is sealed off from the mother cell, the metabolic capacity of the forespore is diminished (Camp & Losick, 2009; Doan et al., 2009). The SpoIIAA-SpoIIIAH and SpoIIQ proteins form a channel between the mother cell and forespore (Meisner, Wang, Serrano, Henriques, & Moran, 2008) through which the mother cell is able to nurture the forespore through the transfer of what are likely small molecules that enable the forespore to continue expressing genes necessary for sporulation (Camp & Losick, 2009). The structure of the basal components of this "feeding tube" channel has been found to be similar to that of type III protein secretion systems (Levdikov et al., 2012; Meisner, Maehigashi, Andre, Dunham, & Moran, 2012). Thus, the activation of σ^G is thought to occur simply because it is the only sigma factor produced at that specific time and location and is dependent on the arrival of metabolites delivered from the mother cell. While the feeding tube is necessary for activation of σ^G, it is still not completely understood how activation of σ^G is precisely linked to the end of engulfment. Indeed, recent observations have indicated

that completion of engulfment is actually linked to the completion of chromosome translocation into the forespore, suggesting that chromosome translocation also contributes to the timing of σ^G activation (Regan, Itaya, & Piggot, 2012).

Similar to σ^E, the subsequent mother-cell specific transcription factor σ^K is produced as an inactive pro-σ^K protein. Pro-σ^K is cleaved by SpoIVFB (Lu, Cutting, & Kroos, 1995), which is an intermembrane protease that is initially held inactive in a complex along with SpoIVFA and BofA (Resnekov & Losick, 1998). Activation of SpoIVFB occurs through the action of the σ^G-regulated SpoIVB processing enzyme. SpoIVB can relieve the inhibition imposed by SpoIVFA and BofA both by cleaving SpoIVFA at multiple sites and by activating the alternate protease CtpB, which can also cleave SpoIVFA (Campo & Rudner, 2006).

Stage IV-V: Cortex and Coat assembly

The mature spore is encased in two distinct concentric shells: an outer shell, called the "coat", which is composed of roughly seventy different proteins, and an inner shell called the "cortex" made of specialized peptidoglycan (Henriques & Moran, 2007; McKenney, Driks, & Eichenberger, 2013). Together, these two shells serve to protect the spore from environmental insults (P. Setlow, 2006). Among the first, if not the first, coat proteins to localize to the outer forespore surface is a small 26-amino-acid protein (a so-called "sprotein" (Hobbs, Fontaine, Yin, & Storz, 2011)), that is exclusively produced in the mother cell, named SpoVM (Levin et al., 1993; van Ooij & Losick, 2003). SpoVM distinguishes the forespore membrane from the mother cell membrane through the recognition of the forespore's positive membrane curvature (Ramamurthi, Lecuyer, Stone, & Losick, 2009). SpoVM tethers a soluble morphogenetic protein called SpoIVA (Ramamurthi, Clapham, & Losick, 2006), which is the structural component of the basement layer of the coat, onto the forespore surface (Price & Losick, 1999; Roels, Driks, & Losick, 1992). While dynamic cytoskeletal nucleotide binding proteins like actin and tubulin hydrolyze nucleotides in order to disassemble, SpoIVA, a static cytoskeletal

element, instead hydrolyzes ATP to drive its self-assembly to form the basement layer of the coat, which acts as a scaffold atop which all other coat proteins are deposited (Castaing, Nagy, Anantharaman, Aravind, & Ramamurthi, 2013; Ramamurthi & Losick, 2008). Curiously, the ATPase domain of SpoIVA resembles that of the TRAFAC class of P-loop GTPases. However, SpoIVA, like the myosin/kinesin family of exceptional ATPases in the TRAFAC GTPase class (Leipe, Wolf, Koonin, & Aravind, 2002), has evolutionarily lost the ability to bind GTP and binds ATP instead.

The coat has been described as having four distinct layers: the basement layer, inner coat, outer coat, and crust (McKenney et al., 2010). Each layer's proper assembly is largely dependent on one (or two, in the case of the crust) major morphogenetic protein that defines each layer. For example, deletion of *spoIVA* results in the mis-assembly of the basement layer (and, by extension, all subsequent layers) (Roels et al., 1992); deletion of *safA*, *cotE,* or *cotZ* and *cotY* result in the improper assembly of the inner coat, outer coat, and crust respectively (Chada, Sanstad, Wang, & Driks, 2003; Costa, Isidro, Moran, & Henriques, 2006; Imamura, Kuwana, Takamatsu, & Watabe, 2011; McKenney et al., 2010; Zheng, Donovan, Fitz-James, & Losick, 1988). Another coat protein, SpoVID, has been shown to drive the "encasement" step of coat morphogenesis where coat proteins completely encapsulate the developing forespore (Driks, Roels, Beall, Moran, & Losick, 1994; McKenney et al., 2010; Wang et al., 2009).

A recent study monitoring the dynamics of spore coat assembly found that proteins in the coat can be divided into six classes based on their localization dynamics. Spore coat proteins initially assemble as a scaffold in a focus on the mother cell side of the forespore. The encasement of the forespore by specific classes of coat proteins then occurs in coordinated waves that are largely driven by transcription (McKenney & Eichenberger, 2012). Coat assembly occurs predominantly in the mother cell where the coat is assembled on the surface of the outer forespore membrane. Interestingly, the discovery that the SpoIIIAH-SpoIIQ complex, which requires the forespore-specific synthesis of SpoIIQ, is necessary for successful

encasement suggests that the forespore may also participate in coordinating the assembly of the coat (McKenney & Eichenberger, 2012).

Although the coat is spatially separated from the cortex by the outer forespore membrane, deletion of either *spoVM* or *spoIVA* not only abrogates the initiation of coat assembly, but also abolishes cortex assembly (Coote, 1972; Levin et al., 1993; Piggot & Coote, 1976; Roels et al., 1992) indicating that coat and cortex assembly are somehow linked. Many factors participating in assembly of each individual structure have been identified; however the mechanisms that coordinate temporal assembly of both structures have remained largely mysterious. Recently, a sprotein (37-amino-acids long) named "CmpA", which was encoded by a previously unannotated mother cell-specific sporulation gene, was found to participate with SpoVM in coordinating cortex assembly (Ebmeier, Tan, Clapham, & Ramamurthi, 2012). Specifically, a model emerged wherein cortex peptidoglycan assembly (but not vegetative peptidoglycan assembly) is repressed by a hitherto-unspecified inhibitory activity of CmpA. Cells that successfully initiate coat assembly by SpoVM and SpoIVA overcome the inhibition imposed by CmpA by removing the protein, likely by regulated proteolysis, and continue through the sporulation program to initiate cortex assembly (Ebmeier et al., 2012). Thus, coordination of the assembly of these two large structures appears to be mediated by at least two small proteins, highlighting the general importance of sproteins in biological processes (Hobbs et al., 2011).

The cortex is made of a specialized peptidoglycan that protects the spore from heat and desiccation. The peptidoglycan in the spore resides between the two membrane layers surrounding the forespore and consists of two layers: an inner germ cell wall and an outer cortex. The germ cell wall is a thin layer adjacent to the inner forespore membrane that has a structure similar to that of the vegetative cell wall (Tipper & Linnett, 1976). The cortex, on the other hand, differs in structure from the vegetative cell wall mainly due to a decreased frequency of transpeptidation between glycan chains (Popham & Setlow, 1993b) and the presence of

muramic lactam (Warth & Strominger, 1972). These structural changes in the cortex are brought about by the activities of the low molecular weight penicillin binding proteins, which often have D,D-carboxypeptidase activity (Popham, Gilmore, & Setlow, 1999), and the CwlD and PdaA proteins, which catalyze the production of muramic lactam from muramic acid (Gilmore, Bandyopadhyay, Dean, Linnstaedt, & Popham, 2004). During spore germination the functionally redundant cortex-lytic enzymes SleB and CwlJ (Ishikawa, Yamane, & Sekiguchi, 1998) specifically hydrolyze the cortex peptidoglycan through the recognition of muramic lactam. Mutants with cortexes deficient in muramic lactam are unable to germinate, but can be induced to germinate through exogenous lysozyme treatment (Popham, Helin, Costello, & Setlow, 1996b).

It is currently unclear what exactly the functional role of the cortex's unique peptidoglycan structure is. One theory is that the low degree of crosslinking allows the spore to expand and contract in response to environmental changes (pH, ionic strength, or humidity, for example) without germinating (Ou & Marquis, 1970). Other theories suggest that the low degree of crosslinking may allow the spore to contract (Lewis, Snell, & Burr, 1960) or expand (Gould & Dring, 1975; Popham et al., 1999) during spore maturation to attain spore dehydration. Interestingly, the degree of crosslinking throughout the cortex is not homogenous, but rather increases progressively towards the outer cortex layers (Meador-Parton & Popham, 2000). Disruption of this crosslinking gradient does not appear to have significant effects on spore core dehydration suggesting a broad range of cortex crosslinking is permissible to attain spore core dehydration (Meador-Parton & Popham, 2000).

Synthesis of cortex peptidoglycan occurs through similar mechanisms as vegetative cell wall synthesis. Peptidoglycan precursors are produced and modified in the cytosol of the mother cell by the Mur proteins which are also responsible for modification of peptidoglycan precursors during vegetative cell wall synthesis. During sporulation the production of the Mur proteins is upregulated by σ^K (Vasudevan, Weaver, Reichert, Linnstaedt, & Popham, 2007).

Once properly modified, the peptidoglycan precursors are then tethered to the outer forespore membrane through the formation of the lipid intermediates Lipid I and Lipid II, which are then flipped across the membrane via a Lipid II flippase into the intermembrane space between the outer and inner forespore membranes. Although there are homologs of putative Lipid II flippases that are expressed specifically during sporulation, the identity of the Lipid II flippase during sporulation is currently unknown. The *E.coli* MviN/MurJ protein has been proposed to be a Lipid II flippase (Ruiz, 2008) and SpoVB was identified as its sporulation-specific homolog (Fay & Dworkin, 2009). However, the discovery that the *E. coli* FtsW protein which is a part of the SEDS (shape, elongation, division and sporulation) family has *in vitro* flippase activity (Mohammadi et al., 2011) suggests that its sporulation-specific homolog SpoVE (Ikeda et al., 1989) may also be a Lipid II flippase. Thus, both SpoVB and SpoVE are plausible candidates for being sporulation-specific Lipid II flippases. Consistent with this idea, mutations in either *spoVB* or *spoVE* abrogate cortex assembly and result in a buildup of peptidoglycan precursors in the mother cell (Vasudevan et al., 2007).

After translocation into the intermembrane space the lipid-linked precursors are assembled into glycan chains via transglycosylation and peptide crosslinks between the glycan strands are formed via transpeptidation. Tranglycosylation and transpeptidation are performed by the high molecular weight penicillin-binding proteins (PBPs) to produce the meshwork of peptidoglycan that constitutes the cortex. The vegetative PBPs (PBP2B and PBP3) are upregulated during sporulation while PBP1, PBP2A, PBP4, and PBP5 are downregulated (Sowell & Buchanan, 1983). PBP2d and PBP2c are expressed in the forespore during sporulation (Pedersen et al., 2000; Popham & Setlow, 1993a) and have been proposed to play partially redundant roles in synthesizing the spore germ cell wall (McPherson, Driks, & Popham, 2001).

Spore resistance

There are many different factors of the spore that make it able to survive in the environment during harsh conditions. In general, the coat protects the spore from enzymatic assaults such as lysozyme and the cortex is required for protection from high temperature. The coat's ability to protect the spore from enzymatic assaults has proven useful in resisting predation by bacteriophagous organisms like *Tetrahymena* (Klobutcher, Ragkousi, & Setlow, 2006; Laaberki & Dworkin, 2008). The cortex is believed to maintain the spore's partially dehydrated state (Imae & Strominger, 1976a; Mallidis & Scholefield, 1987; Warth, 1978) and this low water content is associated with resistance to heat (Beaman & Gerhardt, 1986; Koshikawa et al., 1984). Other factors that contribute to heat resistance and reduction in spore water content include mineralization (Atrih & Foster, 2001; Bender & Marquis, 1985; Marquis & Bender, 1985; Slepecky & Foster, 1959) and the presence of the small molecule dipicolinic acid (DPA) (Paidhungat, Setlow, Driks, & Setlow, 2000; P. Setlow, 2006). Additionally, the spore's DNA is bound by small acid soluble proteins (SASPs) that protect the DNA from damage. Spores that lack SASPs are more susceptible to DNA damaging treatments such as exposure to UV irradiation (B. Setlow & Setlow, 1987) and hydrogen peroxide (B. Setlow & Setlow, 1993). A more in depth discussion of spore resistance mechanisms can be found in Leggett et al. (Leggett, McDonnell, Denyer, Setlow, & Maillard, 2012).

Interest in the ability of spores to survive extraterrestrial environments dates back several decades to when Hagen et al. tested the survival of spores in a simulated Martian environment in an effort to determine the feasibility of extant life on other planets (Hagen, Hawrylewicz, & Ehrlich, 1964). Although the search for extant life is still ongoing, there is significant concern about the contamination of extraterrestrial locations by Earth's organisms carried on space crafts (Nicholson, Schuerger, & Race, 2009). In order to minimize the contamination risk, much research has been done to explore how and under what conditions terrestrial microorganisms may survive and replicate. In particular, understanding how spores,

one of Earth's hardiest cell types, are able to withstand the harsh conditions of space may help the space biological research field to minimize terrestrial contamination. A recent study by Moeller et al., determined that spore survival in a simulated Mars environment is dependent largely on SASPs, the coat, and dipicolinic acid (Moeller, Schuerger, Reitz, & Nicholson, 2012) indicating that survival in Martian environments may depend on the spore's numerous protective factors.

Applications of sporulation studies

Aside from utilizing sporulation as a model system to understand basic biological processes, other applications of studying sporulation derive from the robust nature of the spore. Bacterial cells have been successfully utilized as whole-cell biosensing systems that rely on genetically modified bacteria which are able to express reporter genes in the presence of an analyte of interest in a dose-dependent matter. Advantages of these systems include low-cost, sensitivity, rapid results and the ability to measure the bioavailability of target analytes (Rawson, Willmer, & Turner, 1989). However, one disadvantage has thus far been a lack of stability of the cells used in whole-cell biosensing systems in the field. A solution to this problem has been to use organisms that are able to undergo sporulation. Once they have formed spores, the biosensors can then be stored easily for extended periods of time until they are ready to be deployed (Date, Pasini, & Daunert, 2010). The harmless nature of *B.subtilis* and its genetic tractability, which facilitates the introduction of analyte based reporters, makes it particularly attractive for this purpose. Further studies into sporulation may help in the optimization of spore-based biosensors.

The spore's unique features also make it amenable for a multitude of other applications. The spore's outermost layer is composed of proteins making it easy to decorate the spore with proteins of interest through the incorporation of fusion proteins into the organism's genome. Moreover, such engineered proteins are initially synthesized in the mother cell cytosol and are

displayed in the extracellular milieu on the surface of the spore only after mother cell lysis, thereby potentially avoiding protein misfolding issues that may arise when using purified proteins that are subsequently conjugated to a surface. Such display systems may have multiple uses, including the utilization of spores as surface display systems for enzymes or for use as vaccination platforms (Hinc et al., 2010; Isticato et al., 2001; Mauriello et al., 2004).

Concluding thoughts

Since the initial descriptions by Ferdinand Cohn about 140 years ago of heat resistant spores formed by *Bacillus subtilis* (Cohn, 1877), sporulation has been used as a model system to study a "simple" example of cell differentiation and continues to be used to study fundamental cell biological processes. The non-essential nature of many factors involved in sporulation has greatly facilitated progress made in the field. However, there are still many unanswered questions due to the complex interdependencies and redundancies that are inherent to robust developmental programs.

Despite decades of study, the basic question of how a precursor cell may differentiate into two morphologically distinct, but genetically identical, daughter cells that exhibit different cell fates remains. For example, although in eukaryotes, membrane remodeling events, such as those involved in organelle morphogenesis, endocytosis, and protein trafficking, have been extensively studied, the molecular details underpinning how the architecture of the flat polar septum is altered as the mother cell engulfs the forespore remain an active area of research. Regarding morphogenesis, the spore coat has been a model system for understanding how complex, asymmetric structures may be assembled in an orderly fashion. For years, this structure resisted detailed *in vitro* investigations, since extensive covalent cross-links prevented the extraction of many coat proteins from mature spores. However, advances in bacterial cell biological techniques have revealed detailed interaction networks between the approximately seventy proteins that make up the coat, and an outstanding challenge will be to recreate these

networks *in vitro* in order to ultimately assemble this structure biochemically. At the heart of the study of sporulation remains the differential, but sequential, activation of transcription factors specifically in the mother cell and forespore that can reveal mechanisms by which adjacent cells can communicate with one another. In *B. subtilis*, the molecular details of how σ^F, which is activated in the forespore and sets off the cascade of sigma factor activation, have been exquisitely worked out, yet the cell biological mechanisms that can explain how this activation occurs exclusively in the forespore has been largely unclear. A related question is how asymmetric cell division mechanistically arises in the first place. Additionally, the mysterious chemicals that are transferred from the mother cell to the forespore via the "feeding tube" in order to activate σ^G exclusively in the forespore await discovery and may reveal how activation of a transcription factor may be linked to completion of a morphological event. In total, then, a remarkable developmental process exhibited by a bacterium originally isolated from the soil at the dawn of the era of modern microbiology will likely continue to provide answers to fundamental biological questions. Developing approaches and strategies to unravel these unanswered questions may provide new tools for further understanding other more complex developmental processes as well.

Chapter 2

Small proteins link coat and cortex assembly

A version of this chapter has been published and appears in:

Ebmeier SE*, Tan IS*, Clapham KR, Ramamurthi KS (2012). Small proteins link coat and cortex assembly during sporulation in *Bacillus subtilis*. *Molecular Microbiology*.
*These authors contributed equally to the work.

INTRODUCTION

Understanding the mechanisms that underlie how cells differentiate into genetically identical, but morphologically distinct, daughter cells is a central challenge in developmental biology. One aspect that contributes to the proper morphology of an organism is the presence of complex static structures whose assemblies must be carefully orchestrated during developmental programs (Hartwell & Weinert, 1989; Keaton & Lew, 2006; Richman & Handrigan, 2011). A genetically tractable system to study the morphogenesis of such cellular structures is the process of bacterial endospore formation (sporulation), a simple developmental program in which a normally growing cell differentiates into two different cell types (Errington, 2003; Piggot & Hilbert, 2004; Stragier & Losick, 1996). In the rod-shaped bacterium *Bacillus subtilis*, nutrient deprivation triggers sporulation, whereupon the cell responds by elaborating an asymmetrically-placed division septum that results in two genetically identical, but unequally-sized, daughter cells: the smaller "forespore" that eventually matures into a dormant spore and the larger "mother cell" that nourishes the forespore as it matures (Fig. 2.1A). The two daughter cells initially lie side-by-side, held together by a cell wall that surrounds both cells. Next, the mother cell swallows the forespore in a process called engulfment. As a result, the forespore becomes a double membrane-bound cell inside the mother cell cytosol. Eventually, the mother cell lyses in a programmed event and the small cell, now a dormant spore, is released into the environment.

Mature spores of *B. subtilis* are about one micron in diameter and are encased in two concentric shells that protect the spore's genetic material from various environmental insults (Henriques & Moran, 2007; P. Setlow, 2006). The outer shell, called the "coat", is composed of some seventy different proteins and, being the outermost structure, is responsible for the spore's characteristic appearance (Driks, 2002, 2004). Coat proteins are synthesized in the mother cell and are deposited onto the surface of the developing forespore (Driks et al., 1994;

H. Kim et al., 2006; McKenney et al., 2010; McKenney & Eichenberger, 2012; Webb, Decatur, Teleman, & Losick, 1995). Coat morphogenesis is initiated by the assembly of a basement layer around the developing forespore that is composed largely of a structural protein called SpoIVA which polymerizes to form a platform atop which coat proteins assemble (Driks et al., 1994; Price & Losick, 1999; Ramamurthi & Losick, 2008; Roels et al., 1992). SpoVM, a 26 amino acid-long amphipathic protein, interacts with SpoIVA and the membrane, thereby anchoring SpoIVA onto the forespore surface (Levin et al., 1993; Ramamurthi et al., 2006; van Ooij & Losick, 2003). A third protein, SpoVID, is required to drive the encasement of coat proteins around the developing forespore (Driks et al., 1994; McKenney et al., 2010; Wang et al., 2009). The inner shell (the "cortex"), made of a specialized peptidoglycan (Gilmore et al., 2004; Imae & Strominger, 1976a; Meador-Parton & Popham, 2000; Popham & Setlow, 1993b), is built between the two membranes encircling the forespore and is responsible for maintaining the spore's shape (Atrih & Foster, 1999). Cortex assembly is largely directed from the mother cell, where peptidoglycan precursors are synthesized and subsequently transported across the surface of the forespore into the inter-membrane space between the double membranes that encircle the forespore (Vasudevan et al., 2007). The transported precursors are then assembled into peptidoglycan polymers by transglycosylases and transpeptidases located in this compartment (Popham et al., 1999; Popham, Illades-Aguiar, & Setlow, 1995; Popham & Stragier, 1991).

Several observations indicated that, although the coat and cortex are spatially separated by a membrane, successful initiation of cortex assembly is absolutely dependent on successful initiation of coat assembly at the forespore surface, suggesting that the morphogenesis of both structures is linked. For example, sporulation-defective mutants that display defects in initiating coat assembly are concomitantly defective in cortex assembly (Coote, 1972; Piggot & Coote, 1976). Indeed, in the absence of either SpoIVA or SpoVM not only does the coat fail to form

Figure 2.1. Ile^{15} of VM is required for cortex morphogenesis. (A) Schematic representation of sporulation in *B. subtilis*. After asymmetric division (top), the larger mother cell (MC) and the forespore (FS) lie side-by-side, held together by a cell wall (not shown for simplicity). Plasma membrane is depicted in black. Next, the mother cell engulfs the forespore (middle). Eventually, the forespore becomes a double membrane-bound cell inside the mother cell cytosol (bottom). The proteins that comprise the coat (Ct, dark gray) are synthesized in the mother cell and are deposited on the forespore surface. The cortex (Cx, light gray) is built in the space between the two membranes that encapsulate the forespore. For simplicity, early localization of certain coat proteins to the engulfing membrane in panel two is not shown (McKenney & Eichenberger, 2012). (B-F) Electron micrographs of negatively stained thin sections of sporulating wild type (B, strain PY79), or *VM* deletion (C, strain KR94) strains of *B. subtilis* collected five hours after induction of sporulation. *VM* deletion strain in (C) was complemented with a wild type copy (D, strain KR103) or the *I15A* allele (E, strain KR322) of *VM* at an ectopic locus (*amyE*) on the chromosome. (F) Strain in (E) harboring a spontaneous suppressor mutation in the *cmpA* gene (strain KRC56). All images are oriented such that the engulfed forespore is to the right and the mother cell is to the left. Cortex (Cx) in the micrographs is labeled with a black bar; scale bar: 500 nm. Strain genotypes are listed in Table S1.

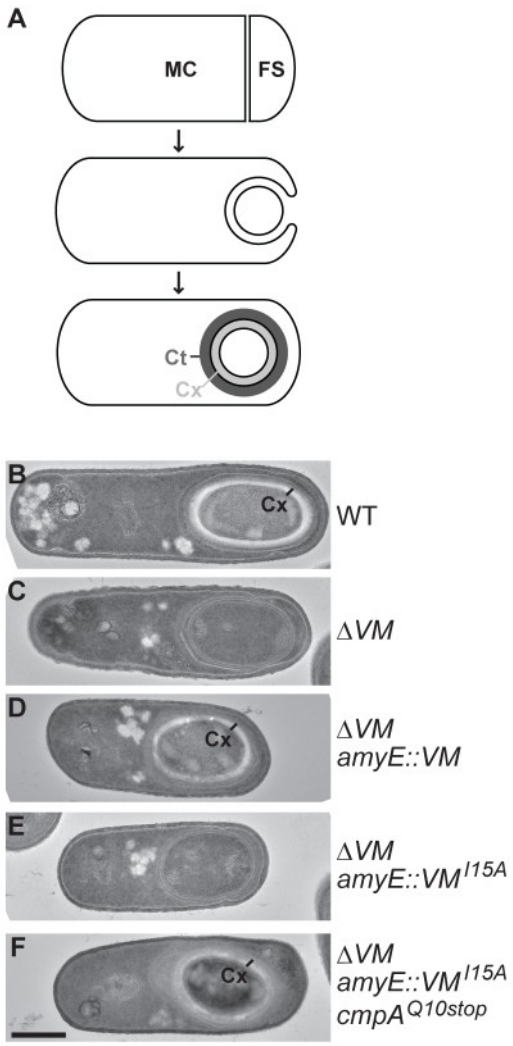
A
MC
FS
Ct
Cx
B
Cx
WT
C
ΔVM
D
Cx
ΔVM
amyE::VM
E
ΔVM
amyE::VM I15A
F
Cx
ΔVM
amyE::VM I15A
cmpA Q10stop

properly, but cortex assembly also fails to initiate (Levin et al., 1993; Roels et al., 1992). Moreover, point mutations in *spoIVA* that disrupt coat assembly also abolish cortex assembly, and the isolation of mutant alleles of *spoIVA* that are defective for the assembly of one structure, but not the other, have not been reported (Catalano, Meador-Parton, Popham, & Driks, 2001). It is important to note that removal of other major coat morphogenetic proteins [for example, SafA, CotE, CotZ, or SpoVID (Beall, Driks, Losick, & Moran, 1993; McKenney et al., 2010; Takamatsu, Kodama, Nakayama, & Watabe, 1999; Zheng et al., 1988)] do not abrogate the morphogenesis of the cortex, suggesting a unique role for SpoIVA and SpoVM in orchestrating coat and cortex assembly. Although many of the factors that are required for the formation of either structure have been very well characterized, the mechanism that temporally orchestrates the morphogenesis of both spatially separated structures has remained largely mysterious.

Here, we report the discovery of a sporulation pathway that links cortex morphogenesis to successful initiation of coat assembly. This pathway involves the small protein SpoVM and another small sporulation protein herein named the Cortex morphogenetic protein A (CmpA), encoded by a previously un-annotated, 37-codon-long open reading frame that is also expressed under the control of two mother cell-specific transcription factors (σ^E and SpoIIID). Deletion of *cmpA* suppressed the sporulation defect of a mutant allele of *spoVM* that was capable of initiating coat assembly, but failed to initiate cortex assembly. In contrast, artificially overproducing CmpA delayed steps of sporulation that require peptidoglycan synthesis and reduced sporulation efficiency. CmpA localized to the surface of the forespore early during sporulation while coat assembly was initiating, but was undetectable in cells that had successfully progressed through the sporulation program. Taken together, we propose a model in which CmpA represses premature cortex assembly until coat assembly successfully initiates, whereupon its inhibition is relieved by a post-translational mechanism.

RESULTS

VM coordinates coat and cortex assembly during sporulation

Deletion of *spoVM* (hereafter, simply "*VM*") causes a severe reduction in sporulation efficiency due to defects in assembling the spore coat and cortex (Levin et al., 1993); Fig. 2.1B-C; contrast the presence of the cortex, which is seen as a white ring, labeled "Cx", in the WT cell encircling the forespore which excludes the stain to the absence of such a ring in the Δ*VM* strain). In order to understand how VM coordinates the assembly of both structures we sought to first identify amino acid residues in VM, by alanine scanning mutagenesis, that would specifically abrogate cortex assembly, while still permitting the initiation of coat assembly. Substitution of Ile^{15} of VM with Ala resulted in a severe sporulation defect in cells harboring VM^{I15A} as the only copy of *VM* [1.2 X 10^{-6} relative to wild type; Table 2.2; (van Ooij & Losick, 2003)]. Examination of these cells by electron microscopy revealed that cortex assembly was abrogated, similar to strains in which the *VM* gene had been deleted (Fig. 2.1E; compare to Fig. 2.1C).

In order to ensure that initiation of coat assembly was not affected in strains harboring VM^{I15A}, we first examined the localization of VM^{I15A} fused to green fluorescent protein (GFP) using fluorescence microscopy. In otherwise wild type cells, VM-GFP localized almost exclusively around the surface of the developing forespore, whereas a previously characterized variant, VM^{P9A}-GFP, promiscuously mis-localized to the membrane surrounding the mother cell as well [Fig. 2.2A-B; (Ramamurthi et al., 2009; van Ooij & Losick, 2003)]. In comparison, localization of VM^{I15A}-GFP was similar to that of wild type VM, suggesting that substitution of I15 with Ala did not affect localization of VM (Fig. 2.2C). Because VM is responsible for anchoring the basement layer of the coat to the forespore surface, we next examined the ability of VM^{I15A} to recruit SpoIVA (hereafter, simply "IVA"), which is a major structural component of the

Table 2.1. Strains used in this chapter.

Strain	Genotype	Reference
PY79	Prototrophic derivative of *B. subtilis* 168	Youngman *et al.* (1984)
CVO1195	*amyE::spoVM-gfp cat*	van Ooji and Losick (2003)
CVO1395	*amyE::spoV ^{P9A}-gfp cat*	van Ooji and Losick (2003)
CVO1399	*Δ spoVM::spc amyE::spoVM^{F3A}cat*	van Ooji and Losick (2003)
CVO1402	*Δ spoVM::spc amyE::spoVM^{I6A}cat*	van Ooji and Losick (2003)
CVO1405	*Δ spoVM::spc amyE::spoVM^{P9A}cat*	van Ooji and Losick (2003)
KR94	*Δ spoVM::tet*	Ramamurthi et al. (2006)
KR103	*Δ spoVM::tet amyE::spoVM cat*	Ramamurthi et al. (2006)
KR320	*Δ spoVM::tet amyE::spoVM^{L8A} cat*	Ramamurthi et al. (2006)
KR321	*Δ spoVM::tet amyE::spoVM^{L12A} cat*	Ramamurthi et al. (2006)
BJK458	*amyE::P$_{hyperspank}$-gfp spc*	Kain and Losick (2008)
KR322	*Δ spoVM::tet amyE::spoVM^{I15A}cat*	
KRC56	*Δ spoVM::tet amyE::spoVM^{I15A}cat cmpA^{Q10stop}*	
KRC125	*Δ spoVM::tet amyE::spoVM cat cmpA^{Q10stop}*	
SE44	*Δ spoVM::tet amyE::spoVM^{I15A}-gfp cat*	
KR165	*Δ spoVM::tet amyE::spoVM cat thrC::gfp-spoIVA spc*	
SE6	*Δ spoVM::tet amyE::spoVM^{I15A} cat thrC::gfp-spoIVA spc*	
SE50	*Δ spoVM::tetR amyE::spoVM^{P9A}cat thrC::gfp-spoIVA spc*	
SE55	*Δ spoVM::tet amyE::spoVM cat::erm cotE::pcotE-gfp cat*	
KR603	*Δ spoVM::tet amyE::spoVM^{P9A}cat::erm cotE::pcotE-gfp cat*	
SE47	*Δ spoVM::tet amyE::spoVM^{I15A}cat::erm cotE::pcotE-gfp cat*	
SE178	*Δ cmpA::erm*	
SE54	*Δ spoVM::tet amyE::erm*	
SE57	*Δ spoVM::tet amyE::spoVM^{F3A}cat cmpA^{Q10Stop}*	
SE58	*Δ spoVM::tet amyE::spoVM^{I6A}cat cmpA^{Q10Stop}*	
SE59	*Δ spoVM::tet amyE::spoVM^{P9A}cat cmpA^{Q10Stop}*	
SE60	*Δ spoVM::tet amyE::spoVM^{L12A}cat cmpA^{Q10Stop}*	
SE61	*Δ spoVM::tet amyE::spoVM^{L8A}cat cmpA^{Q10Stop}*	
SE222	*amyE::P$_{cmpA}$-lacZ cat*	
SE234	*amyE:: P$_{cmpA}$-lacZ cat Δ spo0A::erm*	
SE235	*amyE:: P$_{cmpA}$-lacZ cat Δ sigE::erm*	
SE236	*amyE:: P$_{cmpA}$-lacZ cat Δ sigG::erm*	
SE246	*amyE:: P$_{cmpA}$-lacZ cat Δ sigK::erm*	
IT232	*amyE:: P$_{cmpA}$-lacZ cat Δ spoIIID::erm*	
SE230	*amyE::cmpA-lacZ cat*	
SE241	*amyE::spoVM -lacZ cat*	
SE209	*thrC::cmpA-gfp spec*	
SE211	*Δ spoVM::tet amyE::VM(I15A)cat Δ cmpA::erm thrc::cmpA-gfp*	
SE364	*amyE::P$_{hyperspank}$-cmpA-gfp spc*	
SE367	*Δ spoVM::tet amyE::P$_{hyperspank}$-cmpA-gfp spc*	
SE374	*Δ spoVM::tet amyE::P$_{hyperspank}$-cmpA-gfp spc thrC::spoVM^{I15A} erm*	
SE381	*Δ spoVM::tet amyE::P$_{hyperspank}$-cmpA-gfp spc thrC::spoVM erm*	
SE174	*thrC::cmpA spc*	
SE191	*amyE::P$_{hyperspank}$-cmpA spc*	
SE181	*Δ spoVM::tet amyE::spoVM^{I15A}cat Δ cmpA::erm*	
SE188	*Δ spoVM::tet amyE::spoVM^{I15A}cat Δ cmpA::erm thrC::cmpA spc*	

Table 2.2. Sporulation efficiencies of strains harboring various *VM* alleles in the presence or absence of *cmpA* (measured by heat resistance). Standard deviation from mean is reported in parentheses (n≥3).

	cmpA^{WT}		*cmpA*^{Q10stop}	
VM	Strain[a]	Sporulation Efficiency	Strain[a]	Sporulation Efficiency
WT	A	1	I	0.9
Δ	B	< 1 x 10^{-8}	J	< 1 x 10^{-8}
I15A	C	1.2 x 10^{-6}	K	0.28 (0.02)
F3A	D	< 1 x 10^{-8}	L	< 1 x 10^{-8}
I6A	E	< 1 x 10^{-8}	M	5 x 10^{-7} (1 x 10^{-7})
P9A	F	< 1 x 10^{-8}	N	1.7 x 10^{-7} (9 x 10^{-8})
L8A	G	< 1 x 10^{-8}	O	< 1 x 10^{-8}
L12A	H	1 x 10^{-8}	P	2.7 x 10^{-6} (8 x 10^{-7})

a. Strain A: PY79; B: KR94; C: KR322; D: CVO1399; E: CVO1402; F: CVO1405; G: KR320; H: KR321; I: KRC125; J: SE54; K: KRC56; L: SE57; M: SE58; N: SE59; O: SE61; P: SE60. Genotypes are listed in Table 2.1.

basement layer. In cells harboring a wild type copy of *VM*, GFP-IVA localized around the surface of the forespore in a pattern that was similar to the localization of VM-GFP (Price & Losick, 1999). In cells expressing *VM*^{P9A} as the only copy of *VM*, GFP-IVA mis-localized as a cap on the mother cell-proximal side of the forespore. However, GFP-IVA localized normally in the presence of *VM*^{I15A} (Fig. 2.2D-F). Next, we examined the localization of CotE, a later-assembling coat protein that is recruited by IVA and is in turn required for the recruitment of proteins that comprise the outer layers of the spore coat (Zheng et al., 1988). In the presence of wild type *VM*, CotE-GFP encircled the forespore with a biased accumulation on the mother cell-proximal face of the forespore (Webb et al., 1995). In the presence of the mis-localizing VM^{P9A}, CotE-GFP mis-localized as a cap on the mother cell-proximal side of the forespore, but in the presence of VM^{I15A}, the pattern of CotE-GFP localization was similar to wild type (Fig. 2.2G-I).

Figure 2.2. Ile^{15} of VM is not required for initiation of coat assembly. Localization of VM-GFP (A, strain CVO1195), VM^{P9A}-GFP (B, strain CVO1395), or VM^{I15A}-GFP (C, strain SE44) in an otherwise wild type strain. (D-F) Localization of GFP-IVA in the presence of wild type VM (strain KR165), VM^{P9A} (strain SE50), or VM^{I15A} (strain SE6). (G-I) Localization of CotE-GFP in the presence of wild type VM (strain SE55), VM^{P9A} (strain KR603), or VM^{I15A} (strain SE47). Overlay of GFP fluorescence in panels A-I and membranes visualized with the fluorescent dye FM4-64 (added after the cells were harvested for imaging) is shown below each corresponding panel.

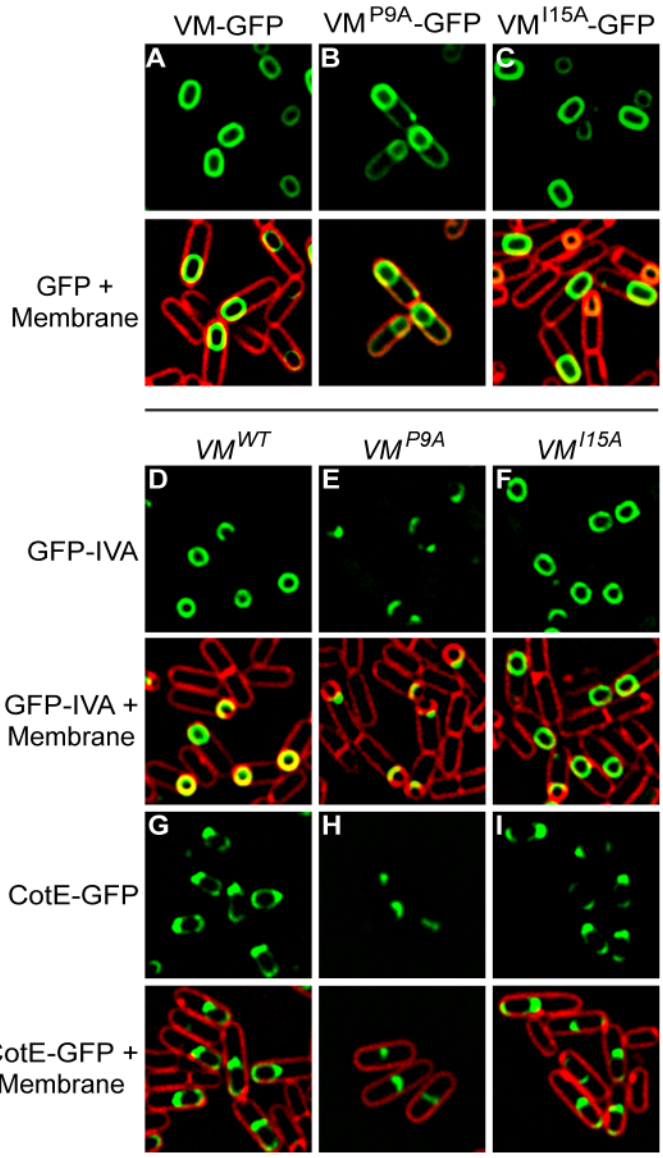
VM-GFP
VM P9A -GFP
VM I15A -GFP
A
B
C
GFP +
Membrane
VM WT
VM P9A
VM I15A
D
E
F
GFP-IVA
GFP-IVA +
Membrane
G
H
I
CotE-GFP
CotE-GFP +
Membrane

Taken together, we conclude that substitution of Ile^{15} of VM with Ala specifically impairs cortex assembly, but not the initiation of coat assembly.

Allele specific suppression of *VM^{I15A}*

In an effort to identify other factors that participate with VM in coordinating cortex assembly with coat assembly, we took advantage of the strong sporulation phenotype caused by *VM^{I15A}* to select for a suppressor mutation that would correct this defect. We therefore subjected cells harboring *VM^{I15A}* to repeated cycles of sporulation, followed by heat treatment to eliminate cells that were unable to sporulate, followed by germination and growth in fresh medium. Our selection yielded an extragenic suppressor mutation which not only corrected the heat resistance defect caused by *VM^{I15A}* to near wild type levels (0.28 ± .02 relative to wild type; Table 2.2, strain K) but also restored cortex assembly (Fig. 2.1F; compare to Fig. 2.1B). The mutation was found to be a single nucleotide transition of cytosine to thymine, located in an intragenic region between *ydcI* and *ydcK*, two genes of unknown function, at approximately 45° relative to the origin of the *B. subtilis* chromosome. Closer examination of this intragenic region revealed a previously un-annotated small putative open reading frame on the complementary strand encoding a 37 amino acid-long protein which we named Cortex morphogenetic protein A (CmpA; Fig. 2.3A-B). The suppressor mutation changed the tenth codon of *cmpA* from CAA, specifying Gln, to TAA, specifying an ochre stop codon, which would presumably result in a truncated CmpA protein product. The upstream region of the *cmpA* ORF harbored a DNA sequence that conformed to a canonical *B. subtilis* ribosome binding site nine bases upstream of the start codon. In addition, the *cmpA* gene was preceded by a sequence that exactly matched the consensus -10 sequence for promoters bound by the mother cell-specific sporulation sigma factor E [σ^E (Eichenberger et al., 2004)], which also drives expression of *VM* (Levin et al., 1993). Although we were unable to find a convincing match for the -35 element recognized by σ^E, the upstream sequence did harbor a nearly perfect match to the consensus

sequence recognized by the transcription factor SpoIIID (Eichenberger et al., 2004). Interestingly, Schmalisch et al. recently identified a small RNA transcript corresponding to this region that was specifically expressed during stationary phase in sporulation medium (Schmalisch et al., 2010). Given the possible sporulation-specific involvement of *cmpA* and its reported expression profile, we investigated whether the gene was conserved in other organisms. BLAST search revealed that *cmpA* is well conserved among closely related spore forming species of the *Bacillales* order (including *Paenibacillus* and *Geobacillus spp*.), but not among the spore forming *Clostridium* species (Fig. 2.3C). Additionally, the σ^E -10 consensus site and the putative SpoIIID binding site were also largely conserved among members of the *Bacillales* order (Fig. 2.4). It is worth noting that in the closely related (but non-spore-forming) *Listeria monocytogenes*, the surrounding chromosomal region is largely conserved, but the open reading frames of *ydcI* and *ydcK* overlap so that the intergenic region harboring *cmpA* is absent. Beyond the conservation of *cmpA* orthologs in other spore forming bacteria, we were unable to identify any conserved motifs that would imply any cellular function.

In order to test if the suppression phenotype was caused by a loss of function of a putative CmpA protein product, we constructed a complete deletion of the *cmpA* ORF by insertion of an antibiotic resistance cassette. Strains harboring a complete deletion of *cmpA* suppressed the VM^{I15A} sporulation defect to similar levels (0.14 ± 0.04 relative to WT; strain SE181) as the spontaneous suppressor harboring a stop codon in *cmpA*, suggesting that a loss of CmpA function was responsible for the suppression phenotype. Complementation of this *cmpA* deletion mutation by introducing *cmpA* (putative *cmpA* ORF plus 126 nucleotides upstream of the start codon) at an ectopic locus in the chromosome (*thr*) restored the sporulation defect of VM^{I15A} ($1.5 \times 10^{-5} \pm 2.9 \times 10^{-6}$ relative to WT; strain SE188), indicating that inactivation of the *cmpA* gene alone was responsible for the suppression of the VM^{I15A} sporulation defect. Next, we wished to determine if the $cmpA^{Q10stop}$ mutation was bypassing the

Figure 2.3. *cmpA* is a small open reading frame that is conserved among spore-forming bacteria. (A) Physical map of the *cmpA* region of the *B. subtilis* chromosome. Arrows depict the direction of transcription. Map is drawn to scale, except that the relative length of the arrow depicting the *cmpA* open reading frame (black) has been exaggerated. (B) Nucleotide sequence of the *cmpA* region of the chromosome. Predicted amino acid sequence of the protein is shown below each codon. Putative ribosome binding site (RBS), -10 binding site for σ^E, and putative SpoIIID binding site are underlined. Consensus nucleotide sequence for the -10 binding site for σ^E and SpoIIID are shown in italics above the chromosomal nucleotide sequence, where capital letters depict highly conserved nucleotides, and "x" is any nucleotide. (C) Amino acid sequence conservation of CmpA among spore forming bacteria. Conserved amino acids are shaded in gray.

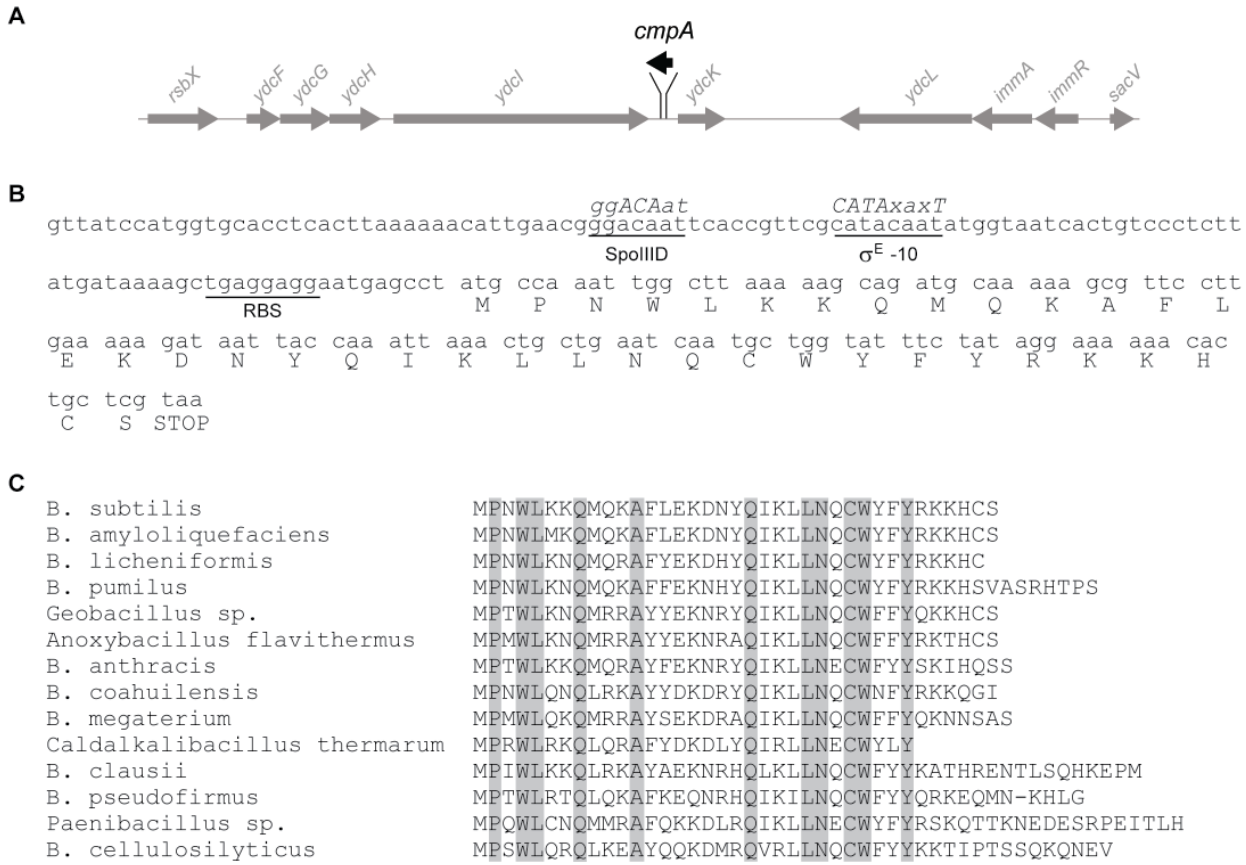

Figure 2.4. Predicted SpoIIID binding site and σ^E -10 consensus sequence upstream of *cmpA* orthologs are widely conserved. One hundred nucleotides immediately upstream of *cmpA* orthologs from various spore forming bacteria are shown (two hundred nucleotides are shown for *B. anthracis*). Predicted SpoIIID binding sites, when identified, are highlighted in the box; sequences resembling the consensus -10 binding sequence for σ^E are underlined.

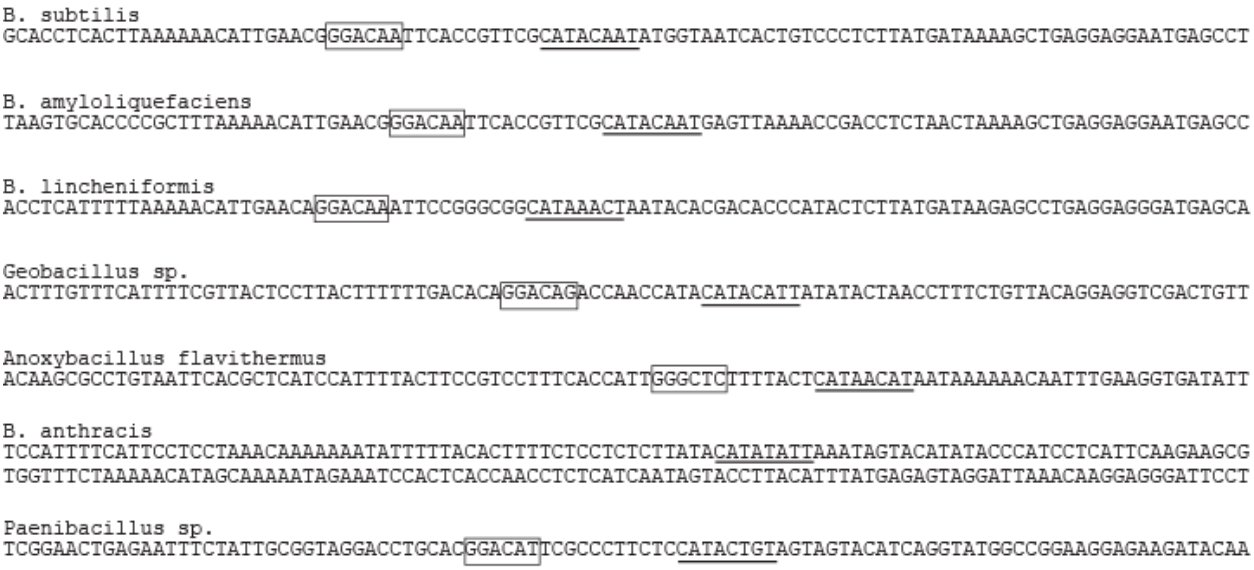

requirement for *VM* altogether and if it was able to suppress the sporulation defects caused by mutant alleles of *VM* other than VM^{I15A}. The results in Table 2.2 show that the $cmpA^{Q10stop}$ mutation did not bypass a Δ*VM* mutation (strain J) and that it was unable to suppress other mutant alleles of *VM* that were known to cause sporulation defects (van Ooij & Losick, 2003). We conclude that truncation of *cmpA* at position 10 results in a loss of function of the protein it encodes and suppresses the sporulation defect of VM^{I15A} in an allele-specific manner. These results led us to hypothesize that *cmpA* encodes a protein that inhibits cortex assembly until coat assembly initiates, and that this inhibition is never properly relieved in cells harboring VM^{I15A}, despite proper initiation of spore coat assembly.

cmpA is a novel sporulation gene regulated by σ^E and SpoIIID

To determine how *cmpA* is transcriptionally regulated, we constructed a strain in which sequences upstream of the *cmpA* ORF (which include the putative promoter, ribosome binding site, and start codon) were fused in frame to the *lacZ* reporter gene. Cultures of the strain harboring this P_{cmpA}-*lacZ* construct were induced to sporulate, and β-galactosidase activity in cell extracts prepared at various time points during sporulation were measured. β-galactosidase activity was undetectable above background before the induction of sporulation, but began to increase at approximately 2.5 hours after induction (Fig. 2.5A). Similar results were obtained for a translation fusion in which the entire *cmpA* ORF was fused in frame to *lacZ*, indicating that the open reading frame was not simply transcribed, but was also translated into a protein product. In comparison, fusion of the promoter and ORF of *VM*, a bona fide σ^E-controlled gene, to *lacZ* displayed a similar timing of expression, though at higher absolute levels of β-galactosidase activity, consistent with the idea that *cmpA* expression also may be driven by σ^E.

To examine the sporulation-specific expression of *cmpA*, we introduced deletions of genes encoding various sporulation-specific transcription factors into the strain harboring P_{cmpA}-

lacZ. Deletion of *spo0A*, which governs the entry of cells into sporulation, *sigE* (which encodes σ^E), or *spoIIID* (a mother cell-specific transcription factor) abolished *cmpA* expression (Fig. 2.5B). In contrast, deletion of *sigG* or *sigK*, which encode sporulation sigma factors that act downstream of σ^E and SpoIIID, did not eliminate *cmpA* expression. Taken together, we conclude that *cmpA* is a gene that is exclusively produced during sporulation and is regulated by the mother cell-specific transcription factors σ^E and SpoIIID.

CmpA localizes to the surface of the forespore

In order to study the subcellular localization of CmpA, we fused *cmpA* in frame to the gene encoding green fluorescent protein (*gfp*) under control of the *cmpA* promoter. When produced under control of its native promoter, though, its fluorescence signal was too faint to be detected by fluorescence microscopy. We therefore cloned the *cmpA-gfp* fusion under control of the IPTG-inducible $P_{hyperspank}$ promoter. Cells that expressed VM^{I15A} along with *cmpA-gfp* as the only copy of *cmpA* displayed an intermediate sporulation efficiency ($6.5 \times 10^{-3} \pm 1.7 \times 10^{-3}$ relative to wild type; strain SE211), indicating that the CmpA-GFP construct was partially functional. To achieve mother cell-specific over-expression of *cmpA-gfp* during sporulation, we exploited a previously described property of sporangia wherein, after the completion of engulfment, activation of xylose-inducible promoters in the forespores was abolished after xylose was added to the growth medium, presumably because the forespore became impermeable to externally added chemicals as it began to metabolically shut down (Camp & Losick, 2009; Doan et al., 2009; Rudner, Pan, & Losick, 2002). To test if IPTG is also unable to induce gene expression in the forespore after completion of engulfment, we examined the production of free GFP in sporulating cells harboring $P_{hyperspank}$-*gfp*. Engulfment was monitored using membrane permeable (TMA-DPH) and membrane impermeable (FM4-64) fluorescent dyes as described previously (Sharp & Pogliano, 1999) in order to measure when the forespore

Figure 2.5. *cmpA* is transcribed only during sporulation and depends on the mother cell-specific transcription factors σ^E and SpoIIID. (A) β-galactosidase accumulation was measured in cells harboring a *spoVM-lacZ* (▼; strain SE241), P_{cmpA}*-lacZ* (●; strain SE222), or *cmpA-lacZ* (■; strain SE230) reporter fusion at various times during sporulation in wild type cells or in cells that did not harbor a *lacZ* reporter [▲; strain PY79, labeled "(-)";]. (B) β-galactosidase accumulation was measured from a P_{cmpA}*-lacZ* reporter fusion at various times during sporulation in wild type (●; strain SE222), and cells harboring a deletion in *sigK* (♦; strain SE246, "$\Delta\sigma^K$"), *sigG* (▼;strain SE236, "$\Delta\sigma^G$"), *spo0A* (■; strain SE234, "Δ*spo0A*"), *sigE* (▲; strain SE235, "$\Delta\sigma^E$"), or *spoIIID* (□; strain IT232, "Δ*spoIIID*"). Symbols represent mean values of three independent measurements; error bars represent standard error of the mean.

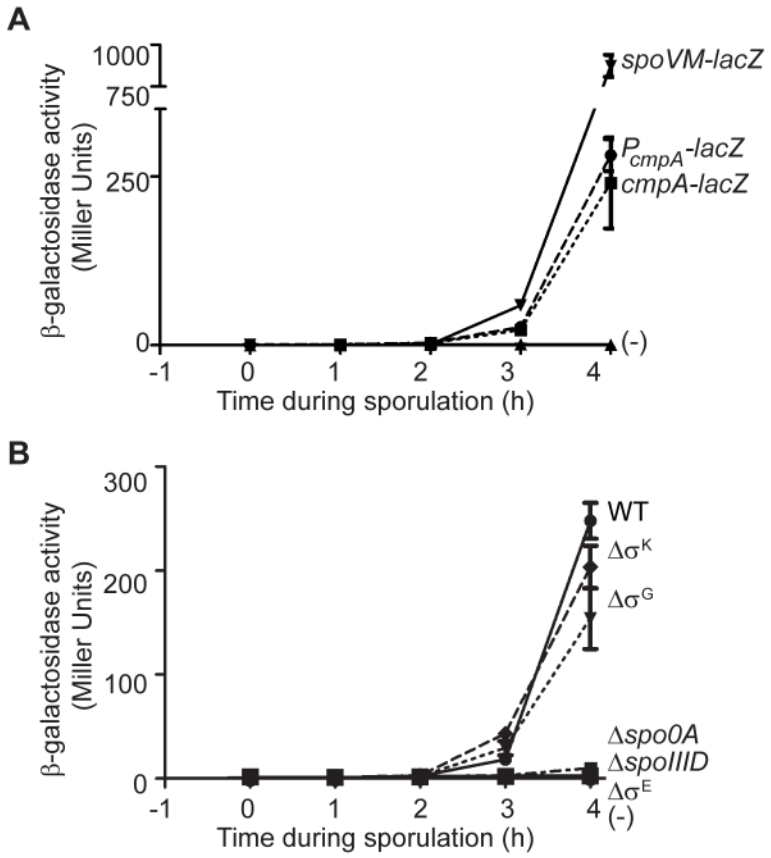

surface separates from the mother cell plasma membrane. Before completion of engulfment (2 hours after the start of sporulation), forespores were detectable using both dyes and, when IPTG was added to cells at this stage, free GFP was uniformly produced in both compartments (Fig. 2.6A, C, E, G). Completion of engulfment (3.5 hours after the start of sporulation) was evident when forespores could not be detected using the membrane impermeable FM4-64, but were visible using TMA-DPH (Fig. 2.6D, F). When IPTG was added to these post-engulfed cells, GFP fluorescence was detected exclusively in the mother cell (Fig. 2.6B, H) indicating that, after engulfment, IPTG only induced gene expression from the $P_{hyperspank}$ promoter in the mother cell.

Three hours after initiation of sporulation, 88% of cells harboring $P_{hyperspank}$-*cmpA-gfp* had completed engulfment, at which time we added inducer to produce CmpA-GFP. Thirty minutes later, we observed that CmpA-GFP production could be monitored by immunoblotting (Fig. 2.7) and that CmpA-GFP localized largely to the forespore surface (Fig. 2.8A). Immunoblotting also allowed us to confirm that the fluorescence signal was due to the production of CmpA-GFP and not free GFP (fig. 2.7). To test if CmpA localization was dependent on VM, we observed the localization of CmpA-GFP in cells harboring a deletion in *VM*. In the absence of VM, CmpA-GFP continued to localize to the forespore surface, but most of the fluorescence signal was present as a focus on the mother cell-proximal side of the forespore (Fig. 2.8B). In the presence of VM^{I15A}, CmpA-GFP localized in a similar pattern as seen in otherwise wild type cells (Fig. 2.8C). Taken together, we conclude that CmpA localizes to the surface of the forespore and that its proper localization either directly or indirectly depends on VM.

CmpA inhibits sporulation and is required for proper coat assembly

The suppression of the VM^{I15A} cortex assembly defect by removing CmpA suggested that CmpA inhibits cortex assembly until coat assembly properly initiates. If so, would overexpression of *cmpA* inhibit cortex assembly? To test this, we first wished to determine if

Figure 2.6. IPTG does not induce expression of genes in the forespore after completion of engulfment. Cells harboring $P_{hyperspank}$-*gfp* were induced to produce GFP either before (left) or after (right) completion of engulfment. (A-B) Fluorescence signal from GFP. (C-D) Membrane stain by the membrane-impermeable dye FM4-64 to monitor the topological separation of the outer forespore membrane from the mother cell plasma membrane in post-engulfed cells. (E-F) Membrane stain by the membrane-permeable dye TMA-DPH to visualize forespores in post-engulfed cells. (G-H) Overlay, GFP and FM4-64. Below, $t_{induction}$, time (hours) after the induction of sporulation at which IPTG was added to cultures to induce expression of *gfp*; t_{imaged}, time (hours) after induction of sporulation at which cells were imaged

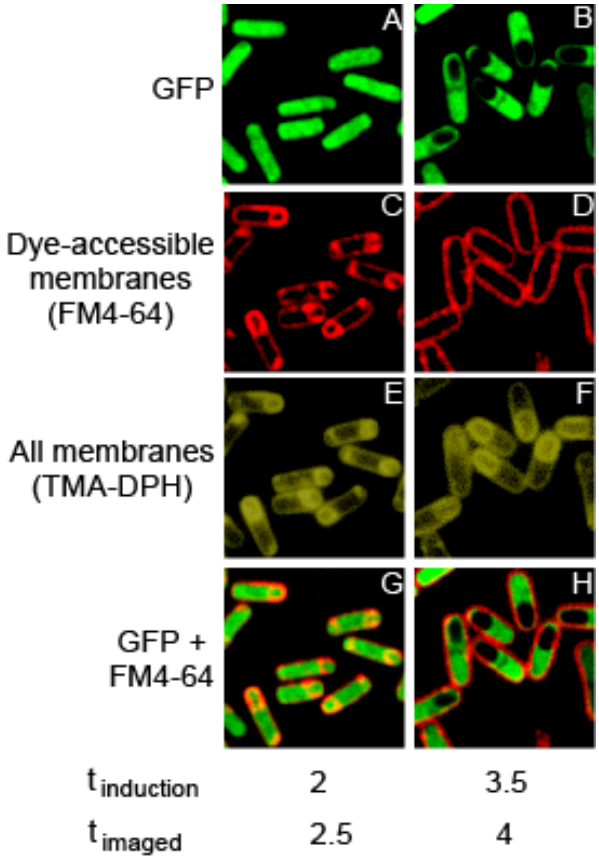

Figure 2.7. Overproduction of CmpA-GFP. Immunoblot analysis of cell extracts taken at t=3.5 hours after the induction of sporulation from cells expressing *cmpA-gfp* under control of its native promoter (left, strain SE209)) or the IPTG-inducible *hyperspank* promoter (right, strain SE364, 1 mM IPTG added at t=3 hours after induction of sporulation) using antibodies to GFP (top) or σ^A, an unrelated protein.

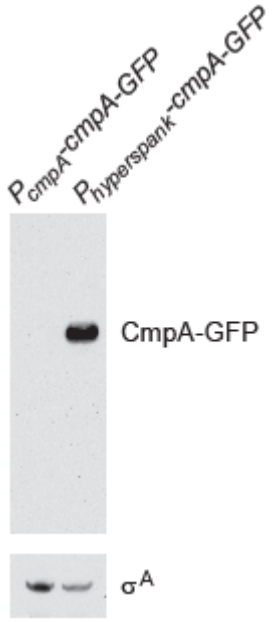

Figure 2.8. CmpA localizes to the surface of the forespore. (A-C) Localization of CmpA-GFP in the presence of wild type *VM* (strain SE364), absence of *VM* (strain SE367), or VM^{I15A} (strain SE374). (D-F) Overlay, GFP fluorescence and membranes in panels A-C visualized with FM4-64 added after cells were harvested for imaging.

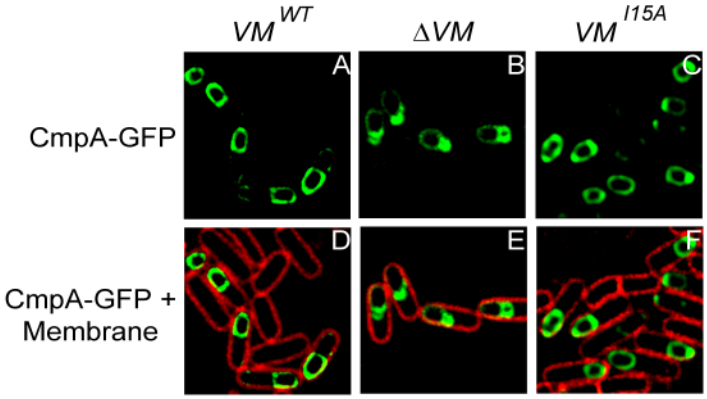

expression of *cmpA* during vegetative growth would also inhibit peptidoglycan assembly in the cell wall and therefore be toxic to cells. We therefore artificially induced the expression of *cmpA* in cells harboring $P_{hyperspank}$-*cmpA* at the *amy* locus during normal growth in CH medium (Sterlini & Mandelstam, 1969) and monitored growth by measuring the turbidity of the culture (Fig. 2.9A, left). Compared to wild type, induced expression of *cmpA* did not appear to be toxic to vegetatively growing cells, and the morphology of cells overexpressing *cmpA* appeared similar to that of wild type cells (Fig. 2.9A, right). Similar results were obtained with cultures grown in DSM medium (Fig. 2.10), indicating that CmpA likely does not affect peptidoglycan assembly during vegetative growth.

To determine if overproduction of CmpA would inhibit cortex assembly, cells harboring $P_{hyperspank}$-*cmpA* at the *amy* locus (in addition to the copy of wild type *cmpA* at its native locus) were induced to sporulate either in the presence or absence of inducer and sporulation efficiency was measured by calculating the number of heat-resistant spores produced in DSM medium as compared to wild type cells. As mentioned above, whereas native levels of CmpA (when fused to GFP) could not be detected by immunoblotting, the fusion was easily detected when expression of *cmpA-gfp* was induced with IPTG, suggesting that the *hyperspank* promoter indeed drives overproduction of CmpA (Fig. 2.7). The results in Table 2.3 show that, whereas the sporulation efficiency of wild type cells was not diminished by addition of inducer, introducing an extra copy of *cmpA*, even in the absence of inducer, reduced sporulation

Table 2.3. Sporulation efficiencies of strains overexpressing *cmpA* (measured by heat resistance). Standard deviation from mean is reported in parentheses (n≥3).

Strain[a]	Description	Inducer	Sporulation Efficiency
A	WT	-	1
		+	1.51 (.38)
B	$P_{hyperspank}$-*cmpA*	-	.48 (.05)
		+	.29 (.12)

a. Strain A:PY79; B: SE191.

Figure 2.9. Overproduction of CmpA arrests sporulation, but not vegetative growth. (A) Left: Representative growth curves of wild type (strain PY79), Δ*cmpA* (strain SE178), or cells (strain SE191) that had (+IPTG) or had not (-IPTG) been induced to overproduce CmpA grown in CH medium from a single experiment. Right: Morphology of the same cells examined by fluorescence microscopy at t = 2.5 hours using the membrane stain TMA-DPH. (B-D) Kinetics of sporulation in cultures of cells (strain SE191) that had (▼; +IPTG) or had not (▲; -IPTG) been induced to overproduce CmpA. Cells were induced to sporulate by resuspension in SM medium, stained with the fluorescent dye TMA-DPH to visualize membranes, and examined by differential interference contrast microscopy (DIC) and epifluorescence microscopy. Fraction of total cells in given fields at various time points that were at Stage 0-1 (B) or Stage II-III (C) of sporulation as determined by membrane staining (cell morphology at each stage is represented by the cartoon above each graph). (D) Fraction of cells at various time points that had elaborated phase bright forespores as determined by DIC. Symbols in (B-D) represent mean values of between 230 and 646 total scored cells from three independent sporulating cultures; error bars represent standard error of the mean. (E) Kinetics of production of heat resistant spores of wild type cells (●; strain PY79), or cells (strain SE191) induced (▼; + IPTG) or not induced (▲; -IPTG) to overproduce CmpA. Symbols represent mean values obtained from three independent measurements; error bars represent standard error of the mean. (F) Change in morphology of cells over time that had not (- IPTG) or had (+ IPTG) been induced to overproduce CmpA as measured by differential interference contrast microscopy. The white arrow at 26 hours indicates a spore-like particle that was not phase bright. (G) Top: Electron micrographs of negatively stained thin sections of wild type (left, strain PY79; arrow indicates a mature spore) or cells overproducing CmpA (right, strain SE191) examined 24 hours after induction of sporulation by nutrient depletion in DSM medium at lower magnification to show a large field of view (scale bar: 2μm). Below, a representative image of a late stage sporangium

and three representative images of mature released spores (left) of wild type cells; on the right, two representative images of cells overproducing CmpA that had been arrested during sporulation (scale bar: 250 nm).

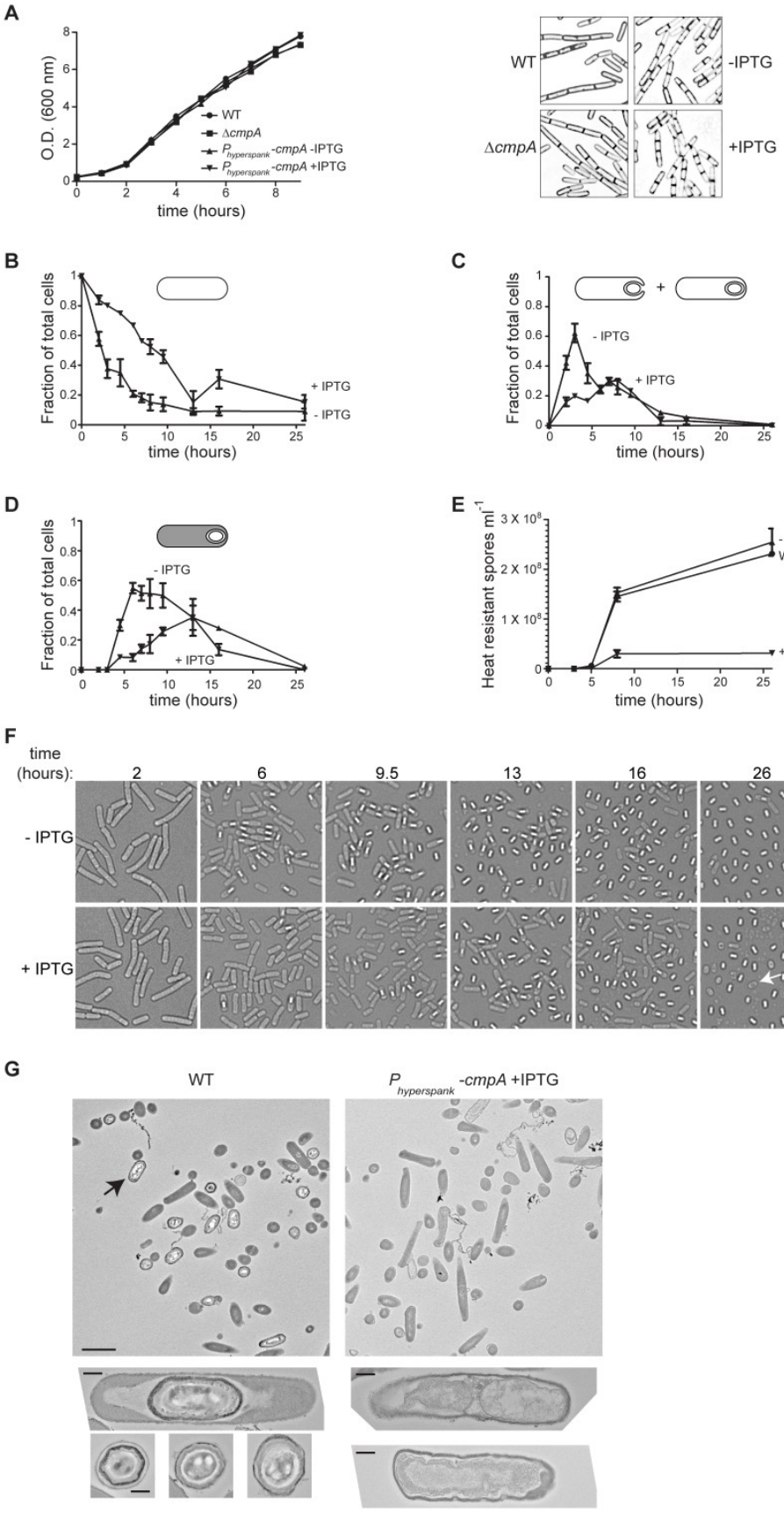
A
O.D. (600 nm)
time (hours)
WT
ΔcmpA
P hyperspank -cmpA -IPTG
P hyperspank -cmpA +IPTG
WT
-IPTG
ΔcmpA
+IPTG
B
Fraction of total cells
time (hours)
+ IPTG
- IPTG
C
Fraction of total cells
time (hours)
- IPTG
+ IPTG
D
Fraction of total cells
time (hours)
- IPTG
+ IPTG
E
Heat resistant spores ml-1
3 X 10^8
2 X 10^8
1 X 10^8
time (hours)
- IPTG
WT
+ IPTG
F
time (hours):
2
6
9.5
13
16
26
- IPTG
+ IPTG
G
WT
P hyperspank -cmpA +IPTG

Figure 2.10. Overproduction of CmpA does not inhibit vegetative growth in DSM medium. Growth curves of wild type (strain PY79), Δ*cmpA* (strain SE178), or cells (strain SE191) that had (+IPTG) or had not (-IPTG) been induced to overproduce CmpA grown in DSM medium.

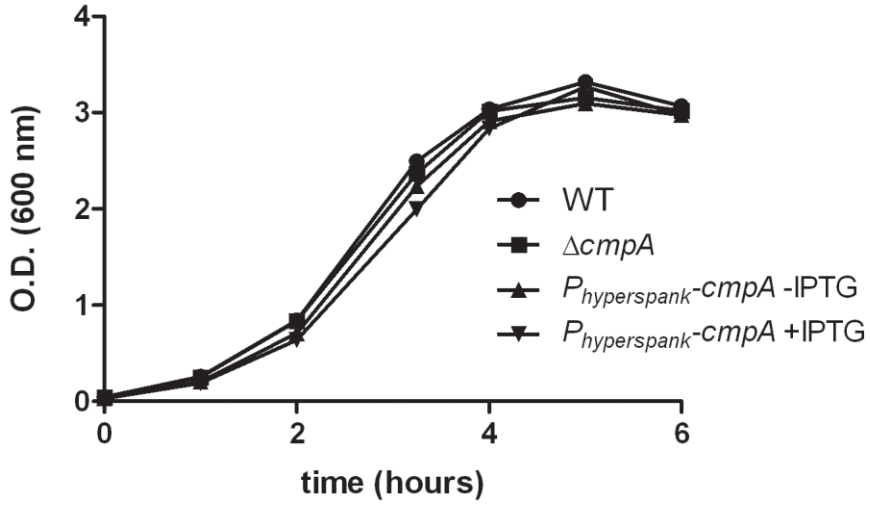

efficiency two-fold to 0.48 ± .05 relative to wild type, presumably due to leaky expression from the *hyperspank* promoter [a true diploid strain harboring a second copy of *cmpA* under control of its native promoter (strain SE174) sporulated with an efficiency of 0.74 ± 0.05 relative to wild type]. When cells were grown in the presence of 1mM IPTG, sporulation efficiency was lowered over three-fold to .29 ± .12 relative to wild type (Table 2.3). To determine the stage at which these cells were impaired, we used a combination of fluorescence and differential interference contrast microscopy to monitor cells harboring $P_{hyperspank}$-*cmpA* at various time points when sporulation was induced by resuspension either in the presence or absence of IPTG, and measured the number of cells that had not yet elaborated polar septa (comprising vegetative cells, and sporangia at Stage 0 or Stage I of sporulation); cells that had elaborated polar septa, were engulfing, or had finished engulfment (sporangia at Stage II or Stage III); or sporangia that had elaborated phase bright forespores (Fig. 2.9B-D). Whereas cells that did not receive IPTG rapidly began to enter sporulation (evidenced by the decrease in the number of Stage 0 and Stage I cells; Fig. 2.9B, "-IPTG"), those cells that were induced to overexpress *cmpA* were delayed in entering sporulation. Concomitantly, the majority of cells that did not receive IPTG had either begun or finished engulfment by hour 3. In contrast, cells that received IPTG displayed a delayed entry into the engulfment stage, with a wide peak centered around hour 8 of sporulation (Fig. 2.9C). Similarly, cells that did not receive IPTG began to elaborate phase bright forespores from hour 5 to hour 8 of sporulation, whereas for IPTG-induced cells, the peak number of cells harboring phase bright forespores did not occur until hour 13 of sporulation (Fig. 2.9D). Finally, heat resistant spores accumulated at a similar rate in cultures un-induced with IPTG compared to the accumulation of spores in cultures of wild type cells (final sporulation efficiency of strain SE191, un-induced with IPTG 26 hours after induction of sporulation by resuspension was 1.1 ± 0.2 relative to wild type; Fig. 2.9E). In contrast, cells that were induced to overproduce CmpA accumulated heat-resistant spores with an efficiency of only 0.13 ± .02 relative to wild type in resuspension medium (Fig. 2.9E). Examining the morphology of these

cells at various time points by differential interference contrast microscopy revealed that the elaboration of phase bright spores and released spores was both reduced and delayed when cells were induced to over-produce CmpA (Fig. 2.9F). Interestingly, in cultures that received IPTG we noticed an additional peak in the number of cells that we scored as "Stage 0" or "Stage I" cells at t=16 (Fig. 2.9B) which coincided with a drop in the number of cells harboring phase bright forespores (Fig. 2.9D). This drop was not accompanied by an increase in heat resistant spores at t=16 (Fig. 2.9E), suggesting that some cells that initially elaborated phase bright forespores failed to progress through the sporulation program and became eventually unaccounted for (perhaps due to lysis), resulting in a relative increase in cells scored as "Stage 0-1" in the population. Additionally, we noticed that cells overproducing CmpA released many bodies that were similar in size and shape to mature spores, but were not phase bright (Fig. 2.9F, t=26 hours, indicated with an arrow). Examination of CmpA-overproducing cells by electron microscopy also revealed that far fewer mature spores were produced. Additionally, those cells that were present largely failed to assembly a cortex (Fig. 2.9G, right; Fig. 2.11). Taken together, we conclude that overexpression of *cmpA* results in a delay in engulfment (and likely, polar septation), a delay in the appearance of phase bright forespores, and an almost eight-fold decrease in the production of heat resistance spores, apparently due to defects in the initiation of cortex assembly. Curiously, although vegetatively growing cells are largely unaffected by artificially produced CmpA, overexpression of *cmpA* at the onset of sporulation arrests or delays sporulation at stages that are known to require peptidoglycan synthesis (Henriques & Moran, 2007; Meyer et al., 2010), suggesting that CmpA specifically affects peptidoglycan assembly during sporulation.

How, then, does the cell relieve the inhibition of sporulation imposed by CmpA? In order to investigate this, we monitored the presence of CmpA-GFP in cells harboring either wild type *VM* or in those harboring VM^{I15A}, which are unable to progress beyond the CmpA block. After the majority of cells had completed engulfment, we added inducer to produce CmpA-GFP

Figure 2.11. Overproduction of CmpA arrests sporulation. Gallery of additional electron micrographs of negatively stained thin sections of cells overproducing CmpA (strain SE191) examined 24 hours after induction of sporulation by nutrient depletion in DSM medium at lower magnification (top) to show a large field of view (scale bar: 2 □m). Below, representative images of cells overproducing CmpA that had been arrested during sporulation at higher magnification (scale bar: 250 nm).

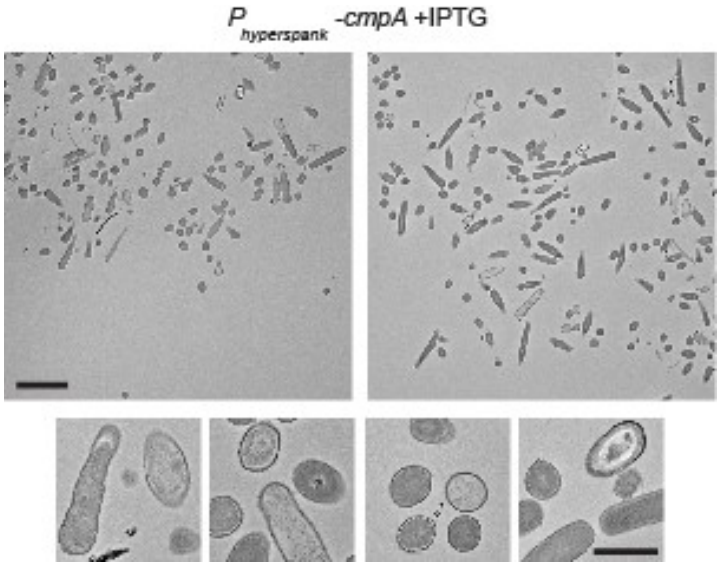

exclusively in the mother cell (because the CmpA-GFP fusion is largely non-functional, it did not inhibit sporulation despite its overproduction). At an early stage of sporulation, before the elaboration of phase bright spores, CmpA-GFP was present around the forespores of cells that harbored either VM^{WT} or VM^{I15A} (Fig. 2.12A-B, arrows). However, 5.5 hours after the induction of sporulation, CmpA-GFP was undetectable in greater than 91% of wild type cells that had elaborated a phase-bright forespore, despite the continued presence of inducer in the medium that drove transcription of *cmpA-gfp* (n=144; the remaining 9% of cells harbored only residual amounts of CmpA-GFP that did not encircle the forespore; Fig. 2.12C, arrowhead). Interestingly, those few cells that had not yet elaborated a phase bright forespore at this later time point still retained CmpA-GFP around the forespore (Fig. 2.12C, arrow). In contrast, in greater than 80% of cells (n=184) expressing VM^{I15A} that elaborated a phase-bright forespore, CmpA-GFP was still present at the later time point and completely encircled the forespore (the remaining approximately 20% retained significant amounts of CmpA-GFP, but the fluorescence signal did not completely encircle the forespore; Fig. 2.12D). Although fusion of GFP to CmpA could artificially stabilize the protein in the presence of VM^{I15A}, our observation that in cells harboring wild type *VM* CmpA-GFP eventually becomes undetectable suggests that the fusion is able to be removed. Taken together, we conclude that once cells progress beyond the stage of sporulation at which they begin to elaborate phase-bright spores, CmpA is post-translationally removed, perhaps to overcome its inhibitory effects. Conversely, in those cells that fail to progress beyond this stage, CmpA remains present. The data are therefore consistent with a model in which the inhibitory effect of CmpA must be removed before cells can progress through the sporulation program.

Would premature removal of CmpA, then, have an effect on the sporulation program? Deletion of *cmpA* did not reduce sporulation efficiency when cells were grown in DSM medium (Table 2.2, strain I), but we wondered if sporulation would proceed faster in the absence of inhibitory activity of CmpA. To test this, we measured the appearance of heat resistant spores

Figure 2.12. CmpA is undetectable in cells that progress through sporulation. CmpA-GFP localization in cells harboring either wild type *VM* (A, strain SE381) or VM^{I15A} (B, strain SE374) 3.5 hours after the induction of sporulation, when expression of *cmpA-gfp* was induced by addition of 1 mM IPTG at 3 hours after induction of sporulation. Arrows indicate representative cells that have not elaborated a phase-bright forespore. (C-D) CmpA-GFP localization in cells harboring either wild type *VM* (C) or VM^{I15A} (D) 5.5 hours after the induction of sporulation. Arrowheads indicate representative cells that have elaborated a phase-bright forespore. (E-H) DIC images corresponding to panels A-D. (I-L) Overlay, GFP fluorescence and DIC. (M) Kinetics of sporulation, as measured by production of heat-resistant spores, of either wild type (●; strain PY79) or Δ*cmpA* (■; strain SE178) cells induced to sporulate by resuspension.

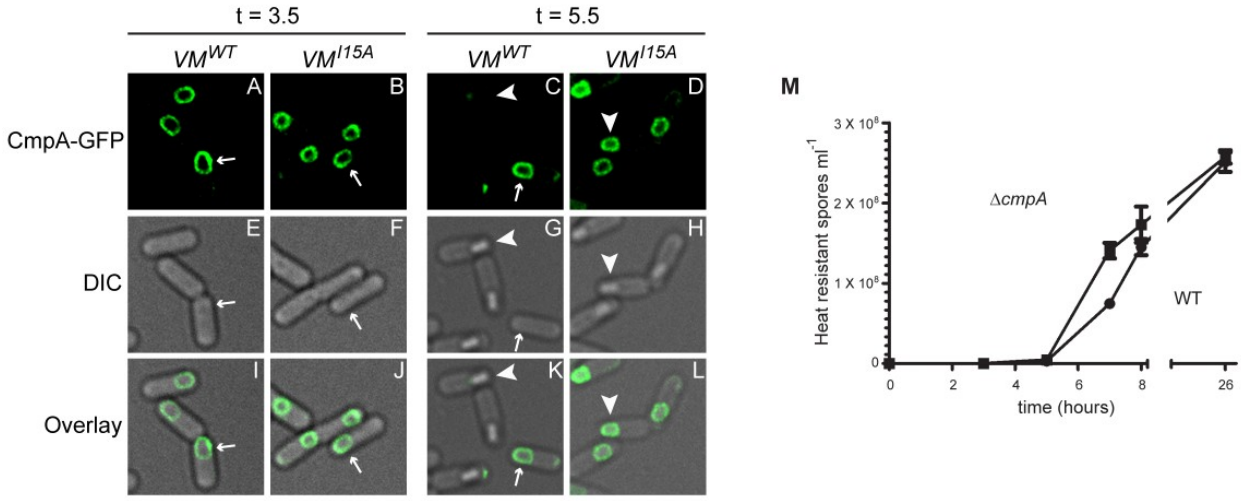

at various time points after the induction of sporulation by resuspension in wild type cells and cells harboring a *cmpA* deletion. At hour 26 after the induction of sporulation, both strains produced a similar number of heat-resistant spores (approximately 2.5 X 10^8 ml^{-1}; Fig. 2.12M). However, examination of earlier time points revealed that at hour 5, the Δ*cmpA* strain had produced about 4.6 X 10^6 heat resistant spores ml^{-1}, whereas the wild type strain had only produced 3.0 X 10^6 spores. This difference was more apparent by hour 7, when the Δ*cmpA* strain had already produced 1.4 X 10^8 heat resistant spores, whereas wild type cells had only produced about 7.5 X 10^7 spores. Taken together, we conclude that when the CmpA-mediated inhibition of sporulation is removed, cells progress more quickly through the sporulation program.

The remarkable conservation of *cmpA* exclusively among other spore forming bacteria led us to wonder what selective pressure assured the maintenance of this gene and what the consequences of unchecked progression through sporulation could be. Heat resistance of *Bacillus* spores correlates with cortex integrity, whereas resistance to lysozyme treatment correlates with coat integrity (Gould & Hitchins, 1963; Melly et al., 2002). Thus, it is conceivable that deletion of *cmpA*, a cortex inhibitor, would result in unrestricted cortex assembly and would therefore not affect heat resistance. Could unrestricted cortex assembly in the absence of CmpA result in coat maturation defects? Δ*cmpA* mutants were not impaired in their ability to correctly localize CotE-GFP to the forespore surface, nor did their mature spores display any obvious gross morphology defects as measured by electron microscopy (Fig. 2.13). We therefore sought to employ a more sensitive technique to assess coat assembly by measuring the ability of Δ*cmpA* spores to resist lysozyme treatment, a resistance property conferred by the coat. Deletion of *cmpA* affected the rate of sporulation as measured by heat resistance (Fig. 2.12M), but had little or no effect on the absolute number of spores produced. In contrast, Δ*cmpA* spores were more than three-fold more sensitive to lysozyme treatment than wild type

Figure 2.13. Deletion of *cmpA* does not result in obvious coat morphology defects.

Localization of CotE-GFP in wild type cells (A, strain CW271) or Δ*cmpA* deletion mutant (B, strain SE224. Overlay of GFP fluorescence in panels A-B and membranes visualized with the fluorescent dye FM4-64 (added after the cells were harvested for imaging) is shown below each corresponding panel. (C-D) Electron micrographs of negatively stained thin sections of released spores of wild type (strain PY79) or Δ*cmpA* strain (strain SE178). Scale bar: 100 nm.

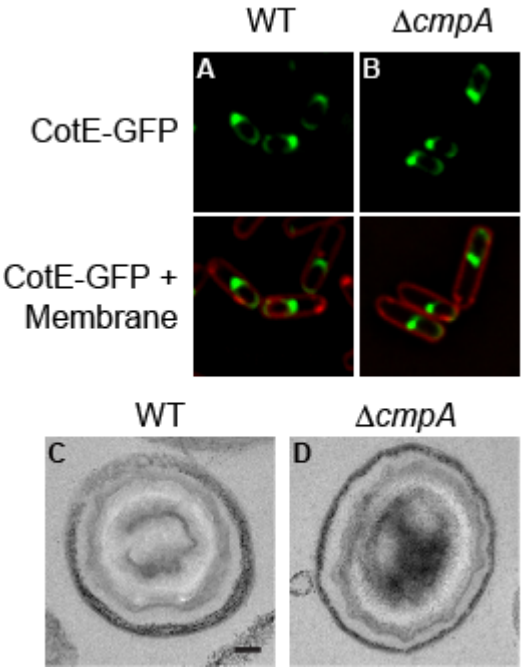

cells (0.29 ± 0.21; Table 2.4), suggesting that they harbored a coat maturation defect that was undetectable by examining the localization of early coat proteins by fluorescence microscopy.

Table 2.4. Sporulation efficiencies of strains harboring various *VM* alleles in the presence or absence of *cmpA* (measured by lysozyme resistance). Standard deviation from mean is reported in parentheses (n≥3).

VM	*cmpA*^{WT}		Δ*cmpA*	
	Strain[a]	Sporulation Efficiency	Strain	Sporulation Efficiency
WT	A	1	D	0.29 (0.21)
Δ	B	$< 1 \times 10^{-8}$	-	ND
I15A	C	1.9×10^{-8} (1.7×10^{-8})	E	0.21 (0.17)

a. Strain A: PY79; B: KR94; C: KR322; D: SE178; E: SE181.

DISCUSSION

Spores of *B. subtilis* are encased in two concentric shells: an outer proteinaceous "coat" and an inner "cortex" made of peptidoglycan. Assembly of the cortex is dependent on the successful initiation of coat assembly and therefore the morphogenesis of both structures must be carefully coordinated during sporulation. Significant progress has been made in understanding how coat assembly initiates and continues self-assembling, how the synthesis of peptidoglycan precursors that comprise the cortex is regulated, and how these precursors are incorporated into the assembling cortex. However, despite the identification of factors that are required for the assembly of both structures, the mechanisms that mediate communication between the coat and cortex during spore morphogenesis are largely unknown. Here, we describe a pathway whereby two small proteins ["sproteins" (Hobbs et al., 2011)] produced in the mother cell, the 26 amino acid-long VM that initiates coat assembly, and a newly discovered 37 amino acid-long protein which we have named CmpA that seems to repress cortex assembly, ensure that the morphogenesis of both cellular structures is temporally coordinated.

Our model that CmpA is a repressor of cortex assembly is based on three observations. First, deletion of the *cmpA* gene suppressed the cortex assembly defect in cells harboring the *VM*^{I15A} allele of *spoVM*, which were otherwise arrested at a stage of sporulation immediately preceding cortex assembly. Cells in which *cmpA* was deleted produced heat resistant spores more quickly than wild type cells, but were sensitive to lysozyme (suggesting that the coat was somehow improperly assembled). We interpret these results to mean that unchecked cortex assembly results in coat assembly defects. Second, overproduction of CmpA before the onset of sporulation caused a three to eight-fold decrease in the production of heat-resistant spores, consistent with a block in cortex assembly. Examining the kinetics of sporulation in these cells revealed that they were delayed in polar septation, engulfment, and the production of phase bright spores, steps which either require peptidoglycan synthesis or are coincident with cortex assembly (Henriques & Moran, 2007; Meyer et al., 2010). Furthermore, electron microscopy

revealed that overproduction of CmpA abrogated cortex assembly. Third, in wild type cells CmpA-GFP was detectable during stages of sporulation preceding the elaboration of phase-bright spores, but was undetectable after phase-bright spores were evident. In contrast, in cells harboring VM^{I15A}, which were arrested at a stage immediately preceding cortex assembly, CmpA-GFP remained localized around the forespore despite becoming phase bright.

Taken together, our results suggest a "checkpoint" model whereby VM and CmpA orchestrate coat and cortex assembly (Fig. 2.14). We propose that, as engulfment proceeds, VM is synthesized in the mother cell, localizes to the surface of the developing forespore, and anchors IVA, an ATPase that polymerizes to form the basement layer of the coat. CmpA, which is produced in the mother cell under the control of the same sigma factor that governs expression of *VM* and *IVA* (albeit at much lower levels), also localizes to the forespore surface, uniformly surrounds it, and represses the initiation of cortex assembly. It is important to note that transcription of the *cmpA* gene is additionally regulated by SpoIIID, which would likely delay synthesis of CmpA until the completion of engulfment and after coat assembly had commenced, since, as we observed (Fig. 2.9), premature synthesis of CmpA delayed the onset of engulfment. Conversely, in the absence of CmpA, the production of heat-resistant spores proceeds more quickly. As a consequence, coat assembly exhibited subtle defects, suggesting that carefully orchestrating the assembly of the cortex is required for proper coat assembly. The precise mechanism by which CmpA localizes is unknown, but its uniform localization pattern depends directly or indirectly on the presence of VM. Successful formation of the basement layer of the coat (which comprises localization of VM, recruitment of IVA, and subsequent polymerization of IVA), then triggers the inactivation of CmpA repression by the eventual removal of CmpA. Since transcription of the *cmpA* gene was driven by an inducible promoter in the experiments presented here, our preliminary evidence suggests that the inactivation of CmpA is a post-transcriptional event, perhaps repression of *cmpA* mRNA translation and/or proteolysis of CmpA protein (Fig. 2.12).

Figure 2.14. CmpA is a checkpoint that orchestrates coat and cortex morphogenesis. A sporulating *B. subtilis* cell is depicted (below) in which membranes are yellow and peptidoglycan is gray. Top: magnification of the outer and inner forespore membranes and cortex (gray mesh), in which VM (red) has inserted into the phospholipid bilayer. CmpA (blue) localizes to the surface of the forespore and participates in the inhibition of cortex assembly. Recruitment of IVA (green) and successful initiation of assembly of the basement layer of the coat results in depletion of CmpA, thereby relieving cortex assembly inhibition.

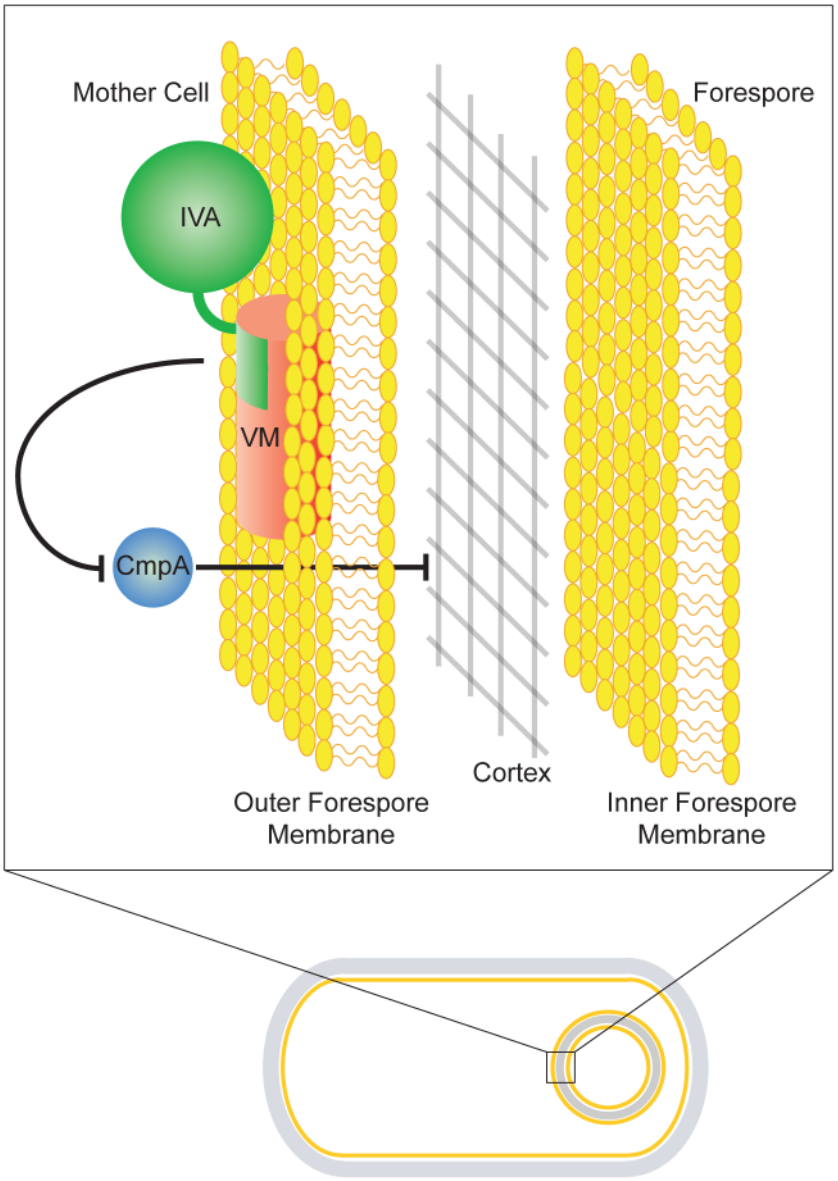

The model immediately raises two outstanding questions that remain to be answered. First, what downstream targets are directly or indirectly inhibited by CmpA? Deletion of three other sporulation genes, *spoVB*, *spoVD*, or *spoVE* results in a phenotype similar to that caused by the VM^{I15A} allele, in which coat assembly proceeds normally, but cortex assembly is blocked. SpoVB is a putative lipid II flippase that has been proposed to transport peptidoglycan precursors synthesized in the mother cell into the intermembrane space between the double membranes surrounding the forespore to be incorporated into the assembling cortex (Popham & Stragier, 1991). SpoVD is a membrane-bound class B penicillin binding protein that is required for cortex peptidoglycan synthesis (Daniel, Drake, Buchanan, Scholle, & Errington, 1994; Fay, Meyer, & Dworkin, 2010). Its activity was recently shown to be controlled by a thioredoxin-like protein called StoA (Y. Liu, Carlsson Moller, Petersen, Soderberg, & Hederstedt, 2010), which is also required for efficient cortex assembly (Erlendsson, Moller, & Hederstedt, 2004). SpoVE is an integral membrane protein that is also required for cortex peptidoglycan synthesis and belongs to the "SEDS" family of proteins that have been implicated in bacterial shape determination (Fay et al., 2010; Real et al., 2008). Recently, Mohammadi et al. demonstrated that at least one SEDS family member, *E. coli* FtsW, displays lipid II flippase activity in vitro (Mohammadi et al., 2011). All three proteins therefore represent excellent candidate targets for direct or indirect inhibition by CmpA. The observation that induced, premature expression of *cmpA* was not toxic to vegetative cells, but delayed several sporulation-specific steps that are thought to require peptidoglycan synthesis (polar septation, engulfment, and cortex morphogenesis) suggests that the target of CmpA inhibition may be a sporulation-specific factor.

Second, what signals the relief of CmpA inhibition of cortex assembly? The presence of an inhibitory element that prevents progression through a developmental program is reminiscent of cell cycle checkpoint proteins, defined as extrinsic control elements in which loss-of-function

mutations may be isolated that allow a "relief of dependence" on that factor (Hartwell & Weinert, 1989), and indeed, deletion of *cmpA* not only permits the progression of sporulation, but even permits it to proceed faster. In one well-studied example, the eukaryotic spindle assembly checkpoint in which exit from metaphase does not occur until chromosome segregation proceeds correctly, entry into anaphase is restricted by the checkpoint if sister kinetochores attached to the mitotic spindle fail to exhibit physical tension (indicating that they are being pulled in opposite directions (Musacchio & Salmon, 2007). The checkpoint is relieved only after sister chromatid cohesion is lost. During sporulation, successful initiation of cortex assembly appears to rely not only on proper localization of VM and subsequent recruitment of IVA, but also an additional event that is mediated by the VM Ile^{15} residue. Perhaps a physical event that conveys the completion of the basement layer of the coat such as polymerization of IVA is monitored by the checkpoint to allow progression through the sporulation program.

The discovery of such a small, previously un-annotated, ORF that plays a critical role during a developmental program highlights the importance of sproteins (gene products that arise from ORFs containing fewer than 50 codons) in biology (Hobbs et al., 2011). Indeed, it is worth noting that VM, despite its diminutive size, plays at least four separate roles during sporulation. First, VM recognizes membrane curvature and, along with IVA, marks this patch of forespore membrane as the site for coat assembly (Ramamurthi et al., 2009). Second, VM anchors IVA (and by extension, the entire assembling coat) to the surface of the forespore (Ramamurthi et al., 2006). Third, along with SpoVID, VM is required for the "encasement" step of the spore coat assembly around the developing forespore (Wang et al., 2009). Finally, as we have described here, VM participates in a pathway that coordinates the assembly of two supramolecular structures that are separated by a phospholipid bilayer. Although, as in the case of *VM* and *cmpA*, genes encoding such proteins were discovered using classical genetics due to strong deletion or suppression phenotypes, improved bioinformatics approaches may enable more facile discovery of previously ignored genes that affect various important cellular

functions. Indeed, an important challenge for the future remains to identify, using a combination of methods, other factors that participate in the developmental pathway that links coat morphogenesis to cortex assembly.

EXPERIMENTAL PROCEDURES

Strain construction and growth. Strains are otherwise congenic derivatives of *B. subtilis* PY79 (Youngman, Perkins, & Losick, 1984). *B. subtilis* competent cells were prepared as described previously (Wilson & Bott, 1968). *spoVM*^{I15A} at *amyE* was created using the Quikchange site-directed mutagenesis kit (Agilent Technologies) using complementary primers that harbored the mutation flanked by 15 bases on either side and using plasmid pKC2 (Ramamurthi et al., 2006) as the template to create plasmid pKR59. *cmpA* at *thrC* was created by PCR amplification of the *cmpA* ORF and 126 nucleotides immediately upstream of the ORF using primers "ydcJprom5'Eco" (5' aaagaattcttttgaagctctttgttatccatg) and "ydcJprom3'Bam" (5' aaaggatcctgatgtcgtatctgtcggcg), digesting the PCR product with EcoRI and BamHI, and cloning into the integration vector pDG1731 (Guerout-Fleury, Frandsen, & Stragier, 1996). P_{cmpA}-*lacZ* at *amyE* was created by PCR amplifying 300 nucleotides upstream of the *cmpA* ORF using primers "ydcJ5'promEco" (5' aaagaattcttgatgatgccaatcagttcc) and "ydcJ3'startHind" (5' aaaagcttcataggctcattcctcctcag), digesting with EcoRI and HindIII, and cloning into plasmid pAH124 (Camp & Losick, 2009) to create pSE23. *cmpA-lacZ* at *amyE* was created by PCR amplifying the *cmpA* ORF and upstream sequences using primers "ydcJ5'promEco" and "ydcJnostop3'Hind" (5' aaaaagcttcgagcagtgtttttttcctatag), and cloning into pSE23 as described above to create pSE27. *spoVM-lacZ* at *amyE* was created by cloning the EcoRI/HindIII fragment of pKC13 (Ramamurthi et al., 2006) into pSE27 to create pSE31. $P_{hyperspank}$-*cmpA-gfp* at *amyE* was created by cloning *cmpA* and *gfp* into a vector and introducing a HindIII restriction site at the site of fusion. *cmpA-gfp* was then PCR amplified from the resulting construct using primers "5'SalI(RBS)ydcJ" (5' aaagtcgactaaggaggaatgagcctatgcc) and "3'GfpNheI" (5' aaagctagcttatttgtatagttcatc), digested with SalI and NheI, and cloned into pDR111 (David Rudner). $P_{hyperspank}$-*cmpA* at *amyE* was created by PCR amplifying the cmpA ORF, along with 9 nucleotides upstream (specifying the RBS) and 24 nucleotides downstream, using primers "ydcJ5'RBSHind" (5' aaaaagctttaaggaggaatgagcctatgcc) and "ydcJ3'Nhe" (5'

aaagctagctctatggtaaaataaaagcactg). The fragment was then digested with HindIII and NheI and cloned into pDR111. All plasmids were integrated into the *B. subtilis* chromosome by double recombination at the specified ectopic locus. The *cmpA* deletion was created using the Long Flanking Homology PCR (LFH-PCR) technique (Wach, 1996) using primers "ydcJ_KO_P1" (5' ggacagtatcagcatgacgtcagcc) and "ydcJ_KO_P2" (5' caattcgccctatagtgagtcgtgcagtgcttttattttaccatag); and "ydcJ_KO_P3" (5' ccagcttttgttccctttagtgagctgctttttaagccaatttggc) and "ydcJ_KO_750P4" (5' gcgcgtccattccgccacgaccgcgtgatc). Underlined sequences correspond to DNA sequence in plasmid pAH52 (Ferguson, Camp, & Losick, 2007) used as a template to amplify the erythromycin antibiotic resistance cassette. s*poVM-gfp, gfp-spoIVA* (Ramamurthi et al., 2006), and *cotE-gfp* (Webb et al., 1995) fusions, and the *spo0A*, *sigE*, *sigG*, *sigK*, and *spoIIID* deletions (Chu et al., 2008; Eichenberger et al., 2004; Kenney & Moran, 1987; Kunkel, Kroos, Poth, Youngman, & Losick, 1989) were described previously.

General methods. β-galactosidase activity was measured as previously described (W.L. Nicholson & P. Setlow, 1990). Sporulation efficiency was measured by inducing sporulation by nutrient depletion in Difco sporulation medium (DSM) for at least 24 hours at 37°C. The number of colony forming units that survived heat treatment (80°C for 20 min) or lysozyme treatment (250 μg ml^{-1} for 10 min at 37°C) was determined and reported relative to the CFU obtained in a parallel culture of the wild type PY79 strain. For *cmpA* overexpression experiments, cells were induced to sporulate by resuspension in SM medium (Sterlini & Mandelstam, 1969) containing 1 mM IPTG at the time of resuspension as described below. For microscopy, cells from the IPTG-induced and uninduced cultures were removed at various time points and imaged as described below.

Fluorescence microscopy. Overnight cultures grown at 22°C in CH medium (Sterlini & Mandelstam, 1969) were diluted 1:20 into fresh CH medium and grown for approximately 2.5

hours at 37°C. Cells were induced to sporulate by resuspension in SM medium. If necessary, IPTG was added (1 mM final concentration) to induce expression of *cmpA-gfp* three hours after resuspension (after most cells had completed engulfment). Cells were harvested, resuspended in PBS containing 1 μg ml^{-1} of the fluorescent dye FM4-64 or 46 μg ml^{-1} TMA-DPH to visualize membranes, and placed on a glass bottom culture dish (Mattek Corp.). A 1% agarose pad made with distilled water was cut to size and placed on top of the cell suspension. Cells were viewed with a DeltaVision Core microscope system (Applied Precision) equipped with an environmental control chamber. Images were captured with a Photometrics CoolSnap HQ2 camera. Seventeen planes were acquired every 0.2 μm at 22°C and the data were deconvolved using SoftWorx software.

Electron microscopy. For the images in Fig. 2.1, cells were induced to sporulate by resuspension in SM medium as described above and were harvested 5 hours after induction of sporulation. For the images in Fig. 2.9G, cells were induced to sporulate by nutrient depletion in DSM for 24 hours. Three ml of the culture was harvested, resuspended in three ml PBS and fixed using 4% formaldehyde, 2% glutaraldehyde (final concentration) for at least 2 hours at room temperature. Fixed cells were collected by centrifugation and processed for thin-sectioned TEM analysis. Briefly, the cell pellet was post-fixed in 1% Osmium tetroxide in 0.1M Cacodylate buffer for one hour at room temperature, en bloc stained with 0.5% uranyl acetate in 0.1M acetate buffer for one hour, then dehydrated sequentially in 35%, 50%, 75%, 95%, and 100% ethanol followed by 100% propylene oxide. Cells were infiltrated in an equal volume of 100% propylene oxide and epoxy resin overnight and embedded in pure resin the following day. The epoxy resin was cured at 55^{o}C for 48hrs. The cured block was thin-sectioned and stained in uranyl acetate and lead citrate. The sample was imaged with a Hitachi H7600 TEM equipped with a CCD camera.

Isolation of spontaneous suppressors. Spontaneous suppressor mutations of *spoVM*^{I15A} were isolated as described previously (Ramamurthi et al., 2006). Briefly, strain KR322, harboring *spoVM*^{I15A} as the only copy of *spoVM*, was grown in 100 ml of DSM supplemented with 5 μg ml^{-1} chloramphenicol (Cm) for 24 h at 37°C in order to accumulate spontaneous mutations and sporulate. 40 ml of this culture was removed and incubated at 80°C for 20 min in order to kill any cells that had not completed sporulation successfully. 33 ml of the heat-killed culture was then diluted into 300 ml of fresh DSM/Cm and allowed to sporulate for 24 h as above. The procedure was repeated two more times and candidate survivors from each round were collected for further characterization. The suppressor mutation was mapped by generating a mini Tn-10 transposon library (Steinmetz & Richter, 1994) using strain KRC56 and isolating a clone in which suppression of the *VM*^{I15A} sporulation defect was genetically linked (by transformation) to the antibiotic resistance conferred by the transposon.

Author Contributions

K.R.C did intitial selection to isolate the mutation in *cmpA*. S.E.E. did initial experiments to characterize CmpA. I.S.T. did later experiments to further characterize CmpA. S.E.E., I.S.T. and K.S.R. analyzed and interpreted data.

Chapter 3

Regulated cell death through proteolysis of a morphogenetic protein selectively removes unfit cells from a population of sporulating bacteria

A version of this chapter has been submitted for publication in:

Tan IS, Weiss CA, Popham DL, Ramamurthi KS (in review). Regulated cell death through proteolysis of a morphogenetic protein selectively removes unfit cells from a population of differentiating bacteria.

INTRODUCTION

Maintaining the fidelity of developmental programs is essential for ensuring the correct morphology of an organism. As such, key factors that determine morphogenesis are often subject to multiple layers of regulation (Deves & Bourrat, 2012). The alternative developmental pathway of bacterial endospore formation ("sporulation") provides a relatively simple and genetically tractable system to study cellular morphogenesis and the mechanisms that maintain the robustness of a differentiation program (Errington, 2003; Higgins & Dworkin, 2012; Stragier & Losick, 1996; Tan & Ramamurthi, 2014). In nutrient-rich conditions, the bacterium *Bacillus subtilis* divides symmetrically to yield two genetically and morphologically identical daughter cells. However, upon nutrient deprivation, the bacterium initiates the sporulation pathway by first dividing asymmetrically, resulting in two genetically identical, but morphologically distinct daughter cells (the larger "mother cell" and the smaller "forespore") that will undergo different cell fates (Fig. 3.1A). Next, the mother cell engulfs the forespore and as a result, the forespore resides as a double membrane-bound cell within the mother cell. The forespore is then encased by the spore envelope which contains two concentric shells, whose assemblies are largely mediated by the mother cell (Henriques & Moran, 2007). The inner shell, the cortex, is assembled between the two membranes surrounding the forespore and is composed of a specialized peptidoglycan that eventually protects the spore from wet heat and helps maintain the dehydrated state of the spore core (Leggett et al., 2012; Popham, Helin, Costello, & Setlow, 1996a). The outer shell, the coat, is composed of ~70 different proteins produced in the mother cell and is responsible for protecting the spore from chemical and enzymatic assaults (Driks, 2002; Klobutcher et al., 2006; McKenney et al., 2013; P. Setlow, 2006). Ultimately, the mother cell lyses, thereby releasing the mature spore into the environment.

Assembly of the coat begins with the localization of a small 26-amino acid protein, SpoVM (Levin et al., 1993), which recognizes the outer forespore membrane by preferentially adsorbing onto the forespore's positively curved membrane surface (Ramamurthi et al., 2009).

Figure 3.1. Overexpression of *cmpA* causes defects in cortex maintenance. (A) Schematic of sporulation in *Bacillus subtilis*. Asymmetric division (top) results in the formation of the larger mother cell (MC) and smaller forespore (FS) compartments, which are genetically identical. Next, the mother cell engulfs the forespore (middle). Ultimately, the forespore resides in the mother cell cytosol (bottom). The forespore is encased in two concentric shells: the proteinaceous coat (Ct, dark gray), and the cortex (Cx, light gray), made of a specialized peptidoglycan. Membranes are depicted in black; cell wall material is depicted in light gray. (B-E) Time-lapse microscopy of sporulating wild type (B; strain PY79) and *cmpA* overexpressing (C-E; IT478) cells. Time after induction of sporulation is indicated above. Fate of phase bright forespores in wild type (B) and *cmpA* overexpressing (C) cells. Fate of (D) phase gray forespores in *cmpA* overexpressing cells while still in the mother cell, or phase gray spores (E) after release into the medium. Arrowheads indicate phase gray forespore or released spore. (F-G) Accumulation of cortex peptidoglycan (F) and dipicolinic acid (DPA) (G) during sporulation in wild type (●; PY79) and *cmpA* overexpressing (■; IT478) cells. Symbols represent mean values obtained from three independent measurements; error bars represent standard error of the mean. Strain genotypes are listed in Table 3.7. See also Figure 3.2 and Table 3.1.

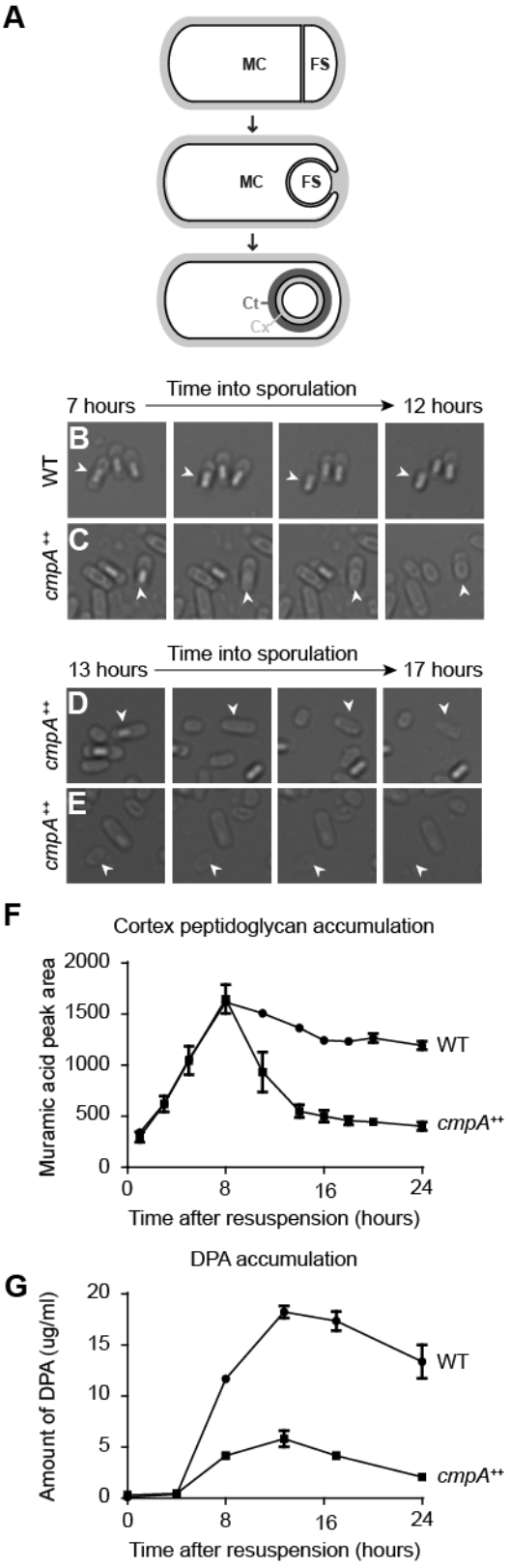
A
MC
FS
MC
FS
Ct
Cx
Time into sporulation
7 hours
12 hours
B
WT
C
cmpA++
Time into sporulation
13 hours
17 hours
D
cmpA++
E
cmpA++
F
Cortex peptidoglycan accumulation
Muramic acid peak area
2000
1500
1000
500
0
WT
cmpA++
0
8
16
24
Time after resuspension (hours)
G
DPA accumulation
Amount of DPA (ug/ml)
20
15
10
5
0
WT
cmpA++
0
8
16
24
Time after resuspension (hours)

SpoVM recruits the morphogenetic protein SpoIVA (Price & Losick, 1999; Ramamurthi et al., 2006; Roels et al., 1992) which polymerizes irreversibly in an ATP-dependent manner around the forespore surface (Castaing et al., 2014; Castaing et al., 2013; Ramamurthi & Losick, 2008). Deletion of either *spoVM* or *spoIVA* results in a mis-assembled coat that is not anchored to the forespore surface (Levin et al., 1993; Roels et al., 1992). Thus, SpoVM and SpoIVA are required for proper assembly of the basement layer, atop which other coat proteins are deposited (McKenney et al., 2010). Interestingly, deletion of *spoVM* or *spoIVA*, but not other major coat proteins, also abolishes the assembly of the spatially separated cortex (Levin et al., 1993; Roels et al., 1992) suggesting that SpoVM and SpoIVA play unique roles in coordinating the assembly of both the coat and the cortex.

Previously, we identified a small (37 codon) unannotated open reading frame in *B. subtilis* (which we termed "*cmpA*"), whose deletion suppressed the sporulation defect imposed by a mutant allele of *spoVM* that permitted initiation of coat assembly, but abrogated cortex assembly (Ebmeier et al., 2012). We found that CmpA is produced in the mother cell during sporulation and that overexpression of *cmpA* reduced sporulation efficiency in otherwise wild type cells (Ebmeier et al., 2012). We proposed that CmpA may participate with SpoVM and SpoIVA in coordinating the orchestration of spore envelope assembly by inhibiting cortex assembly until coat assembly occurred, but the mechanism remained unclear. Here, we report that CmpA ensures proper spore envelope assembly by participating in a sporulation quality control pathway that selectively removes defective sporulating cells through regulated cell death, to ultimately preserve the integrity of the sporulation program in the population. Using classical genetics we identified the AAA+ protease ClpXP (T. A. Baker & Sauer, 2012; Gottesman, 1996) as an additional participant in this pathway and propose that CmpA is an adaptor (Zhou, Gottesman, Hoskins, Maurizi, & Wickner, 2001) that delivers the coat protein SpoIVA for degradation by ClpXP specifically in those cells in which the spore envelope has mis-assembled. Accordingly, we found that amino acid substitutions in CmpA, SpoIVA, or ClpX

that disrupted complex formation led to restoration of SpoIVA stability in cells that had mis-assembled the spore envelope. Additionally, we found that deletion of *cmpA* permitted the completion of the sporulation program by cells harboring mutant alleles of *spoVM* and *spoIVA*, resulting in the formation of viable, but less robust spores. We propose that the persistence of CmpA in cells harboring a spore envelope defect, mediated by the late-acting sporulation transcription factor σ^K, acts as a switch that promotes the degradation of the spore envelope morphogenetic protein SpoIVA, which destabilizes the forespore and leads to cell lysis, thereby specifically removing defective cells and ensuring the fidelity of the sporulation program.

RESULTS

cmpA overexpression causes spore maturation defects

Overexpression of *cmpA* diminished the production of heat resistance of spores, which we interpreted as a defect in cortex assembly (Ebmeier et al., 2012), however the mechanism of cortex assembly inhibition remained unclear. To better understand CmpA's role in cortex assembly we performed single-cell time lapse microscopy of wild type and *cmpA*-overexpressing cells and monitored the fate of forespores that had achieved the phase bright state, an indicator of the spore core's dehydration (Imae & Strominger, 1976b). In both wild type cells and *cmpA*-overexpressing cells, forespores were able to progress to the phase bright state. However, while 74% (n=498) of wild type phase bright forespores were ultimately released into the extracellular milieu upon lysis of the mother cell (Fig. 3.1B, arrow; (Smith & Foster, 1995)), in the *cmpA*-overexpressing cells only 15% (n=222) of phase bright forespores were released and the remaining 85% relapsed into a phase-gray state (Fig. 3.1C, second panel, arrowhead), suggesting that they were unable to maintain spore core dehydration. We observed two fates of these relapsed phase-gray forespores in *cmpA*-overexpressing cells. First, in sporangia harboring unreleased relapsed phase-gray forespores, both the mother cell and phase gray forespore lysed (Fig. 3.1E). Second, we observed that released phase gray forespores would ultimately lyse (Fig. 3.1E). Taken together, the data suggested that overexpression of *cmpA* inhibited the cell's ability to properly maintain its dehydrated spore core and led to cell lysis.

Since cell shape and osmotic stability are governed by the integrity of the cell wall (Holtje, 1998), we next examined the effect of *cmpA*-overexpression on cortex peptidoglycan (PG) levels and composition. To monitor assembly of cortex PG, we harvested soluble cortex PG precursors and assembled cortex PG from wild type and *cmpA*-overexpressing forespores at various time points during sporulation. Both strains initially (~t_0-t_8 hours after resuspension)

Figure 3.2. Overexpression of *cmpA* has no lasting effect on soluble peptidoglycan precursors. Accumulation of soluble peptidoglycan precursors during sporulation in wild type (O; PY79) and *cmpA* overexpressing (■; IT478) cells. Symbols represent mean values obtained from three independent measurements; error bars represent standard error of the mean.

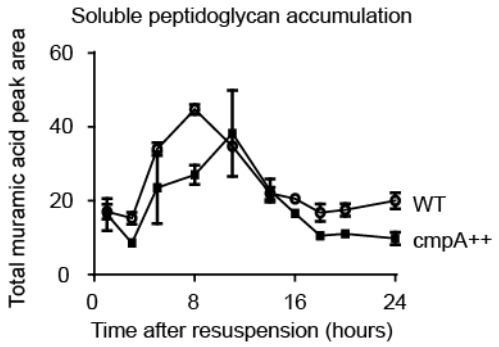

accumulated soluble PG precursors, and depleted this pool coincident with cortex assembly (Fig. 3.2). During this initial period, both strains also accumulated cortex PG as sporulation progressed, indicating that cortex assembly was occurring despite *cmpA* overexpression (Fig. 3.1F). However, whereas wild type cells subsequently maintained steady levels of assembled PG after t_8, indicating the presence of a stable cortex, the recovered cortex PG from *cmpA*-overexpressing cells decreased drastically after this time point (Fig. 3.1F), presumably due to an inability to harvest cells that lysed upon *cmpA*-overexpression (Fig. 3.1D-E). Consistent with a defect in cortex maintenance, we also observed that sporangia overexpressing *cmpA* did not appreciably accumulate dipicolinic acid (DPA) (Fig. 3.1G), a small molecule that displaces water and is required for heat resistance (Paidhungat et al., 2000; B. Setlow, Atluri, Kitchel, Koziol-Dube, & Setlow, 2006). Interestingly, the inability to maintain a stable cortex after apparently normal initial assembly and the inability to accumulate DPA of *cmpA*-overexpressing cells was reminiscent of the phenotypes associated with a *spoIVA* cortex-deficient point mutant (Catalano et al., 2001), suggesting that *cmpA* overexpression may be causing a loss of *spoIVA*'s cortex assembly function.

Two mechanisms could possibly contribute to the instability of the assembled cortex PG: (*1*) mechanical instability of the cortex due to a defect in spore envelope assembly, or (*2*) premature activation of cortex lytic hydrolases responsible for ultimately degrading the cortex during germination. To rule out the second scenario in *cmpA*-overexpressing cells, we deleted *sleB* and *cwlJ*, which encode the two known cortex lytic hydrolases necessary for germination (Heffron, Orsburn, & Popham, 2009), and measured sporulation efficiency. Deletion of *sleB* and *cwlJ* did not suppress the sporulation defect caused by *cmpA* overexpression, (Table 3.1, Strain D) indicating that *cmpA's* inhibition of cortex maturation is not due to a premature activation of cortex lytic enzymes. The data suggest that *cmpA*-overexpression prevents the maintenance of a stable cortex and that this may be due to a mechanical instability of the spore envelope.

Table 3.1. Effect of cortex hydrolase deletion on *cmpA* overexpression sporulation efficiency. Standard deviation from mean is reported in parentheses (n=3). "++" indicates overproduction.

Strain[s]	CmpA	*cwlJ sleB*	Sporulation Efficiency
A	WT	WT	1
B	++	WT	5.7×10^{-3} (6.1×10^{-4})
C	WT	Δ	0.01 (0.003)
D	++	Δ	1.2×10^{-5} (9.5×10^{-6})

[a] Strain A: PY79; B: IT504; C: IT517; D: IT575. Genotypes are listed in Table 2.7.

Identification of other factors interacting with CmpA

To better understand the mechanism of CmpA's inhibition of cortex stability we sought to identify additional factors that participate in this pathway. Since deletion of *cmpA* was initially identified as an extragenic suppressor of cells harboring the cortex-deficient *spoVM*^{I15A} mutation (Ebmeier et al., 2012) we selected for additional spontaneous suppressors that corrected the sporulation defect imposed by *spoVM*^{I15A}. To prevent isolation of more mutations in *cmpA*, we performed the selection in a strain harboring two copies of *cmpA*. From this selection we isolated two suppressors that mapped to *spoIVA* (Table 3.2, Strain C and D). The first suppressor changed Glu423 to Gly, and the second changed the adjacent Leu424 to Phe. The proximity of these two suppressors indicated that this region of SpoIVA may be important for interacting with CmpA or SpoVM and supported our model that SpoVM, SpoIVA and CmpA participate together to orchestrate coat and cortex assembly.

We previously reported that proper CmpA-GFP localization is directly or indirectly dependent on *spoVM* ((Ebmeier et al., 2012); Fig.3.3B); however, the modest mislocalization phenotype, together with the isolation of suppressor mutations in *spoIVA*, suggested that SpoIVA may also be interacting with CmpA. Accordingly, in the absence of SpoIVA, we found

that CmpA-GFP was principally mislocalized in the mother cell cytosol (Fig.3.3C). The deletion of both *spoVM* and *spoIVA* resulted in a similar mislocalization phenotype as the *spoIVA* deletion alone (Fig.3.3D), suggesting that SpoIVA is likely the major localization determinant for CmpA.

Table 3.2. Sporulation efficiencies of additional *spoVM*^{I15A} suppressors. Standard deviation from mean is reported in parentheses (n=3).

Strain[a]	*spoVM*	Suppressor	Sporulation Efficiency
A	WT	-	1
B	*spoVM*^{I15A}	-	5×10^{-6} (1.7×10^{-6})
C	*spoVM*^{I15A}	*spoIVA*^{E423G}	0.49 (0.16)
D	*spoVM*^{I15A}	spoIVA^{L424F}	0.22 (0.11)

[a] Strain A: PY79; B: KR322; C: SE249; D: IT89; Genotypes are listed in Table S7.

Next, we exploited the heat sensitivity caused by *cmpA* overexpression ((Ebmeier et al., 2012); Table 3.3, Strain F) to select for spontaneous suppressors that would correct this phenotype. This selection yielded three suppressors that mapped to the *clpX* locus, which encodes for the ATPase subunit of the ClpXP protease ((Gottesman, Clark, de Crecy-Lagard, & Maurizi, 1993; Wojtkowiak, Georgopoulos, & Zylicz, 1993); Table 3.3, Strain G, H, I). All three suppressors (D21Y, I34M, and E44G) resulted in

amino acid changes in the N-terminus of ClpX, which is implicated in substrate binding (Wojtyra, Thibault, Tuite, & Houry, 2003). A fourth suppressor mapped to *clpP,* which encodes the proteolytic subunit of ClpXP (Table S3, Strain J). This mutation (D187N) was located near the hydrophobic pocket off ClpP that has been proposed to interact with the “IGF loop” of ClpX (Y. I. Kim et al., 2001) and may therefore affect interactions between ClpX and ClpP.

Table 3.3. Sporulation efficiencies of *B. subtilis* strains overproducing CmpA and harboring various alleles of *clpX* and *clpP*. Standard deviation from mean is reported in parentheses (n=3). "++" indicates overproduction.

Strain[a]	CmpA	Suppressor	Sporulation Efficiency
E	WT	-	1
F	++	-	0.006 (0.004)
G	++	*clpX*^{D21Y}	0.39 (0.28)
H	++	*clpX*^{I34M}	0.62 (0.33)
I	++	*clpX*^{E44G}	0.62 (0.31)
J	++	*clpP*^{D187N}	0.35 (0.14)

[a] Strain E: PY79; F: IT504; G: IT525; H: IT367; I: IT342; J: IT531. Genotypes are listed in Table 3.7.

ClpX is required for entry into sporulation ((J. Liu, Cosby, & Zuber, 1999); Table 3.4, strain L), and overproduction of ClpX resulted in only a mild sporulation defect (Table 3.4, strain O). However, co-overproduction of ClpX and CmpA resulted in a 2×10^5-fold defect in sporulation efficiency relative to wild type (Table 3.4, strain P), which was worse than the ~300-fold defect caused by overproduction of CmpA alone (Table 3.4, strain O), indicating that co-overproduction of CmpA and ClpX exhibits a synergistic inhibition of sporulation. To test if the suppression by the N-terminal ClpX mutations were due to a loss-of-function of the N-terminus, we deleted the N-terminus of ClpX and determined whether it was sufficient to suppress the defect caused by CmpA overproduction. Cells overproducing ClpX$^{\Delta 1\text{-}53}$ (the endogenous copy of *clpX* was present in this strain to ensure entry into sporulation) and CmpA sporulated at near wild type levels despite overproduction of CmpA (Table 3.4, strain Q), suggesting that the isolated suppressor mutations likely conferred a loss of function in ClpX's N-terminus. We conclude that the loss of ClpX's ability to bind a substrate is sufficient for cells to overcome the sporulation defect imposed by CmpA overproduction.

Figure 3.3. CmpA-GFP localization is dependent on *spoIVA*. (A-D) Localization of CmpA-GFP in wild type (A; SE364), Δ*spoVM* (B; IT86), Δ*spoIVA* (C; IT114) and Δ*spoVM* Δ*spoIVA* (D; IT113) cells. (E-H) Overlay of DIC and GFP fluorescence from A-D, respectively. See also Table S2.

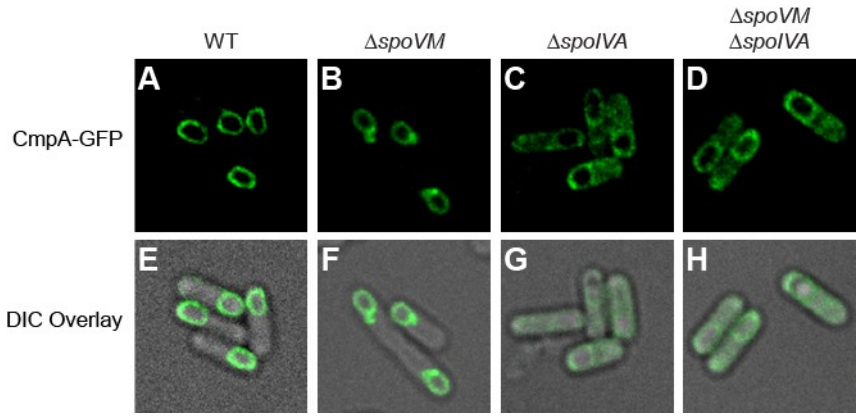

In addition to being the ATPase subunit of ClpXP protease, ClpX may also function alone as a folding chaperone for particular substrates (Schirmer, Glover, Singer, & Lindquist, 1996). The additional ClpP^{D187N} suppressor suggested it was a loss of ClpXP function that suppressed CmpA overproduction, but to specifically test this we constructed a ClpX^{F270W} variant harboring a substitution in the IGF loop that diminishes ClpX interaction with ClpP (Y. I. Kim et al., 2001). Similar to the ClpX$^{\Delta 1-53}$ N-terminal truncation variant, co-overproduction of ClpX^{F270W} with CmpA restored sporulation efficiency to near wild type levels (Table 3.4, strain R), suggesting that abrogating the interaction between ClpX and ClpP corrects the CmpA overproduction defect. Taken together, the genetic data are consistent with a model in which binding and degradation of one or more substrates by ClpXP is responsible for the sporulation defect imposed by CmpA overproduction.

Table 3.4. Sporulation efficiencies of CmpA-overproducing *B. subtilis* strains harboring various alleles of *clpX*.

Strain[a]	*amyE*	*clpX*	*thrC*	IPTG	Sporulation Efficiency
K	-	-	-	-	1
L	-	Δ	-	-	0.006
M	P_{IPTG}-*cmpA*	-	-	+	0.003
N	P_{IPTG}-*cmpA*	Δ	-	+	0.009
O	-	-	P_{IPTG}-*clpX*	+	0.25
P	P_{IPTG}-*cmpA*	-	P_{IPTG}-*clpX*	+	4.8×10^{-5}
Q	P_{IPTG}-*cmpA*	-	P_{IPTG}-*clpX*$^{\Delta 1-53}$	+	0.68
R	P_{IPTG}-*cmpA*	-	P_{IPTG}-*clpX*^{F270W}	+	0.38

[a] Strain K: PY79; L: IT482; M: SE191; N: IT483; O: IT479; P: IT545; Q: IT571 R: IT616. Genotypes are listed in Table 3.7.

CmpA is a ClpXP adaptor for binding SpoIVA

Since CmpA overproduction inhibited cortex maturation and ClpX acted synergistically with CmpA to inhibit sporulation (Table 3.4, Strain P), we hypothesized that CmpA may be an adaptor protein that delivers a protein required for cortex maturation to ClpXP for degradation. To isolate a non-functional CmpA variant for use as a negative control to test this hypothesis, we first performed alanine scanning mutagenesis of the 37 codon *cmpA* open reading frame. We then characterized the resulting mutants by monitoring the localization of each variant fused to GFP (Fig. 3.4) and assessed each variant's function by measuring their ability to suppress the *spoVM*^{I15A} sporulation defect (Table 3.5). In the presence of *cmpA*^{P2A}, cells harboring *spoVM*^{I15A} sporulated at near wild type levels (Table 3.5, strain IT139), similar to cells harboring a deletion of *cmpA*, suggesting that substitution of Pro2 with Ala completely abolished CmpA function. Nonetheless, CmpA^{P2A}-GFP localized to the surface of the forespore (Fig. 3.4), indicating that its localization was not impaired.

To test if CmpA and ClpX interact we produced a ClpX construct harboring a C-terminal His_6 tag. To promote stabilization of the hexameric form of ClpX that would bind adaptors and substrates, but would be unable to degrade bound substrates, we introduced a substitution (E182A) in ClpX's Walker B motif that disrupts ATP hydrolysis, but not ATP binding (T. A. Baker & Sauer, 2012). We then overproduced ClpX^{E182A}-His_6 (hereafter, simply ClpX-His_6) from a chromosomal locus in *B. subtilis* cells that also produced low levels of wild type ClpX to enable entry into sporulation. We then purified ClpX-His_6 from either vegetative or sporulating cells that also produced CmpA-GFP or CmpA^{P2A}-GFP (Fig. 3.5). In vegetative cells, in the absence of other sporulation factors, CmpA-GFP, but not CmpA^{P2A}-GFP, co-purified with ClpX-His_6 (Fig. 3.5A), suggesting that the loss-of-function of CmpA^{P2A} *in vivo* is due to its inability to interact with ClpX. To test if the I34M substitution in ClpX, which the genetic analysis suggested caused some loss in ClpX function, affected CmpA binding, we purified ClpX^{I134M}-His_6 (also harboring a Walker B disruption) from vegetative cells that produced CmpA-GFP. Whereas ClpX-His_6 co-

Table 3.5. Mean sporulation efficiencies of strains harboring *VM*^{I15A} and various alleles of *cmpA* (measured by heat resistance). *amyE* and *thrC* are ectopic loci that alleles of *spoVM* and *cmpA* were complemented at. Standard deviation from mean (n≥3) is reported in parentheses. Genotypes are listed in Table S7.

Strain	*spoVM*	*cmpA*	*amyE*	*thrC*	Sporulation Efficiency (relative to PY79)
PY79	WT	WT	--	--	1
KR322	Δ	WT	*spoVM*^{I15A}	--	1.2×10^{-6}
SE181	Δ	Δ	*spoVM*^{I15A}	--	.15
IT139	Δ	Δ	*spoVM*^{I15A}	*cmpA*^{P2A}	.18 (.071)
CW13	Δ	Δ	*spoVM*^{I15A}	*cmpA*^{N3A}	3.9×10^{-3} (3.4×10^{-3})
IT141	Δ	Δ	*spoVM*^{I15A}	*cmpA*^{W4A}	.24 (.13)
IT165	Δ	Δ	*spoVM*^{I15A}	*cmpA*^{L5A}	.12 (.050)
CW16	Δ	Δ	*spoVM*^{I15A}	*cmpA*^{K6A}	8.9×10^{-4} (9.6×10^{-4})
CW31	Δ	Δ	*spoVM*^{I15A}	*cmpA*^{K7A}	5.7×10^{-3} (2.3×10^{-3})
CW139	Δ	Δ	*spoVM*^{I15A}	*cmpA*^{Q8A}	.019 (.011)
CW28	Δ	Δ	*spoVM*^{I15A}	*cmpA*^{M9A}	.12 (.071)
CW34	Δ	Δ	*spoVM*^{I15A}	*cmpA*^{Q10A}	.13 (.090)
CW37	Δ	Δ	*spoVM*^{I15A}	*cmpA*^{K11A}	.027 (.023)
CW53	Δ	Δ	*spoVM*^{I15A}	*cmpA*^{F13A}	.33 (.16)
CW56	Δ	Δ	*spoVM*^{I15A}	*cmpA*^{L14A}	2.7×10^{-4} (1.0×10^{-4})
CW163	Δ	Δ	*spoVM*^{I15A}	*cmpA*^{E15A}	3.7×10^{-4} (7.8×10^{-5})
CW125	Δ	Δ	*spoVM*^{I15A}	*cmpA*^{K16A}	.038 (.019)
CW103	Δ	Δ	*spoVM*^{I15A}	*cmpA*^{D17A}	.08 (.07)
CW166.1	Δ	Δ	*spoVM*^{I15A}	*cmpA*^{N18A}	1.7×10^{-6} (1.4×10^{-6})
CW131	Δ	Δ	*spoVM*^{I15A}	*cmpA*^{Y19A}	5.7×10^{-6} (2.3×10^{-6})
CW142	Δ	Δ	*spoVM*^{I15A}	*cmpA*^{Q20A}	6.1×10^{-3} (7.7×10^{-3})
IT166	Δ	Δ	*spoVM*^{I15A}	*cmpA*^{I21A}	.11 (.18)

IT179	Δ	Δ	*spoVM*^{I15A}	*cmpA*^{K22A}	.018 (.031)
IT168	Δ	Δ	*spoVM*^{I15A}	*cmpA*^{L23A}	.045 (.75)
IT147	Δ	Δ	*spoVM*^{I15A}	*cmpA*^{L24A}	.16 (.13)
IT169	Δ	Δ	*spoVM*^{I15A}	*cmpA*^{N25A}	.049 (.036)
CW128	Δ	Δ	*spoVM*^{I15A}	*cmpA*^{Q26A}	2.2×10^{-4} (3.1×10^{-4})
CW169.1	Δ	Δ	*spoVM*^{I15A}	*cmpA*^{C27A}	8.4×10^{-6} (3.1×10^{-6})
CW172	Δ	Δ	*spoVM*^{I15A}	*cmpA*^{W28A}	.093 (.049)
CW79	Δ	Δ	*spoVM*^{I15A}	*cmpA*^{Y29A}	1.6×10^{-3} (1.4×10^{-3})
CW82	Δ	Δ	*spoVM*^{I15A}	*cmpA*^{F30A}	5.9×10^{-6} (5.5×10^{-6})
CW107	Δ	Δ	*spoVM*^{I15A}	*cmpA*^{Y31A}	.09 (.01)
CW145	Δ	Δ	*spoVM*^{I15A}	*cmpA*^{R32A}	3.7×10^{-3} (1.6×10^{-3})
CW148	Δ	Δ	*spoVM*^{I15A}	*cmpA*^{K33A}	4.6×10^{-3} (1.7×10^{-3})
CW151	Δ	Δ	*spoVM*^{I15A}	*cmpA*^{K34A}	.031 (.015)
CW175	Δ	Δ	*spoVM*^{I15A}	*cmpA*^{H35A}	1.8×10^{-3} (6.8×10^{-4})
CW182	Δ	Δ	*spoVM*^{I15A}	*cmpA*^{C36A}	2.3×10^{-4} (1.4×10^{-4})
CW185	Δ	Δ	*spoVM*^{I15A}	*cmpA*^{S37A}	1.5×10^{-3} (7.2×10^{-4})

Figure 3.4. Localization and persistence of CmpA-GFP mutants.

(A, C, E, G) Localization of CmpA-GFP or indicated CmpA-GFP variants 3.5 h after induction of sporulation. Top row: GFP fluorescence; bottom row: overlay, GFP and DIC.(B, D, F, H) Localization of CmpA-GFP or indicated CmpA-GFP variants after induction of sporulation. Top row: GFP fluorescence; middle row: DIC; bottom row: overlay, GFP and DIC.

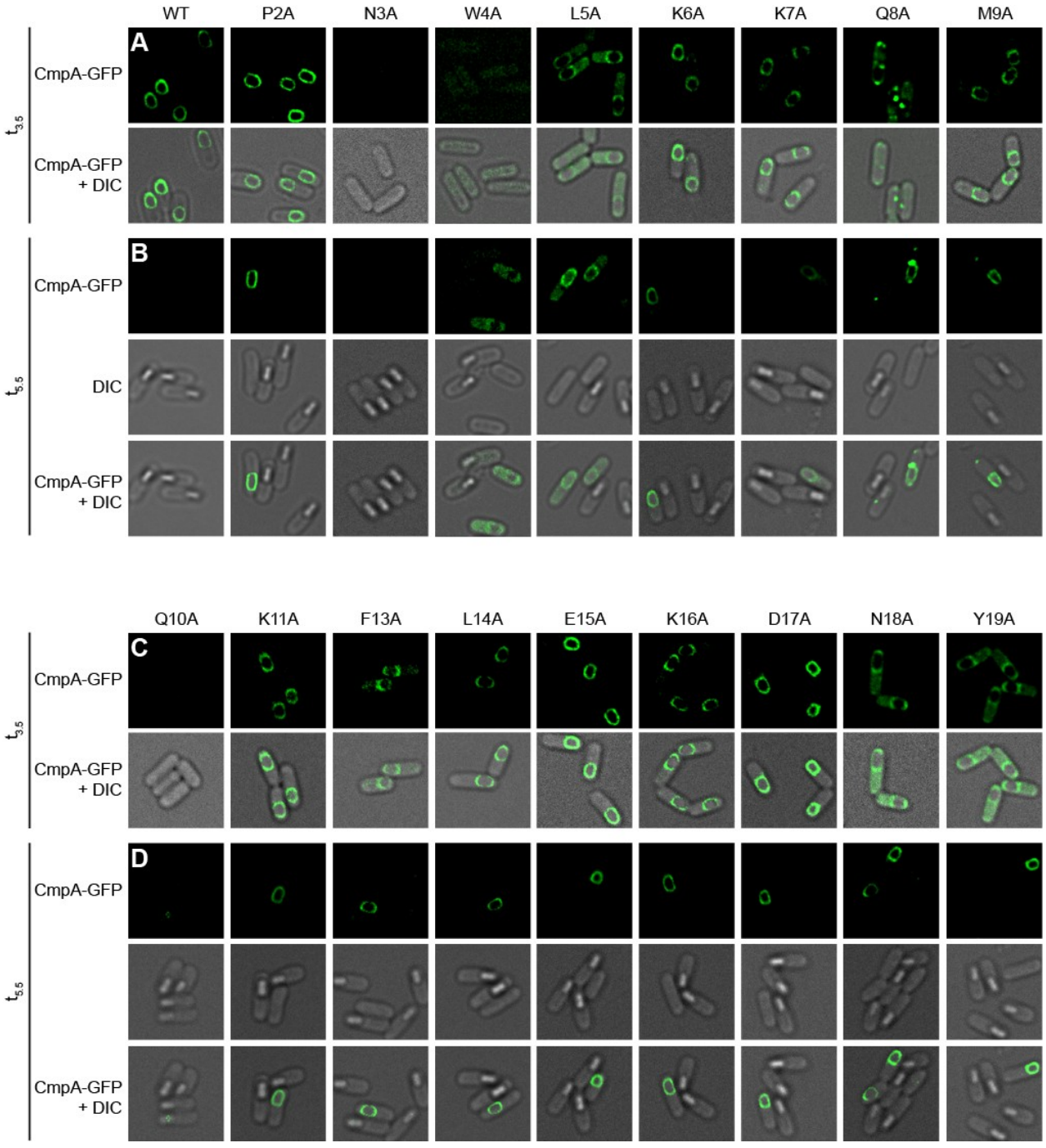
WT
P2A
N3A
W4A
L5A
K6A
K7A
Q8A
M9A
A
B
CmpA-GFP
CmpA-GFP + DIC
DIC
$t_{3.5}$
Q10A
K11A
F13A
L14A
E15A
K16A
D17A
N18A
Y19A
C
D

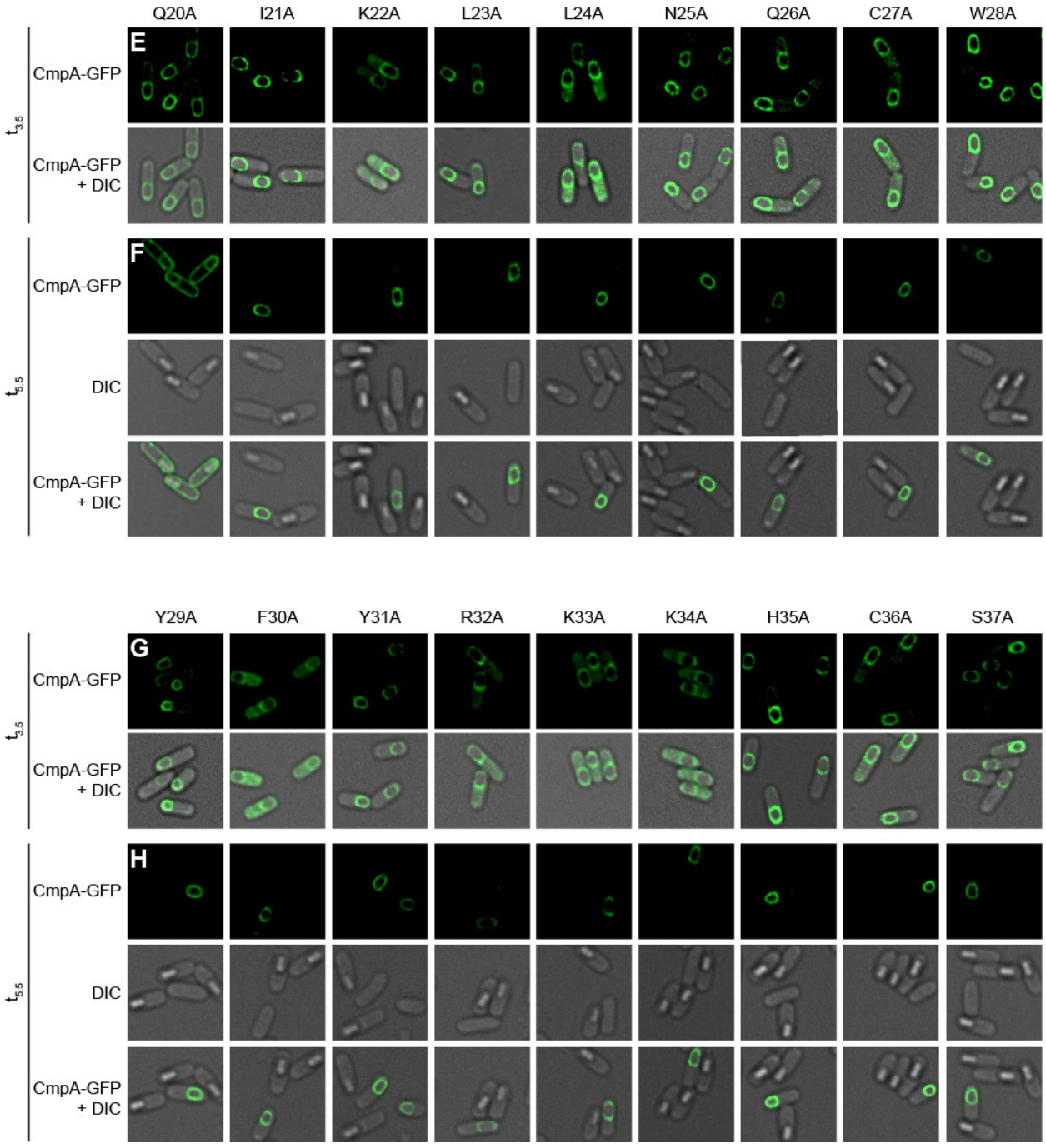
Q20A
I21A
K22A
L23A
L24A
N25A
Q26A
C27A
W28A
E
CmpA-GFP
CmpA-GFP + DIC
t3.5
F
CmpA-GFP
DIC
CmpA-GFP + DIC
t5.5
Y29A
F30A
Y31A
R32A
K33A
K34A
H35A
C36A
S37A
G
CmpA-GFP
CmpA-GFP + DIC
t3.5
H
CmpA-GFP
DIC
CmpA-GFP + DIC
t5.5

Figure 3.5. ClpX, CmpA and SpoIVA form a complex. (A-B) Extracts of vegetative *B. subtilis* producing CmpA-GFP and ClpX-His_6 (A; IT735) or $ClpX^{I34M}$-His_6 (B; T751) were applied to a Ni^{2+}-agarose affinity column and eluted. The presence of ClpX and CmpA-GFP in the total (T), unbound (UB), wash (W), or eluate (E) fractions was monitored by immunoblotting. (C-F) Extracts of sporulating *B. subtilis* producing $CmpA^{P2A}$-GFP and ClpX-His_6 (C; IT760); $ClpX^{I34M}$-His_6 and CmpA-GFP (D; IT751); ClpX-His_6, CmpA-GFP, and $SpoIVA^{L424F}$ (E; IT818); or CmpA-GFP-His_6 (F; IT784) were applied to a Ni^{2+}-agarose affinity chromatography and eluted. The presence of ClpX, CmpA-GFP, and SpoIVA were monitored in each fraction by immunoblotting. (G) Schematic summarizing the interactions between variants of ClpX, CmpA, and SpoIVA (ClpX, pink; ClpP, orange; CmpA, purple; SpoIVA, green).

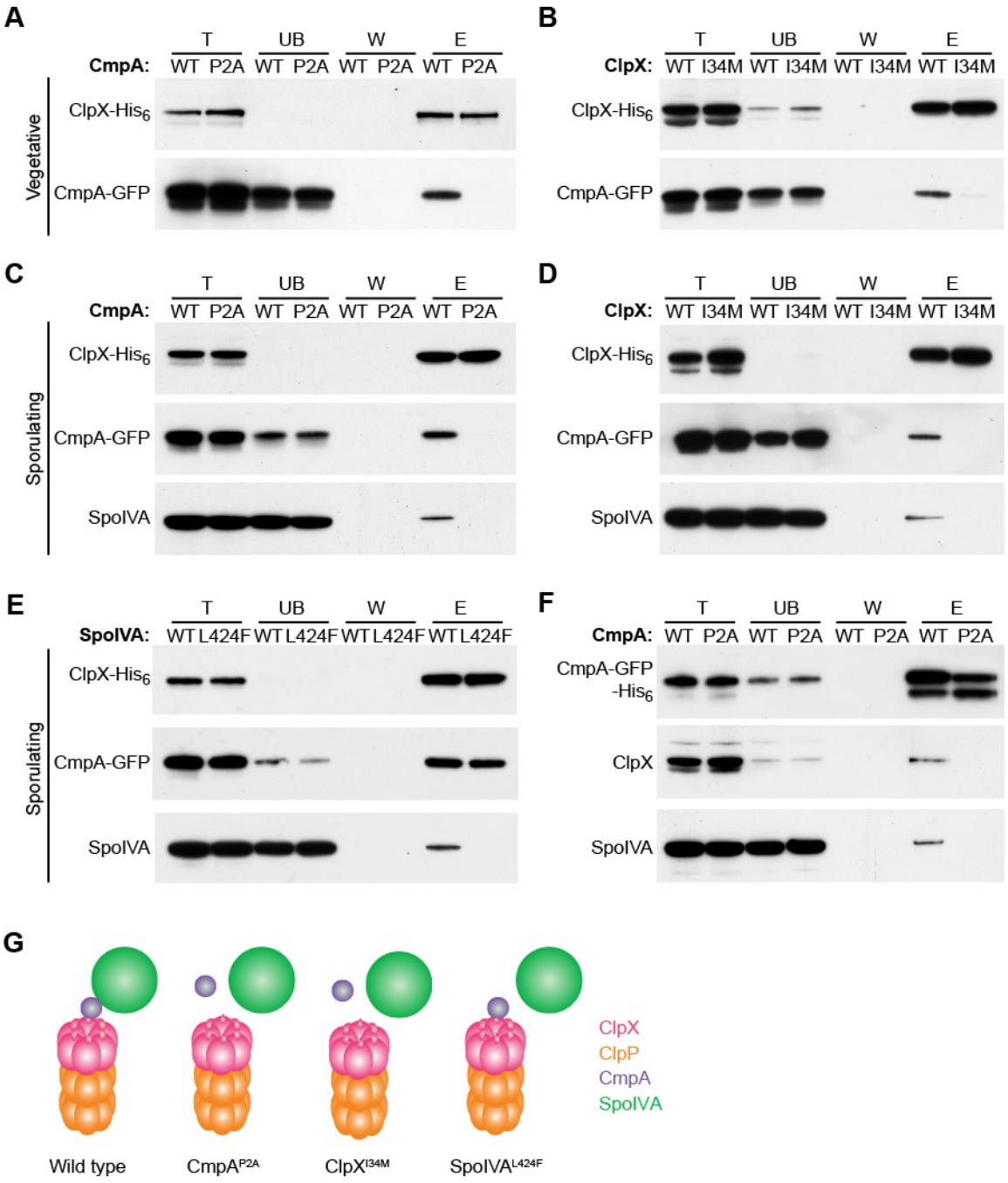
A
T UB W E
CmpA: WT P2A WT P2A WT P2A WT P2A
Vegetative
ClpX-His6
CmpA-GFP
B
T UB W E
ClpX: WT I34M WT I34M WT I34M WT I34M
ClpX-His6
CmpA-GFP
C
T UB W E
CmpA: WT P2A WT P2A WT P2A WT P2A
Sporulating
ClpX-His6
CmpA-GFP
SpoIVA
D
T UB W E
ClpX: WT I34M WT I34M WT I34M WT I34M
ClpX-His6
CmpA-GFP
SpoIVA
E
T UB W E
SpoIVA: WT L424F WT L424F WT L424F WT L424F
Sporulating
ClpX-His6
CmpA-GFP
SpoIVA
F
T UB W E
CmpA: WT P2A WT P2A WT P2A WT P2A
CmpA-GFP -His6
ClpX
SpoIVA
G
ClpX
ClpP
CmpA
SpoIVA
Wild type
CmpAP2A
ClpXI34M
SpoIVAL424F

purified with CmpA-GFP, the amount of CmpA-GFP that co-purified with ClpX^{I34M}-His$_6$ was diminished (Fig. 3.5B). Together, the data indicated that ClpX and CmpA interact, and that disruption of Pro2 of CmpA or Ile34 of ClpX results in a loss of function *in vivo* and *in vitro*.

Since our genetic analysis identified mutations in *spoIVA* (E423G and L424F; Table 3.2) that suppressed the *spoVM^{I15A}* defect and CmpA-GFP localization was dependent on SpoIVA (Fig. 3.3), we wondered if SpoIVA would bind to ClpX and CmpA. In sporulating cells, SpoIVA co-purified with ClpX-His$_6$, along with CmpA-GFP (Fig. 3.5C). However, in the presence of CmpA^{P2A}-GFP, SpoIVA was not detected in the eluate (Fig. 3.5C), suggesting that SpoIVA binding to ClpX requires CmpA. Additionally, in sporulating cells, while SpoIVA co-purified with ClpX-His$_6$, SpoIVA did not co-purify with ClpX^{I134M}-His$_6$ even in the presence of wild type CmpA-GFP (Fig. 3.5D). Further, whereas wild type SpoIVA co-purified with ClpX-His$_6$ and CmpA-GFP, the suppressor variant SpoIVA^{L424F} did not (Fig. 3.5E). Consistent with the results from the co-purification performed in vegetative cells (Fig. 3.5A), CmpA-GFP continued to co-purify with ClpX-His$_6$ even in the presence of SpoIVA^{L424F}, suggesting that SpoIVA is not required for CmpA interaction with ClpX. Finally, to test if all three proteins exist in a single complex, we repeated the co-purification experiment, but this time placed the affinity tag on CmpA-GFP. In sporulating cells producing low levels of wild type ClpX (to allow entry into sporulation) and overproducing ClpX^{E182A}, purification of CmpA-GFP-His$_6$, but not CmpA^{P2A}-GFP-His$_6$, led to the co-purification of ClpX and SpoIVA (Fig. 3.5F). Taken together, we conclude that ClpX, CmpA, and SpoIVA exist in complex with one another, SpoIVA is not required for ClpX-CmpA complex formation, and disruption of Pro2 in CmpA, the N-terminal substrate binding domain of ClpX or Leu424 in SpoIVA abolishes formation of the ternary complex (Fig. 3.5G). The data thus far are consistent with a model in which CmpA delivers SpoIVA to ClpXP for degradation.

Spore envelope morphogenetic defects cause CmpA-driven SpoIVA degradation

To test if SpoIVA is a substrate for degradation by ClpXP, we first examined the steady state levels of SpoIVA by immunoblotting cell extracts harvested from cells containing the *spoVM*^{I15A} mutation that activates the CmpA pathway. SpoIVA was detectable in wild type cells at $t_{3.5}$ of sporulation, and similar levels of SpoIVA were maintained through $t_{5.5}$ (Fig. 3.6A-B). However, in the presence of *spoVM*^{I15A}, SpoIVA levels rapidly diminished by $t_{5.5}$, but SpoIVA levels were restored to near wild type levels upon *cmpA* deletion, even in the presence of *spoVM*^{I15A} (Fig. 3.6A-B). To test if the decrease in SpoIVA levels was due to degradation and not a difference in SpoIVA production, we inhibited translation by addition of spectinomycin and measured SpoIVA levels at different time points. Whereas wild type strains maintained steady levels of synthesized SpoIVA even 2 h after inhibition of translation, in strains expressing *spoVM*^{I15A} SpoIVA was rapidly depleted and almost undetectable after 2 h (Fig. 3.6C-D). Deletion of *cmpA*, though, prevented degradation of SpoIVA in cells expressing *spoVM*^{I15A}, suggesting that in cells harboring mutations causing spore envelope defects, such as *spoVM*^{I15A}, SpoIVA is degraded in a CmpA-dependent manner.

To determine if SpoIVA is degraded in a particular subpopulation of sporulating cells, we examined the localization and stability of GFP-SpoIVA in cells expressing *spoVM*^{I15A} using fluorescence microscopy (Fig. 3.7A-K). At $t_{3.5}$ of sporulation, localization and levels of GFP-SpoIVA were similar in otherwise wild type and *spoVM*^{I15A} cells (Fig. 3.7A-B). At $t_{5.5}$, when most sporangia had elaborated a phase-bright forespore, wild type cells maintained similar amounts of GFP-SpoIVA (Fig. 3.7F, 5K). However, in the presence of *spoVM*^{I15A}, sporangia that had elaborated a phase-bright forespore were largely devoid of GFP-SpoIVA signal (Fig. 3.7G, 3.7K). When *cmpA* was deleted, though, GFP-SpoIVA levels returned to near wild type levels despite the presence of *spoVM*^{I15A} (Fig. 3.7H, 3.7K), consistent with the observation that SpoIVA degradation was prevented by deletion of *cmpA* (Fig. 3.6C-D). We then reasoned that

Figure 3.6. SpoIVA is degraded in a *cmpA* dependent manner in the *spoVM*^{I15A} mutant. (A) Cell extracts were prepared from sporulating cells of Δ*spoIVA* (KP73), or strains harboring wild type *spoVM* (KR103), *spoVM*^{I15A} (KR322), or *spoVM*^{I15} Δ*cmpA* (SE181) at times (h) indicated after induction of sporulation. SpoIVA and, as a control, σ^A were detected by immunoblotting. (B) Quantification of SpoIVA band intensities of each strain in (A) relative to σ^A levels at each time point and represented as a fraction compared to the level at $t_{3.5}$ (●, *spoVM*^{WT}; ■, *spoVM*^{I15A}; ▲, *spoVM*^{I15} Δ*cmpA*). (C) Strains KR103, KR322, and SE181 were induced to sporulated. At $t_{4.5}$, spectinomycin (200 μg ml^{-1}) was added to inhibit translation and cell extracts were prepared from aliquots taken at the times (min) indicated. SpoIVA and σ^A were detected by immunoblotting. (D) Quantification of SpoIVA band intensities in (C) relative to σ^A levels at each time point and represented as a fraction compared to the level at t_0 after addition of spectinomycin (●, *spoVM*^{WT}; ■, *spoVM*^{I15A}; ▲, *spoVM*^{I15} Δ*cmpA*). All symbols represent mean values obtained from three independent measurements; error bars represent standard error of the mean.

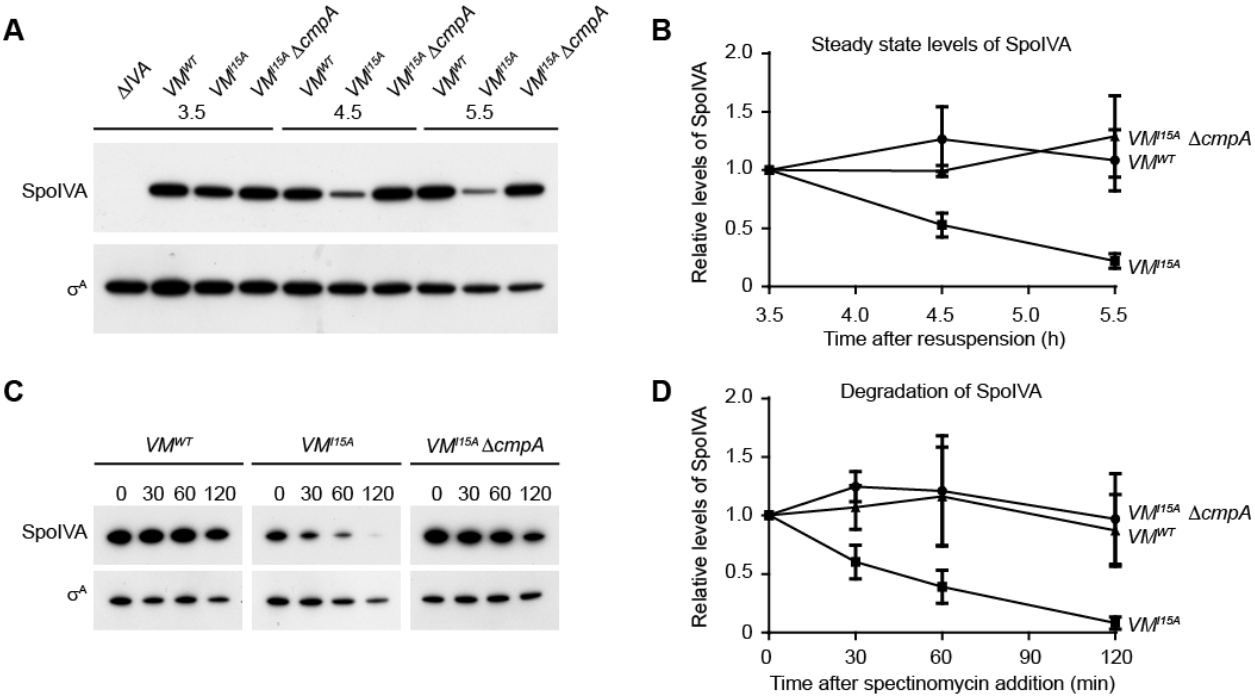

disruption of the CmpA-ClpX-SpoIVA complex through the use of the loss-of-function *clpX* point mutants should also restore SpoIVA stability at $t_{5.5}$ and found that this was indeed the case (Fig. 3.7I-K).

We also examined the persistence of GFP-SpoIVA^{L424F} (Fig. 3.7L-R), with the expectation that this variant would display an increased resistance to degradation since it did not bind to ClpX (Fig. 3.5E). In wild type cells GFP-SpoIVA^{L424F} behaved similarly to GFP-SpoIVA in its localization to the forespore and persistence in phase bright forespores (Fig. 3.7L, 5R). Interestingly, in the presence of the *spoVM*^{I15A} mutant and an additional copy of wild type *spoIVA* at the native locus, GFP-SpoIVA^{L424F} was degraded (Fig. 3.7P, 3.7R), but when the native locus harbored *spoIVA*^{L424F} instead, GFP-SpoIVA^{L424F} was largely resistant to degradation (Fig. 3.7Q, 3.7R). The recessive nature of the *spoIVA*^{L424F} allele may be explained by the ability of SpoIVA to polymerize (Ramamurthi & Losick, 2008), whereby wild type molecules of SpoIVA that are degraded in the presence of *spoVM*^{I15A} in a CmpA-dependent manner recruit interacting SpoIVA^{L424F} molecules to ClpX that would not otherwise bind to CmpA and be subject to degradation. We conclude that SpoIVA is degraded in a CmpA-dependent manner in cells harboring a mutation (*spoVM*^{I15A}) that causes improper spore envelope assembly.

Additional factors under σ^K control are required for degradation of SpoIVA and CmpA

Our observation that degradation of GFP-SpoIVA only occurred in cells that had reached the phase bright forespore state led us to wonder whether some factor was preventing degradation at an earlier time point or if an additional factor (beyond CmpA and ClpXP) was required for SpoIVA degradation at a later time point. We therefore first determined if overproduction of CmpA, ClpX or both at an earlier time point was sufficient for degradation of SpoIVA. We overproduced CmpA and ClpX at t_3 of sporulation, added spectinomycin after 15 min to prevent further translation, and monitored SpoIVA levels over the next 2 h. In all instances we saw no significant degradation of SpoIVA (Fig. 3.8) indicating that ClpX and CmpA

Figure 3.7. CmpA-dependent degradation of GFP-SpoIVA in sporangia harboring *spoVM*^{I15A} that elaborate phase bright forespores. (A-J) GFP-SpoIVA in cells harboring *spoVM*^{WT} (A and F, KR165) *spoVM*^{I15A} (B and G, KRC77), *spoVM*^{I15A} Δ*cmpA* (C and H, IT839), *spoVM*^{I15A} *clpX*^{I34M} (D and I, IT884) or *spoVM*^{I15A} *clpX*^{E44G} (E and J, IT883) at $t_{3.5}$ (A-E) and $t_{5.5}$ (F-J) after induction of sporulation. (K) Quantification of GFP-SpoIVA fluorescence in strains shown in (A-J). (L-Q) GFP-SpoIVA^{L424F} in cells harboring *spoVM*^{WT} *spoIVA*^{L424F} (L and O, IT869), *spoVM*^{I15A} *spoIVA*^{WT} (M and P, IT852) or *spoVM*^{I15A} *spoIVA*^{L424F} (N and Q, IT852) at $t_{3.5}$ (L-N) and $t_{5.5}$ (O-Q) after induction of sporulation. (R) Quantification of GFP-SpoIVA^{L424F} fluorescence in strains shown in (L-Q). All bars represent mean values of >80 phase bright forespores; error bars represent standard deviation. Arrows indicate a phase bright forespore. See also Figure S3.

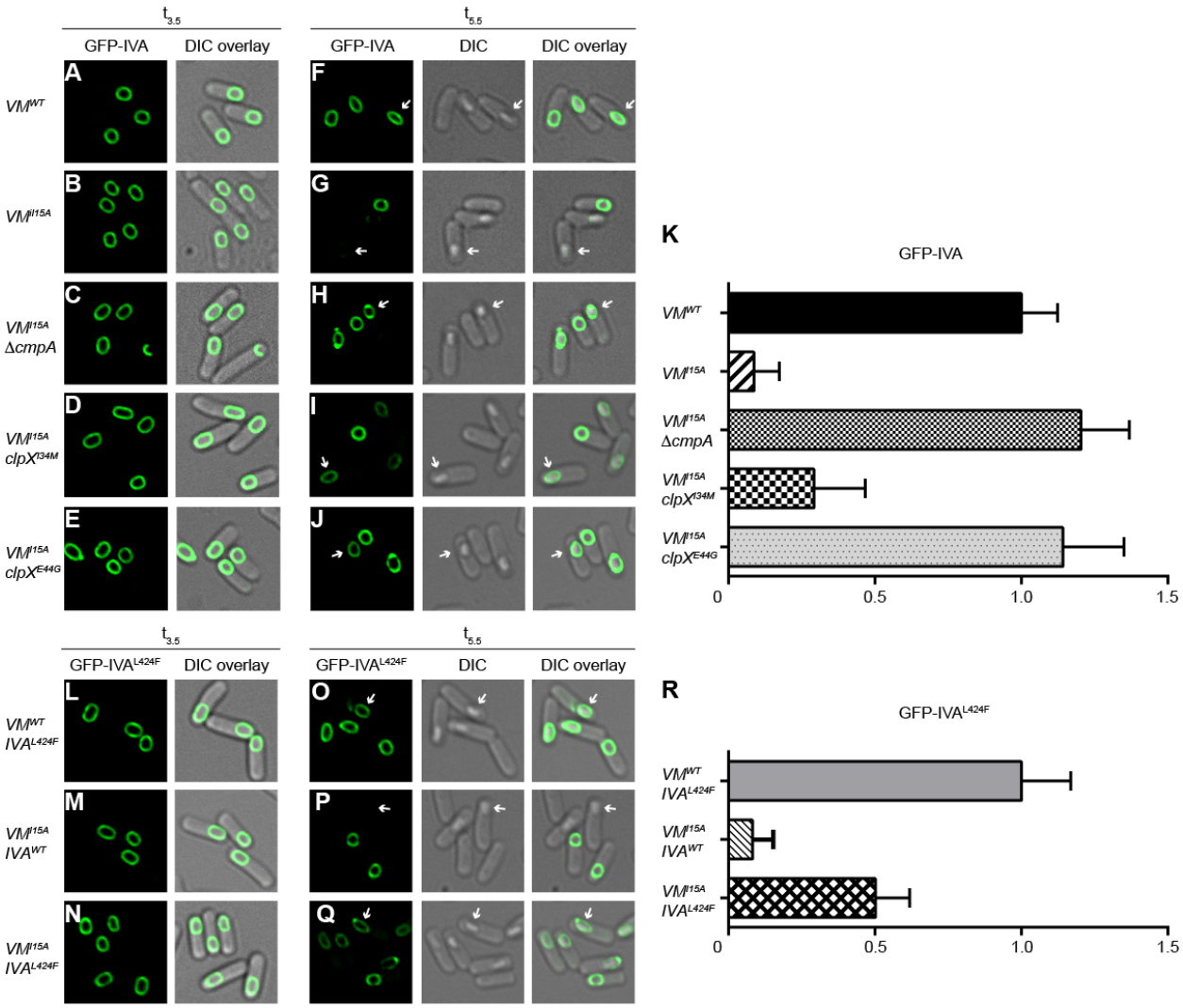
t3.5
GFP-IVA
DIC overlay
t5.5
GFP-IVA
DIC
DIC overlay
VMWT
VMI15A
VMI15A ΔcmpA
VMI15A clpXI34M
VMI15A clpXE44G
A
B
C
D
E
F
G
H
I
J
K
GFP-IVA
VMWT
VMI15A
VMI15A ΔcmpA
VMI15A clpXI34M
VMI15A clpXE44G
0
0.5
1.0
1.5
t3.5
GFP-IVAL424F
DIC overlay
t5.5
GFP-IVAL424F
DIC
DIC overlay
VMWT IVAL424F
VMI15A IVAWT
VMI15A IVAL424F
L
M
N
O
P
Q
R
GFP-IVAL424F
VMWT IVAL424F
VMI15A IVAWT
VMI15A IVAL424F
0
0.5
1.0
1.5

Figure 3.8. Overexpression of *cmpA*, *clpX* or both together are not sufficient to induce degradation of SpoIVA at an early time point (3.5 h after induction of sporulation).

Immunoblot of cell lysate harvested from wild type (PY79), *cmpA* overexpressing (cmpA++; SE191), *clpX* overexpressing (clpX++; IT479) or *cmpA* and *clpX* overexpressing cells (cmpA++ clpX++; IT481). Overexpression was induced at t_3 of sporulation by addition of 1 mM IPTG. Spectinomycin (200ug ml^{-1}) was added at $t_{3.5}$ to arrest translation and cells were harvested at 0, 15, 45 and 75 minutes after addition of spectinomycin.

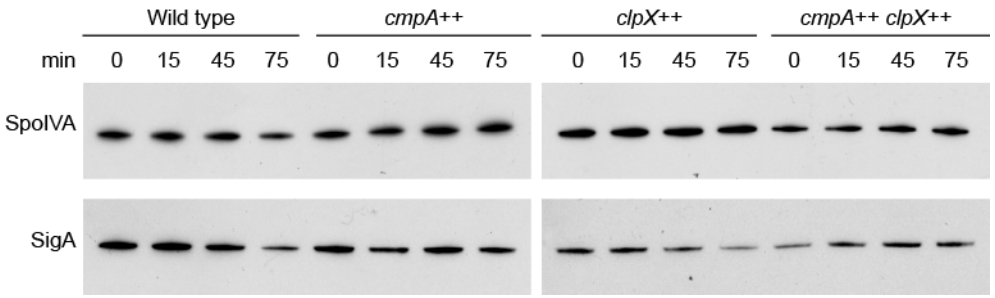

were not sufficient for SpoIVA degradation and that there are likely other factor(s) required for degradation. Since the appearance of phase bright spores is coincident with activation of the late-acting mother cell-specific sigma factor, σ^K, we wondered whether the additional factor(s) were under the control of σ^K and if so, we would expect GFP-SpoIVA degradation to be inhibited by preventing σ^K activation. Thus, we monitored GFP-SpoIVA levels in sporulating cells harboring a deletion in the *spoIVCA* gene, the DNA recombinase required for creating an intact *sigK* gene and producing functional σ^K (Kunkel, Losick, & Stragier, 1990). At an early time point, the absence of σ^K had no effect on GFP-SpoIVA stability and localization in otherwise wild type cells or in cells harboring *spoVM*^{I15A} (Fig. 3.9A, B). However, at a later time point, the absence of σ^K prevented the degradation of GFP-SpoIVA in phase-bright forespores of the *spoVM*^{I15A} mutant (Fig. 3.9D) suggesting that at least one additional factor produced by σ^K is required for CmpA/ClpXP-mediated degradation of SpoIVA.

Since CmpA-GFP is also degraded specifically in wild type cells elaborating phase bright forespores (Ebmeier et al., 2012) we tested if the stability of CmpA-GFP was affected by the absence of σ^K in both wild type and *spoVM*^{I15A} cells. We induced *cmpA-gfp* expression at t_3 of sporulation, and 30 min later we observed that CmpA-GFP localized to the forespore in all the tested strains (Fig. 3.9E-H), similar to wild type cells. At $t_{5.5}$, CmpA-GFP was no longer detectable in otherwise wild type cells that had elaborated a phase-bright forespore (Fig. 3.9I), but persisted in the *spoVM*^{I15A} mutant (Fig. 3.9J), as reported previously (Ebmeier et al., 2012). Surprisingly, in the absence of σ^K, CmpA-GFP not only persisted in cells harboring *spoVM*^{I15A} (Fig. 3.9L), but also persisted in otherwise wild type cells that had elaborated phase bright forespores (Fig. 3.9K), indicating that degradation of CmpA also requires a factor under the control of σ^K. Interestingly, the fluorescence intensity of CmpA-GFP in *spoVM*^{I15A} cells harboring phase bright forespores was more intense than those not harboring phase bright forespores (Fig. 3.9L), and we also observed the slightly promiscuous mis-localization of CmpA-GFP in the absence of σ^K (Fig. 3.9K, L). It is unclear if this mis-localization of CmpA-GFP is the result of

Figure 3.9. Additional factor(s) under σ^K control are required for SpoIVA and CmpA-GFP degradation. (A-D) GFP-SpoIVA in cells harboring *spoVM*^{WT} $\Delta\sigma^K$ (A and C, IT891) or *spoVM*^{I15A} $\Delta\sigma^K$ (B and D, IT892) at $t_{3.5}$ (A-B) or $t_{5.5}$ (C-D) after induction of sporulation. (E-L) CmpA-GFP in cells harboring *spoVM*^{WT}(E and I, IT897), *spoVM*^{I15A} (F and J, IT896), *spoVM*^{WT} $\Delta\sigma^K$ (G and K, IT904) or *spoVM*^{I15A} $\Delta\sigma^K$ (H and L, IT903) at $t_{3.5}$ (E-H) or $t_{5.5}$ (I-L) after induction of sporulation. Arrows indicate a phase bright forespore.

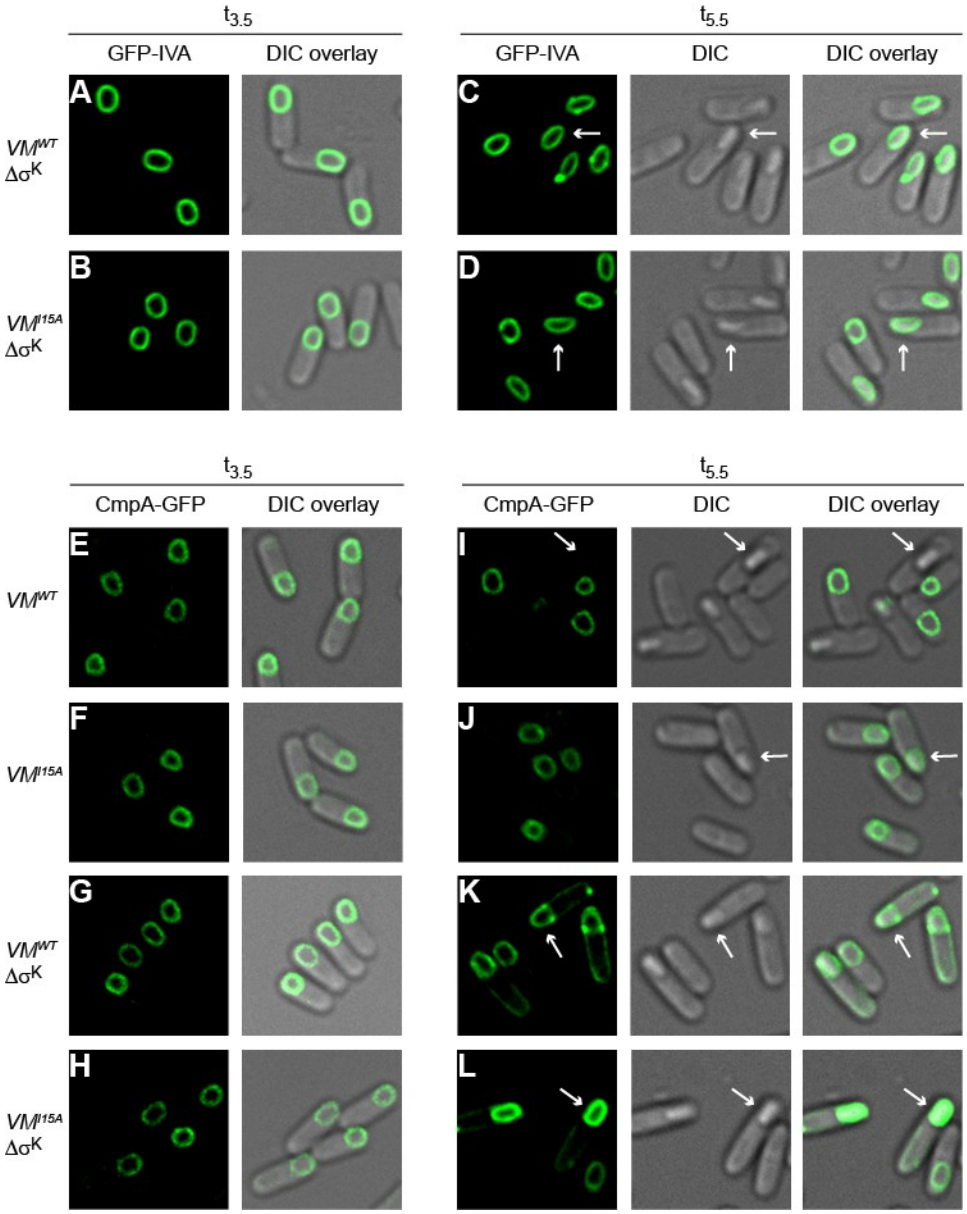

increased CmpA-GFP levels saturating the forespore membrane forcing the overflow of CmpA-GFP to localize to an alternative membrane, or if a σ^K-produced factor is required for persistent localization of CmpA at the forespore. In any case, the data suggest that σ^K controls two parts of the pathway. First, in wild type cells that have successfully initiated spore envelope assembly, σ^K is required for the degradation of CmpA so that the sporulation program may proceed. Second, in cells that are unable to successfully initiate spore envelope assembly, at least one additional factor produced under control of σ^K is required for CmpA/ClpXP-mediated degradation of SpoIVA.

CmpA is part of a quality control mechanism that maintains the integrity of a sporulating population

The degradation of SpoIVA in cells unable to initiate proper spore envelope assembly (in the presence of *spoVM*^{I15A}), followed by the ultimate lysis of those cells, led us to wonder if CmpA participates in a quality control mechanism that selectively removes cells harboring incorrectly assembled spore envelopes from the population. To test this, we examined if deletion of *cmpA* would permit cells harboring other spore envelope initiation defects to proceed past this checkpoint. To this end, we first investigated the effect of *cmpA* deletion on a *spoVM*^{K2A} mutant that behaves similarly to the *spoVM*^{I15A} mutant in that it localizes properly (Fig. 3.10), but produces heat-sensitive spores. Cells harboring *spoVM*^{K2A} produced ~100-fold fewer heat resistant spores and ~150-fold fewer lysozyme resistant spores relative to wild type cells (Table 3.6, Strain T). Removal of the quality control mechanism by deletion of *cmpA* in cells harboring *spoVM*^{K2A} allowed the production of more heat and lysozyme resistant spores (Table 3.6, Strain U), indicating that the sporulation program continued despite the block normally Imposed by *spoVM*^{K2A}, but resulted in a less robust production of spores compared to wild type.

Figure 3.10. SpoVM^{K2A}-GFP localizes to the forespore.

(A-C) Localization of SpoVM-GFP (A; CVO1195), SpoVM^{K2A}-GFP (B; KRC1) and SpoVM^{P9A}-GFP (C; CVO1395). (D-F) Overlay of GFP and membrane stain in (A-C), respectively.

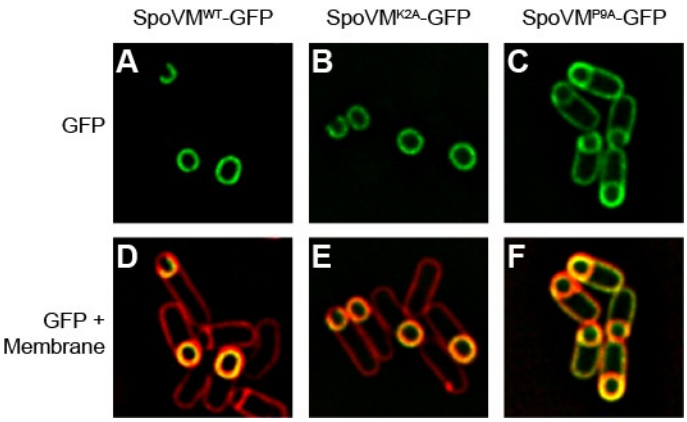

Table 3.6. Sporulation efficiencies of *spoVM* and *spoIVA* mutants with and without deletion of *cmpA.* Standard deviation from mean is reported in parentheses (n=3).

Strain[a]	Mutation	*cmpA*	Sporulation Efficiency	
			Heat Resistance	Lysozyme Resistance
S	WT	-	1	1
T	*spoVM*^{K2A}		0.01 (0.007)	0.007 (0.003)
U	*spoVM*^{K2A}	Δ	0.25 (0.05)	0.47 (0.03)
V	*spoVM*^{I15A}		5×10^{-6} (1.7×10^{-6})	1.8×10^{-6} (1.1×10^{-6})
W	*spoVM*^{I15A}	Δ	0.16 (0.09)	0.05 (0.01)
X	*spoIVA*^{K30A}		3.8×10^{-4} (1.7×10^{-4})	3×10^{-4} (3.2×10^{-4})
Y	*spoIVA*^{K30A}	Δ	0.08 (0.01)	0.03 (0.02)
Z	*spoIVA*$^{T70A-T71A}$		5.8×10^{-6} (3×10^{-6})	2×10^{-6} (1×10^{-6})
AA	*spoIVA*$^{T70A-T71A}$	Δ	0.02 (0.01)	0.002 (7×10^{-4})
BB	Δ*spoIVA*		$<10^{-8}$	$<10^{-8}$
CC	Δ*spoIVA*	Δ	$<10^{-8}$	ND

[a] Strain S: PY79; T: KRC102; U:IT102; V: KR322; W:SE181; X:KR367; Y:IT880; Z: JPC221; AA: IT882; BB: KP73; CC: IT895) Genotypes are listed in Table S7. ND, not determined.

In addition, we examined if deletion of *cmpA* would allow cells producing polymerization-defective variants of SpoIVA to complete the sporulation program despite their inability to properly form the spore envelope. Sporangia harboring SpoIVA variants that fail to polymerize, either due to an inability to bind (SpoIVA^{K30A}) or hydrolyze (SpoIVA$^{T70A-T71A}$) ATP, fail to recruit coat proteins to assemble a coat and produce 10^4-10^6-fold fewer heat resistant spores than wild type ((Castaing et al., 2013; Ramamurthi & Losick, 2008); Table S6, Strains X and Z). Surprisingly, deletion of *cmpA* suppressed this phenotype also, bringing the sporulation efficiency up to ~10-50-fold fewer than wild type (Table S6, Strains Y and AA). Interestingly, deletion of *cmpA* also suppressed the lysozyme sensitivity of these mutants, indicating that coat assembly was permitted to occur, albeit not to wild type levels (Table 3.6, Strains Y and AA).

Finally, deletion of *cmpA* did not suppress the sporulation defect of deleting *spoIVA*, indicating that it is unable to completely bypass the requirement for SpoIVA (Table 3.6, Strains BB and CC). Important to note is that in all instances, while deletion of *cmpA* allowed the mutants to bypass this checkpoint and continue with sporulation, the result was production of spores that had lower sporulation efficiencies than wild type cells. Thus, CmpA appears to be part of a quality control checkpoint system that selectively removes unfit cells that assemble defective spore envelopes from a sporulating population by preventing them from completing the sporulation program.

DISCUSSION

The use of checkpoints ensures that steps in a developmental program properly finish prior to progression into the next stage of the program (Hartwell & Weinert, 1989). Here, we discovered that, during sporulation in *B. subtilis*, the small protein CmpA participates with the ClpXP proteolytic machinery in a developmental checkpoint to monitor proper spore envelope assembly. We propose a model (Fig. 3.11) in which CmpA acts as an adaptor to ClpXP to mediate the degradation of the coat morphogenetic protein SpoIVA specifically in cells that improperly assemble the spore envelope. Degradation of SpoIVA, which acts as a static platform atop which other coat proteins are deposited (Roels et al., 1992), leads to destabilization of defective sporangia and ultimately results in their lysis, thereby releasing nutrients into the environment for others to utilize and removing the defective spores from the population. In cells that properly construct the spore envelope, we propose that degradation of CmpA is a switch that signals successful spore envelope assembly and prevents SpoIVA proteolysis, permitting these cells to continue through the sporulation program. The model suggests that deleting *cmpA*, or disrupting the interactions between CmpA, ClpXP, and SpoIVA bypasses the checkpoint and permits mutant cells elaborating defective spore envelopes to continue through the sporulation program and persist in the population. As with other developmental programs there may be redundant pathways that help offset the deleterious effects of a single mutation. However, without selective pressure, mutations that lower sporulation efficiency readily accumulate and lead to deterioration of the program (Maughan, Masel, Birky, & Nicholson, 2007; Sastalla, Rosovitz, & Leppla, 2010). Since sporulation is a last-resort stress pathway (Gonzalez-Pastor et al., 2003; Sonenshein, 2000) that provides a fitness advantage in fluctuating environments (Siebring et al., 2014), maintaining the fidelity of the program would be a key factor in the long-term survival of the population.

Our model is consistent with several lines of genetic, biochemical, and cytological evidence. First, disruption of sporulation by overexpression of *cmpA* was suppressed by three

Figure 3.11. Model of the CmpA-mediated regulated cell death pathway. Depicted is a population of sporulating *B. subtilis* cells (center, top) in which a single cell has elaborated a defective spore envelope (highlighted in red) and, as a consequence, is removed from the population by cell lysis (center, bottom). Left: the CmpA pathway in a cell elaborating a defective spore envelope. CmpA persists in this cell and acts as an adaptor of ClpXP to mediate degradation of SpoIVA in a σ^K-dependent manner. Right: in cells that successfully initiate spore envelope assembly, CmpA is degraded upon activation of σ^K and, in the absence of SpoIVA degradation, the sporulation program proceeds. SpoIVA, green; SpoVM, red; CmpA, purple; ClpX, pink; ClpP, orange.

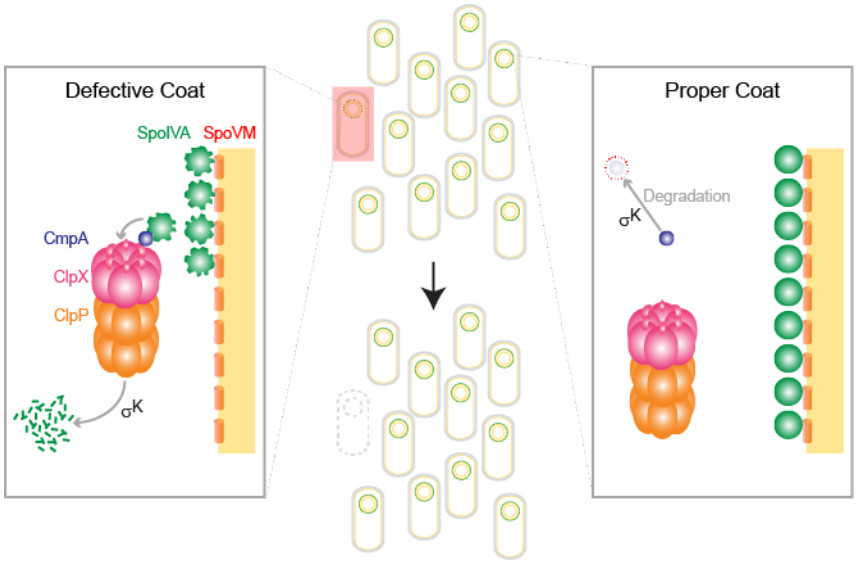

different spontaneous loss-of-function mutations in *clpX* that changed residues in the N-terminus of ClpX (a domain previously implicated in substrate and adaptor binding (Wojtyra et al., 2003)). A fourth spontaneous mutation in *clpP*, that altered a residue near the hydrophobic binding pocket that mediates ClpP's interaction with ClpX, also suppressed the sporulation defect caused by *cmpA* overexpression. Deleting the N-terminus of ClpX, or targeted disruption of the ClpX IGF loop which mediates its interaction with ClpP, also suppressed the *cmpA*-overexpression phenotype *in vivo*, indicating that the inability to degrade one or more factors bypassed the CmpA-mediated sporulation checkpoint. Involvement of SpoIVA as a putative target for degradation by ClpXP arose from two spontaneous mutations in adjacent codons of *spoIVA.* Both mutations altered residues near the interface between the Middle and C-terminal domain of SpoIVA (Castaing et al., 2014), suppressed the sporulation defect imposed by the *spoVM*^{I15A} allele (which arrests sporulation in a CmpA-dependent manner (Ebmeier et al., 2012)) and led to stabilization of SpoIVA.

Biochemical support for the model came from co-purification experiments which demonstrated that CmpA, ClpX, and SpoIVA exist in a complex in extracts of sporulating *B. subtilis* cells. Consistent with our genetic data, amino acid substitutions in CmpA, ClpX, or SpoIVA that bypassed the CmpA checkpoint *in vivo* also failed to form a ternary complex of these proteins *in vitro*. Our analysis with these variants also demonstrated that CmpA and ClpX likely interact with each other via the N-terminus of ClpX, and that this interaction can occur in the absence of SpoIVA. However, the interaction between SpoIVA and ClpX absolutely required CmpA. Together, this behavior is consistent with an adaptor-like function for CmpA, similar to that which has been described for ClpXP adaptors in other systems (Battesti & Gottesman, 2013).

Finally, epifluorescence microscopy analysis of individual cells producing GFP-SpoIVA revealed that degradation of GFP-SpoIVA occurred specifically in cells that had progressed to the phase bright forespore state, which is the same stage in sporulation in which CmpA-GFP

abnormally persists in the *spoVM*^{I15A} mutant (Ebmeier et al., 2012). However, in mutant cells in which formation of the CmpA/ClpX/SpoIVA degradation complex was prevented, GFP-SpoIVA persisted and these cells were able to successfully complete the sporulation program to produce spores albeit at a lowered efficiency compared to wild type. The disappearance of CmpA-GFP in phase bright forespores in wild type cells (Ebmeier et al., 2012), suggests that regulation of the checkpoint may be controlled via degradation of CmpA. CmpA is therefore likely a late stage quality control mechanism that monitors the integrity of the developing spore to ensure the fitness of the spore population. In this pathway, we propose that spore envelope defects arising at a late stage (so-called "Stage IV-V") result in lysis of the sporangium, and that this lysis is an active process that depends on SpoIVA degradation by CmpA and ClpXP. Consistent with this timing, we also report here that the switch that initiates this pathway resides under control of σ^K, the final compartment-specific sporulation sigma factor which is also required for activating cortex synthesis (Vasudevan et al., 2007). We found that not only is at least one factor produced by σ^K required to activate CmpA/ClpXP-mediated degradation of SpoIVA in unfit cells, but that σ^K is also required for degradation of CmpA in properly sporulating cells. We propose that the sporulating cell provides the window between σ^E and σ^K activation for the spore envelope to initiate assembly properly, and upon σ^K activation if the coat has properly assembled, the cell degrades CmpA and sporulation proceeds. However, if the spore envelope improperly assembles, CmpA persists and activation of SpoIVA degradation and cell lysis occurs instead.

Recent reports of "programmed" or "regulated" cell death in bacterial cells have added to the changing view of bacterial communities as more than simply a collection of independently operating cells, and has given rise to the speculation that individual unicellular organisms may initiate cell death to benefit the population as a whole (Bos, Yakhnina, & Gitai, 2012; Dwyer, Camacho, Kohanski, Callura, & Collins, 2012; Erental, Sharon, & Engelberg-Kulka, 2012). Although specific mechanisms for cell death in these cases have been well characterized, the

exact benefit of such an act to a single-celled organism has been difficult to explicitly demonstrate. The use of the term “apoptosis” in these situations has therefore remained controversial (Galluzzi et al., 2012; Hacker, 2013). Unlike regulated cell death pathways described in actively dividing cells, the CmpA pathway occurs during a terminal differentiation program that results in the production of the spore, which is a specialized cell type that preserves the cell’s genetic material in a manner functionally similar to that of germ cells in multi-cellular organisms. The construction of a spore envelope that is robustly resistant to environmental insults is critical for the spore’s survival in harsh environmental conditions. As such, removal of cells harboring mutations that produce defective spore envelopes confers an obvious advantage to a population that needs to protect the integrity of the genome of its “germ line” and ensures the survival of future generations (Gartner, Boag, & Blackwell, 2008; P. Setlow, 2006). In the absence of CmpA, cells run the risk of producing defective spores that may not confer the resistance properties required to protect the cell’s genome.

Why, then, is it more beneficial to completely remove defective spores from a population, rather than allowing a defective spore, which may confer some low level of protection, to persist? Populations of sporulating cells employ a bet-hedging strategy whereby a fraction of the population does not initiate sporulation in order to retain the ability to rapidly respond to a return to favorable growth conditions (Veening et al., 2008). During continued favorable growth conditions, the selective pressure to maintain sporulation can become relaxed, resulting in the enrichment of sporulation-defective cells (Maughan et al., 2007; Sastalla et al., 2010). In the absence of the CmpA pathway, cells harboring mutations that diminish spore envelope assembly can complete sporulation and persist in the population. When these mutant cells resume vegetative growth, and eventually re-sporulate, a population of them will likely employ the bet-hedging strategy and avoid initiating sporulation. In this scenario, this group of non-sporulating cells has the capacity to quickly flourish, upon a sudden increase in nutrient availability, and out-compete the population of wild type cells that initiate sporulation. In this

manner, we propose that the CmpA pathway ensures that mutations that diminish the capacity to produce a functional spore do not become incorporated into the bacterium's "germ line" and ensures that faulty spores, which may be prone to accumulate additional mutations leading to the deterioration of the sporulation program, are removed by lysis.

In this report, we mimicked the occurrence of spore envelope assembly defects by introducing mutations that altered specific coat proteins. However, it is tempting to speculate that the CmpA pathway may serve a more general role in monitoring the integrity of coat basement layer assembly in completely wild type cells. Unlike virus particles that display internal symmetry, endospore coats are more complex and are non-uniformly shaped, suggesting that heterogeneity in assembly is permitted (Chada et al., 2003; Plomp, Carroll, Setlow, & Malkin, 2014). Given a less physically-constrained assembly process (compared to spontaneously self-assembling viral particles, for example), perhaps the CmpA pathway may also selectively discard sporangia that happen to mis-assemble the coat using wild type components, thereby ensuring the integrity of spore envelope assembly in every spore. In this aspect, the degradation of the structural protein SpoIVA, which encases the forespore, is reminiscent of the degradation of the nuclear lamins (the intermediate filaments that help form and maintain the integrity of the nuclear envelope) during apoptosis in metazoans. While degradation of lamins is a feature of apoptosis, the incorrect assembly of lamins to form the nuclear envelope can also induce apoptosis (Burke, 2001). Similarly, SpoIVA may not only be a target for degradation, but its incorrect assembly may potentially also induce CmpA-dependent cell lysis. Thus, the ability of morphogenetic proteins that serve to maintain the integrity of cellular envelopes to play these dual roles in regulated cell death appears to have arisen in evolutionarily and mechanistically distinct systems.

EXPERIMENTAL PROCEDURES

Strain construction

Strains are otherwise isogenic derivatives of *B. subtilis* PY79 (Youngman et al., 1984). Construction of integration plasmids pSE18 and pSE24, for integration of IPTG-inducible *cmpA* ($P_{hyperspank}$-*cmpA*) and *cmpA-gfp* ($P_{hyperspank}$-*cmpA-gfp*), respectively, at *amyE* have been previously described (Ebmeier et al., 2012). To integrate $P_{hyperspank}$-*cmpA* at the *thrC* locus, *cmpA* was subcloned from pSE18 into the integration vector pDP150 (Kearns et al., 2005) to create pIT43. To construct constitutively expressing *cmpA* (P_{sigA}-*cmpA*), *lacI* expression in pSE18 and pIT43 was abolished by deleting the immediate upstream region and start codon of *lacI* in addition to introducing a stop codon using Quikchange site-directed mutagenesis (Agilent Technologies) to create pIT59 and pIT66. $P_{hyperspank}$-*cmpA-gfp* was subcloned from pSE24 using EcoRI and BamHI into the integration vector pSac-cm (Middleton & Hofmeister, 2004) for integration at *sacA* to create pIT80. *clpX* at *thrC* was created by PCR-amplifying the *clpX* ORF, 260 nucleotides upstream and 20 nucleotides downstream with primers '5'BsaI clpX' (aaaaggtctcgaattcgcgcgaatcattcgtgcctt) and '3'BamHI clpX' (cgacggatcctcaggaggtttgtgcttatctt). The PCR fragment was then cloned into the EcoRI and BamHI sites in the integration vector pDG1664 (Guerout-Fleury et al., 1996) to create pIT89. $P_{hyperspank}$-*clpX* at *thrC* and $P_{hyperspank}$-*clpX-His*$_6$ at *amyE* were constructed by PCR-amplifying the *clpX* ORF and introducing a ribosomal binding site (RBS) as well as the restriction sites NheI and SphI using primers '5' NheI RBS clpX' (aaaagctagctaaggaggaatgagcctatgtttaaatttaacgagga) and '3' SphI clpX' (aaaagcatgcctcctgagtgttaccac) or '3' SphI 6xHisclpX' (aaaagcatgcttagtggtgatggtgatgatgtgcagatgttttatcttg) to add a His_6 tag. The PCR fragments were then digested with NheI and SphI and *clpX* was cloned into pDP 150 to create pIT60 while *clpX-His*$_6$ *was* cloned into pDR111 to create pIT76. $P_{hyperspank}$-*clpX*$^{\Delta 1-53}$ at *amyE* was constructed by PCR-amplifying the *clpX* ORF starting at the nucleotides that encode for amino acid 54 and introducing a RBS, start codon and restriction sites NheI and SphI using the primers '5' NheI

RBS N-term t-clpX' (aaaagctagctaaggaggaatgagcctatggaagaagtagaattt) and '3' SphI clpX'. The PCR fragment was digested with NheI and SphI and cloned into pDR111.

All plasmids were integrated into the *B. subtilis* chromosome by double recombination at the specified ectopic locus.

General methods

Sporulation efficiency was measured by inducing sporulation in Difco sporulation medium (DSM) for at least 24 h at 37°C and subjecting spores to heat treatment (80°C for 20 min) or lysozyme treatment (250 μg ml^{-1} for 1 h at 37°C). Cultures were then serially diluted and colony-forming units (cfu) that survived were determined and reported relative to the cfu obtained in a parallel culture of the wild-type PY79 strain.

Microscopy

Microscopy was performed as previously described (Eswaramoorthy et al., 2014). Cells were induced to sporulate by resuspension in SM medium (Sterlini & Mandelstam, 1969). When required, IPTG was added (1 mM final concentration) to induce expression wild type or variants of *clpX* or *cmpA*. At various time points 1 ml of culture was harvested and resuspended in 100 μl PBS. 5 μl was spotted on a glass bottom culture dish (Mattek Corp.) and covered with a 1% agarose pad made with distilled water. Cells were viewed with a DeltaVision Core microscope system (Applied Precision) equipped with an environmental control chamber. Fluorescence was quantified using Softworx Suite 2.0 (Applied Precision/GE Healthcare).

DPA and peptidoglycan harvesting

DPA was harvested and measured as previously described (W. L. Nicholson & P. Setlow, 1990). 5 ml of sporulating cell culture was harvested at each time point and the cell pellet was resuspended in 500 μl distilled water. Cells were boiled for 20 min to release DPA into the

water. The amount of DPA was determined by a colorimetric assay, in which changes in absorption at OD_{440} caused by complex formation between ferrous iron and DPA was measured (Janssen, Lund, & Anderson, 1958). Peptidoglycan was harvested and analyzed as previously described (Meador-Parton & Popham, 2000; Vasudevan et al., 2007). Briefly, 1ml of sporulating cell culture was pelleted, washed, acid hydrolyzed in 6N HCl and subjected to amino acid/sugar analysis.

Isolation of spontaneous suppressors

Spontaneous suppressor mutations were isolated as described previously (Ramamurthi et al., 2006). Mutant strains were grown in 30 ml of DSM for at least 24 h at 37°C in order to sporulate and accumulate spontaneous mutations. The culture was then incubated at 80°C to kill cells which did not sporulated successfully. The 30 ml culture was re-inoculated into 300 ml of fresh DSM, allowed to germinate, grow and sporulate for at least 24 h at 37°C. The procedure was repeated with re-inoculation of 30 ml of heat-killed culture until an increase in sporulation efficiency was observed (usually three rounds). Candidate spontaneous suppressors were collected and characterized. Suppressor mutations were mapped by linkage analysis and whole genome sequencing.

Co-purification and cell lysate harvesting

Overnight cultures were grown in CH media and induced to sporulate in 20 ml resuspension medium. IPTG (1 mM final concentration) was added to induce expression of tagged or untagged versions of wild type and mutant CmpA and ClpX at approximately 2 h after resuspension. 20 ml of culture was then harvested approximately 2 h after IPTG induction. Cells were harvested and protoplasted as previously described (Ramamurthi & Losick, 2008) in protoplast buffer (0.5 M sucrose, 20 mM $MgCl_2$, 10 mM potassium phosphate at pH 6.8, 0.1 mg ml^{-1} lysozyme) for 25 min at 37°C. Protoplasts were collected by centrifugation and

resuspended in 1 ml of ice cold 0.5X PD buffer (Y. I. Kim et al., 2001) without ATP regenerating system (hereafter referred to as 0.5X PD buffer). PMSF (1mM final concentration) was added to cell lysate and cell debris was removed by centrifugation. The supernatant was collected and incubated with Ni-NTA agarose beads (Qiagen) equilibrated in 0.5X PD buffer for 10 min at 4°C with inversion. Beads were washed with 0.5X PD buffer containing 20mM imidazole. Bound proteins were eluted with 250 µl of 0.5× PD buffer containing 250mM imidazole. Fractions were analyzed by immunoblotting using rabbit antisera raised against purified *E. coli* ClpX (gift from Sue Wickner), GFP, or SpoIVA. Cells were harvested and protoplasted as described above. Protoplasts were resuspended in 500 µl 5% tricholoroacetic acid (TCA) to lyse cells and precipitate proteins. After incubation on ice for 15 min, precipitate was collected by centrifugation and washed three times with 1 ml acetone. Precipitated pellet was air-dried overnight at room temperature, then resuspended in 300 µl 1× LDS NuPAGE Buffer (Invitrogen) and heated at 55°C for 10 min with shaking. Fractions were analyzed by immunoblotting using rabbit antisera raised against SpoIVA or σ^A.

Table 3.7. Strains used in this chapter.

Strain	Genotype	Source
PY79	Prototrophic derivative of *B. subtilis* 168	Youngman et al., 1984
IT478	*amyE::P$_{sigA}$-cmpA spec*	
IT504	*thrC::P$_{sigA}$-cmpA erm*	
IT517	*ΔsleB::spec ΔcwlJ::tet*	
IT575	*ΔsleB::spec ΔcwlJ::tet thrC::P$_{sigA}$-cmpA erm*	
SE249	*spoIVA^{E423G} ΔspoVM::tet amyE::spoVM^{I15A} cat thrC::cmpA spec*	
IT89	*spoIVA^{L424F} ΔspoVM::tet amyE::spoVM^{I15A} cat thrC::cmpA spec*	
KR322	*ΔspoVM::tet amyE::spoVM^{I15A} cat*	Ebmeier et al., 2012
SE364	*amyE::P$_{hyperspank}$-cmpA-gfp spec*	
IT86	*ΔspoVM::tet amyE::P$_{hyperspank}$-cmpA-gfp spec*	
IT113	*ΔspoVM::tet ΔspoIVA::kan amyE::P$_{hyperspank}$-cmpA-gfp spec*	
IT114	*ΔspoIVA::kan amyE::P$_{hyperspank}$-cmpA-gfp spec*	
IT525	*amyE::P$_{sigA}$-cmpA spec thrC::P$_{sigA}$-cmpA erm clpX^{D21Y}*	
IT367	*amyE::P$_{sigA}$-cmpA spec thrC::P$_{sigA}$-cmpA erm clpX^{I34M}*	
IT342	*amyE::P$_{sigA}$-cmpA spec thrC::P$_{sigA}$-cmpA erm clpX^{E44G}*	
IT531	*amyE::P$_{sigA}$-cmpA spec thrC::P$_{sigA}$-cmpA erm clpP^{D187N}*	
IT482	*ΔclpX::kan*	
IT483	*ΔclpX::kan amyE::P$_{hyperspank}$-cmpA spec*	
IT479	*thrC::P$_{hyperspank}$-clpX erm*	
IT545	*amyE::P$_{hyperspank}$-cmpA spec thrC::P$_{hyperspank}$-clpX erm*	
IT571	*amyE::P$_{hyperspank}$-clpX$^{Δ1-53}$ spec thrC::P$_{hyperspank}$-cmpA erm*	
IT616	*amyE::P$_{hyperspank}$-cmpA spec thrC::P$_{hyperspank}$-clpX^{F270W} erm*	
SE178	*ΔcmpA::erm*	
SE181	*ΔspoVM::tet amyE::spoVM^{I15A} cat ΔcmpA::erm*	

IT261	*amyE::$P_{hyperspank}$-cmpA^{P2A}-gfp spec*
IT131	*thrC::cmpA^{P2A} spec*
IT139	*ΔspoVM::tet amyE::spoVM^{I15A} cat ΔcmpA::erm thrC::cmpA^{P2A}spec*
IT138	*ΔcmpA::erm thrC::cmpA^{P2A} spec*
IT183	*ΔspoVM::tet amyE::spoVM^{I15A} cat thrC::cmpA^{P2A} spec*
CW6	*amyE::$P_{hyperspank}$-cmpA^{N3A}-gfp spec*
CW8	*thrC::cmpA^{N3A} spec*
CW13	*ΔspoVM::tet amyE::spoVM^{I15A} cat ΔcmpA::erm thrC::cmpA^{N3A} spec*
CW12	*ΔcmpA::erm thrC::cmpA^{N3A} spec*
CW14	*ΔspoVM::tet amyE::spoVM^{I15A} cat thrC::cmpA^{N3A} spec*
IT252	*amyE::$P_{hyperspank}$-cmpA^{W4A}-gfp spec*
IT132	*thrC::cmpA^{W4A} spec*
IT141	*ΔspoVM::tet amyE::spoVM^{I15A}cat ΔcmpA::erm thrC::cmpA^{W4A} spec*
IT140	*ΔcmpA::erm thrC::cmpA^{W4A} spec*
IT184	*ΔspoVM::tet amyE::spoVM^{I15A} cat thrC::cmpA^{W4A} spec*
IT180	*amyE::$P_{hyperspank}$-cmpA^{L5A}-gfp spec*
IT153	*thrC::cmpA^{L5A} spec*
IT165	*ΔspoVM::tet amyE::spoVM^{I15A} cat ΔcmpA::erm thrC::cmpA^{L5A} spec*
IT160	*ΔcmpA::erm thrC::cmpA^{L5A} spec*
IT185	*ΔspoVM::tet amyE::spoVM^{I15A} cat thrC::cmpA^{L5A} spec*
CW7	*amyE:: ^{I15A}-cmpA^{K6A}-gfp spec*
CW9	*thrC::cmpA^{K6A} spec*
CW16	*ΔspoVM::tet amyE::spoVM^{I15A} cat ΔcmpA::erm thrC::cmpA^{K6A} spec*
CW15	*ΔcmpA::erm thrC::cmpA^{K6A} spec*
CW17	*ΔspoVM::tet amyE::spoVM^{I15A} cat thrC::cmpA^{K6A} spec*
CW21	*amyE:: $P_{hyperspank}$-cmpA^{K7A}-gfp spec*
CW23	*thrC::cmpA^{K7A} spec*
CW31	*ΔspoVM::tet amyE::spoVM^{I15A} cat ΔcmpA::erm thrC::cmpAK7A*

	spec
CW32	*∆cmpA::erm thrC::cmpA^{K7A} spec*
CW33	*∆spoVM::tet amyE::spoVM^{I15A} cat thrC::cmpA^{K7A} spec*
IT181	*amyE::P^{I15A}-cmpA^{Q8A}-gfp spec*
IT123	*thrC::cmpA^{Q8A} spec*
CW139	*∆spoVM::tet amyE::spoVM^{I15A} cat ∆cmpA::erm thrC::cmpA^{Q8A} spec*
CW140	*∆cmpA::erm thrC::cmpA^{Q8A} spec*
CW141	*∆spoVM::tet amyE::spoVM^{I15A} cat thrC::cmpA^{Q8A} spec*
CW20	*amyE:: P$_{hyperspank}$-cmpA^{M9A}-gfp spec*
CW22	*thrC::cmpA^{M9A} spec*
CW28	*∆spoVM::tet amyE::spoVM^{I15A} cat ∆cmpA::erm thrC::cmpA^{M9A} spec*
CW29	*∆cmpA::erm thrC::cmpA^{M9A} spec*
CW30	*∆spoVM::tet amyE::spoVM^{I15A} cat thrC::cmpA^{M9A} spec*
CW24	*amyE:: P$_{hyperspank}$-cmpA^{Q10A}-gfp spec*
CW26	*thrC::cmpA^{Q10A} spec*
CW34	*∆spoVM::tet amyE::spoVM^{I15A} cat ∆cmpA::erm thrC::cmpA^{Q10A} spec*
CW35	*∆cmpA::erm thrC::cmpA^{Q10A} spec*
CW36	*∆spoVM::tet amyE::spoVM^{I15A} cat thrC::cmpA^{Q10A} spec*
CW25	*amyE:: P$_{hyperspank}$-cmpA^{K11A}-gfp spec*
CW27	*thrC::cmpA^{K11A} spec*
CW37	*∆spoVM::tet amyE::spoVM^{I15A} cat ∆cmpA::erm thrC::cmpA^{K11A} spec*
CW38	*∆cmpA::erm thrC::cmpA^{K11A} spec*
CW39	*∆spoVM::tet amyE::spoVM^{I15A} cat thrC::cmpA^{K11A} spec*
CW49	*amyE:: P$_{hyperspank}$-cmpA^{F13A}-gfp spec*
CW51	*thrC::cmpA^{F13A} spec*
CW53	*∆spoVM::tet amyE::spoVM^{I15A} cat ∆cmpA::erm thrC::cmpA^{F13A}*

	spec
CW54	*Δcmp A::erm thrC::cmpA^{F13A} spec*
CW55	*ΔspoVM::tet amyE::spoVM^{I15A} cat thrC::cmpA^{F13A} spec*
CW50	*amyE:: P$_{hyperspank}$-cmpA^{L14A}-gfp spec*
CW52	*thrC::cmpA^{L14A} spec*
CW56	*ΔspoVM::tet amyE::spoVM^{I15A} cat Δcmp A::erm thrC::cmpA^{L14A} spec*
CW57	*Δcmp A::erm thrC::cmpA^{L14A} spec*
CW58	*ΔspoVM::tet amyE::spoVM^{I15A} cat thrC::cmpA^{L14A} spec*
CW112	*amyE:: P$_{hyperspank}$-cmpA^{E15A}-gfp spec*
CW158	*thrC::cmpA^{E15A} spec*
CW163	*ΔspoVM::tet amyE::spoVM^{I15A} cat Δcmp A::erm thrC::cmpA^{E15A} spec*
CW164	*Δcmp A::erm thrC::cmpAE15A spec*
CW165	*ΔspoVM::tet amyE::spoVM^{I15A} cat thrC::cmpA^{E15A} spec*
CW110	*amyE:: P$_{hyperspank}$-cmpA^{K16A}-gfp spec*
CW121	*thrC::cmpA^{K16A} spec*
CW125	*ΔspoVM::tet amyE::spoVM^{I15A} cat Δcmp A::erm thrC::cmpA^{K16A} spec*
CW126	*Δcmp A::erm thrC::cmpA^{K16A} spec*
CW127	*ΔspoVM::tet amyE::spoVM^{I15A} cat thrC::cmpAK16A spec*
CW99	*amyE:: P$_{hyperspank}$-cmpA^{D17A}-gfp spec*
CW101	*thrC::cmpA^{D17A} spec*
CW103	*ΔspoVM::tet amyE::spoVM^{I15A} cat Δcmp A::erm thrC::cmpA^{D17A} spec*
CW104	*Δcmp A::erm thrC::cmpA^{D17A} spec*
CW105	*ΔspoVM::tet amyE::spoVM^{I15A} cat thrC::cmpA^{D17A} spec*
CW113	*amyE:: P$_{hyperspank}$-cmpA^{N18A}-gfp spec*
CW159.1	*thrC::cmpA^{N18A} spec*
CW166.1	*ΔspoVM::tet amyE::spoVM^{I15A} cat Δcmp A::erm thrC::cmpA^{N18A}*

	spec
CW167.1	*ΔcmpA::erm thrc::cmpA^{N18A} spec*
CW168.1	*ΔspoVM::tet amyE::spoVM^{I15A} cat thrC::cmpA^{N18A} spec*
CW123	*amyE:: P$_{hyperspank}$-cmpA^{Y19A}-gfp spec*
CW124	*thrC::cmpA^{Y19A} spec*
CW131	*ΔspoVM::tet amyE::spoVM^{I15A} cat ΔcmpA::erm thrC::cmpA^{Y19A} spec*
CW132	*ΔcmpA::erm thrC::cmpA^{Y19A} spec*
CW133	*ΔspoVM::tet amyE::spoVM^{I15A} cat thrC::cmpA^{Y19A} spec*
IT351	*amyE:: P$_{hyperspank}$-cmpA^{Q20A}-gfp spec*
IT133	*thrC::cmpA^{Q20A} spec*
CW142	*ΔspoVM::tet amyE::spoVM^{I15A} cat ΔcmpA::erm thrC::cmpA^{Q20A} spec*
CW143	*ΔcmpA::erm thrC::cmpA^{Q20A} spec*
CW144	*ΔspoVM::tet amyE::spoVM^{I15A} cat thrC::cmpA^{Q20A} spec*
IT195	*amyE:: P$_{hyperspank}$-cmpA^{I21A}-gfp spec*
IT154	*thrC::cmpA^{I21A} spec*
IT166	*ΔspoVM::tet amyE::spoVM^{I15A} cat ΔcmpA::erm thrC::cmpA^{I21A} spec*
IT161	*ΔcmpA::erm thrC::cmpA^{I21A} spec*
IT188	*ΔspoVM::tet amyE::spoVM^{I15A} cat thrC::cmpA^{I21A} spec*
CW154	*amyE:: P$_{hyperspank}$-cmpA^{K22A}-gfp spec*
IT155	*thrC::cmpA^{K22A} spec*
IT179	*ΔspoVM::tet amyE::spoVM^{I15A} cat ΔcmpA::erm thrC::cmpA^{K22A} spec*
IT162	*ΔcmpA::erm thrC::cmpA^{K22A} spec*
IT189	*ΔspoVM::tet amyE::spoVM^{I15A} cat thrC::cmpA^{K22A} spec*
IT221	*amyE:: P$_{hyperspank}$-cmpA^{L23A}-gfp spec*
IT156	*thrC::cmpA^{L23A} spec*
IT168	*ΔspoVM::tet amyE::spoVM^{I15A} cat ΔcmpA::erm thrC::cmpA^{L23A} spec*

IT163 *Δcmp*A::*erm thrC::cmpA*^{L23A} *spec*

IT190 *ΔspoVM::tet amyE::spoVM*^{I15A} *cat thrC::cmpA*^{L23A} *spec*

CW155 *amyE::* $P_{hyperspank}$*-cmpA*^{L24A}*-gfp spec*

IT134 *thrC::cmpA*^{L24A} *spec*

IT147 *ΔspoVM::tet amyE::spoVM*^{I15A} *cat Δcmp*A::*erm thrC::cmpA*^{L24A} *spec*

IT146 *Δcmp*A::*erm thrC::cmpA*^{L24A} *spec*

IT191 *ΔspoVM::tet amyE::spoVM*^{I15A} *cat thrC::cmpA*^{L24A} *spec*

CW134 *amyE::* $P_{hyperspank}$*-cmpA*^{N25A}*-gfp spec*

IT157 *thrC::cmpA*^{N25A} *spec*

IT169 *ΔspoVM::tet amyE::spoVM*^{I15A} *cat Δcmp*A::*erm thrC::cmpA*^{N25A} *spec*

IT164 *Δcmp*A::*erm thrC::cmpA*^{N25A} *spec*

IT192 *ΔspoVM::tet amyE::spoVM*^{I15A} *cat thrC::cmpA*^{N25A} *spec*

CW111 *amyE::* $P_{hyperspank}$*-cmpA*^{Q26A}*-gfp spec*

CW122 *thrC::cmpA*^{Q26A} *spec*

CW128 *ΔspoVM::tet amyE::spoVM*^{I15A} *cat Δcmp*A::*erm thrC::cmpA*^{Q26A} *spec*

CW129 *Δcmp*A::*erm thrC::cmpA*^{Q26A} *spec*

CW130 *ΔspoVM::tet amyE::spoVM*^{I15A} *cat thrC::cmpA*^{Q26A} *spec*

CW114 *amyE::* $P_{hyperspank}$*-cmpA*^{C27A}*-gfp spec*

CW160 *thrC::cmpA*^{C27A} *spec*

CW169.1 *ΔspoVM::tet amyE::spoVM*^{I15A} *cat Δcmp*A::*erm thrC::cmpA*^{C27A} *spec*

CW170 *Δcmp*A::*erm thrC::cmpA*^{C27A} *spec*

CW171 *ΔspoVM::tet amyE::spoVM*^{I15A} *cat thrC::cmpA*^{C27A} *spec*

CW115 *amyE::* $P_{hyperspank}$*-cmpA*^{W28A}*-gfp spec*

CW161 *thrC::cmpA*^{W28A} *spec*

CW172 *ΔspoVM::tet amyE::spoVM*^{I15A} *cat Δcmp*A::*erm thrC::cmpA*^{W28A} *spec*

CW173 *Δcmp*A::*erm thrC::cmpA*^{W28A} *spec*

CW174 *ΔspoVM::tet amyE::spoVM^{I15A} cat thrC::cmpA^{W28A} spec*

CW157 *amyE:: P$_{hyperspank}$-cmpA^{Y29A}-gfp spec*

CW75 *thrC::cmpA^{Y29A} spec*

CW79 *ΔspoVM::tet amyE::spoVM^{I15A} cat ΔcmpA::erm thrC::cmpA^{Y29A} spec*

CW80 *ΔcmpA::erm thrC::cmpA^{Y29A} spec*

CW81 *ΔspoVM::tet amyE::spoVM^{I15A} cat thrC::cmpA^{Y29A} spec*

CW74 *amyE:: P$_{hyperspank}$-cmpA^{F30A}-gfp spec*

CW76 *thrC::cmpA^{F30A} spec*

CW82 *ΔspoVM::tet amyE::spoVM^{I15A} cat ΔcmpA::erm thrC::cmpA^{F30A} spec*

CW83 *ΔcmpA::erm thrC::cmpA^{F30A} spec*

CW84 *ΔspoVM::tet amyE::spoVM^{I15A} cat thrC::cmpA^{F30A} spec*

CW100 *amyE:: P$_{hyperspank}$-cmpA^{Y31A}-gfp spec*

CW102 *thrC::cmpA^{Y31A} spec*

CW107 *ΔspoVM::tet amyE::spoVM^{I15A} cat ΔcmpA::erm thrC::cmpA^{Y31A} spec*

CW108 *ΔcmpA::erm thrC::cmpA^{Y31A} spec*

CW109 *ΔspoVM::tet amyE::spoVM^{I15A} cat thrC::cmpA^{Y31A} spec*

CW135 *amyE:: P$_{hyperspank}$-cmpA^{R32A}-gfp spec*

CW137 *thrC::cmpA^{R32A} spec*

CW145 *ΔspoVM::tet amyE::spoVM^{I15A} cat ΔcmpA::erm thrC::cmpA^{R32A} spec*

CW146 *ΔcmpA::erm thrC::cmpA^{R32A} spec*

CW147 *ΔspoVM::tet amyE::spoVM^{I15A} cat thrC::cmpA^{R32A} spec*

CW136 *amyE:: P$_{hyperspank}$-cmpA^{K33A}-gfp spec*

CW138 *thrC::cmpA^{K33A} spec*

CW148 *ΔspoVM::tet amyE::spoVM^{I15A} cat ΔcmpA::erm thrC::cmpA^{K33A} spec*

CW149 *ΔcmpA::erm thrC::cmpA^{K33A} spec*

CW150 *ΔspoVM::tet amyE::spoVM^{I15A} cat thrC::cmpA^{K33A} spec*

CW116 *amyE:: P$_{hyperspank}$-cmpA^{K34A}-gfp spec*

CW117 *thrC::cmpA^{K34A} spec*

CW151 *ΔspoVM::tet amyE::spoVM^{I15A} cat ΔcmpA::erm thrC::cmpA^{K34A} spec*

CW152 *ΔcmpA::erm thrC::cmpA^{K34A} spec*

CW153 *ΔspoVM::tet amyE::spoVM^{I15A} cat thrC::cmpA^{K34A} spec*

CW118 *amyE:: P$_{hyperspank}$-cmpA^{H35A}-gfp spec*

CW162 *thrC::cmpA^{H35A} spec*

CW175 *ΔspoVM::tet amyE::spoVM^{I15A} cat ΔcmpA::erm thrC::cmpA^{H35A} spec*

CW176 *ΔcmpA::erm thrC::cmpA^{H35A} spec*

CW177 *ΔspoVM::tet amyE::spoVM^{I15A} cat thrC::cmpA^{H35A} spec*

CW119 *amyE:: P$_{hyperspank}$-cmpA^{C36A}-gfp spec*

CW180 *thrC::cmpA^{C36A} spec*

CW182 *ΔspoVM::tet amyE::spoVM^{I15A} cat ΔcmpA::erm thrC::cmpA^{C36A} spec*

CW183 *ΔcmpA::erm thrc::cmpA^{C36A} spec*

CW184 *ΔspoVM::tet amyE::spoVM^{I15A} cat thrc::cmpA^{C36A} spec*

CW120 *amyE:: P$_{hyperspank}$-cmpA^{S37A}-gfp spec*

CW181 *thrC::cmpA^{S37A} spec*

CW185 *ΔspoVM::tet amyE::spoVM^{I15A} cat ΔcmpA::erm thrC::cmpA^{S37A} spec*

CW186 *ΔcmpA::erm thrC::cmpA^{S37A} spec*

CW187 *ΔspoVM::tet amyE::spoVM^{I15A} cat thrC::cmpA^{S37A} spec*

IT735 *amyE::P$_{hyperspank}$-clpX^{E182A}-His$_6$ spec ΔclpX::kan thrC::clpX erm sacA::P$_{hyperspank}$-cmpA-gfp cat*

IT751 *amyE::P$_{hyperspank}$-clpX$^{I34M, E182A}$-His$_6$ spec ΔclpX::kan thrC::clpX erm sacA::P$_{hyperspank}$-cmpA-gfp cat*

IT760 *amyE::P$_{hyperspank}$-clpX^{E182A}-His$_6$ spec ΔclpX::kan thrC::clpX erm sacA::P$_{hyperspank}$-cmpA^{P2A}-gfp cat*

IT818	*amyE::$P_{hyperspank}$-clpX^{E182A}-His_6 spoIVA^{L424F} yphF::erm sacA::$P_{hyperspank}$-cmpA-gfp cat*
IT828	*amyE::$P_{hyperspank}$-clpX^{E182A}-His_6 ΔyphF::erm sacA::$P_{hyperspank}$-cmpA-gfp cat*
IT784	*amyE::$P_{hyperspank}$-clpX^{E182A} spec sacA::$P_{hyperspank}$-cmpA-gfp-His_6 cat*
IT829	*amyE::$P_{hyperspank}$-clpX^{E182A} spec sacA::$P_{hyperspank}$-cmpA^{P2A}-gfp-His_6 cat*
KP73	*ΔspoIVA::kan*
KR103	*ΔspoVM::tet amyE::spoVM^{WT} cat*
KR165	*ΔspoVM::tet amyE::spoVM^{Wt} cat thrC::gfp-spoIVA spec*
KRC77	*ΔspoVM::tet amyE::spoVM^{I15A} cat thrC::gfp-spoIVA spec*
IT839	*ΔspoVM::tet amyE::spoVM^{I15A} cat thrC::gfp-spoIVA spec ΔcmpA::erm*
IT852	*ΔspoVM::tet amyE::spoVMspoVM^{I15A} cat thrC::gfp-spoIVA^{L424F} spec*
IT869	*ΔspoVM::tet amyE::spoVM^{WT} cat thrC:: gfp -spoIVA^{L424F} spec ΔyphF::erm spoIVA^{L424F}*
IT870	*ΔspoVM::tet amyE::spoVM^{I15A} cat thrC:: gfp -spoIVA^{L424F} spec ΔyphF::erm spoIVA^{L424F}*
IT883	*ΔspoVM::tet amyE:: spoVM^{I15A} cat thrC::gfp-spoIVA spec clpX^{E44G}*
IT884	*ΔspoVM::tet amyE:: spoVM^{I15A} cat thrC::gfp-spoIVA spec clpX^{I34M}*
SE191	*amyE::$P_{hyperspank}$-cmpA spec*
IT481	*amyE::$P_{hyperspank}$-cmpA spec thrC::$P_{hyperspank}$-clpX erm*
CVO1195	*amyE:: spoVM-gfp cat*
KRC1	*amyE::spoVM(K2A)-gfp cat*
CVO1395	*amyE::spoVM(P9A)-gfp cat*

Author Contributions

C.A.W characterized the majority of CmpA point mutants. D.L.P. analyzed harvested peptidoglycan. I.S.T. did remaining experiments. I.S.T. and K.S.R. analyzed and interpreted data.

Chapter 4

Additional factors contributing to the orchestration of coat and cortex assembly

INTRODUCTION

The linked assembly of the coat and cortex during sporulation was first observed when researchers observed that the deletion of genes encoding the coat proteins SpoVM and SpoIVA also prevented cortex assembly (Roels et al., 1992; Levin et al, 1993). Since then, the major components involved in the assembly of each individual structure have been identified, but other than SpoVM and SpoIVA, the factors coordinating the linked assembly of coat and cortex have largely remained elusive. Despite the identification of the CmpA-dependent cell death pathway, the precise roles of SpoVM and SpoIVA in cortex assembly are still unknown. To further understand the complex interactions that coordinate coat and cortex assembly we selected for additional suppressors of cortex-deficient mutants.

RESULTS

SpoVM$^{G13V, I15A}$

From a selection using the *spoVM*^{I15A} mutant we isolated an intragenic suppressor which changed the glycine at residue 13 of SpoVM to valine and brought the sporulation efficiency up to 0.2 relative to wild type (Table 4.1, Strain C). While wild type cells normally degrade CmpA-GFP in cells that have reached the phase bright forespore state, *spoVM*^{I15A} cells are unable to degrade CmpA-GFP in phase bright forespores. Our model suggests that the inability of SpoVM to signal proper coat assembly in the *spoVM*^{I15A} mutant is the reason for CmpA-GFP persistence and led us to wonder whether the intragenic suppressor was able to restore CmpA-GFP degradation. When we monitored CmpA-GFP localization and persistence in the *spoVM*^{G13V,I15A} suppressor mutant we found that CmpA-GFP localized similarly to wild type at an early time point (Fig. 4.1C) and CmpA-GFP degradation was also restored similarly to wild type in phase bright forespores (Fig. 4.1F). The data therefore suggested that SpoVM may be undergoing a structural change to signal proper coat assembly and that this structural change facilitates degradation of CmpA-GFP upon reaching the phase bright state.

Figure 4.1. CmpA-GFP degradation in phase bright forespores is restored by the *spoVM*$^{G13V, I15A}$ suppressor. Localization and persistence of CmpA-GFP in wild type (A,D), *spoVM*^{I15A} (B, E) or *spoVM*^{G13V,I15A} cells at $t_{3.5}$ (A-C) or $t_{5.5}$ (D-F) after induction of sporulation. Arrows indicate a phase bright forespore.

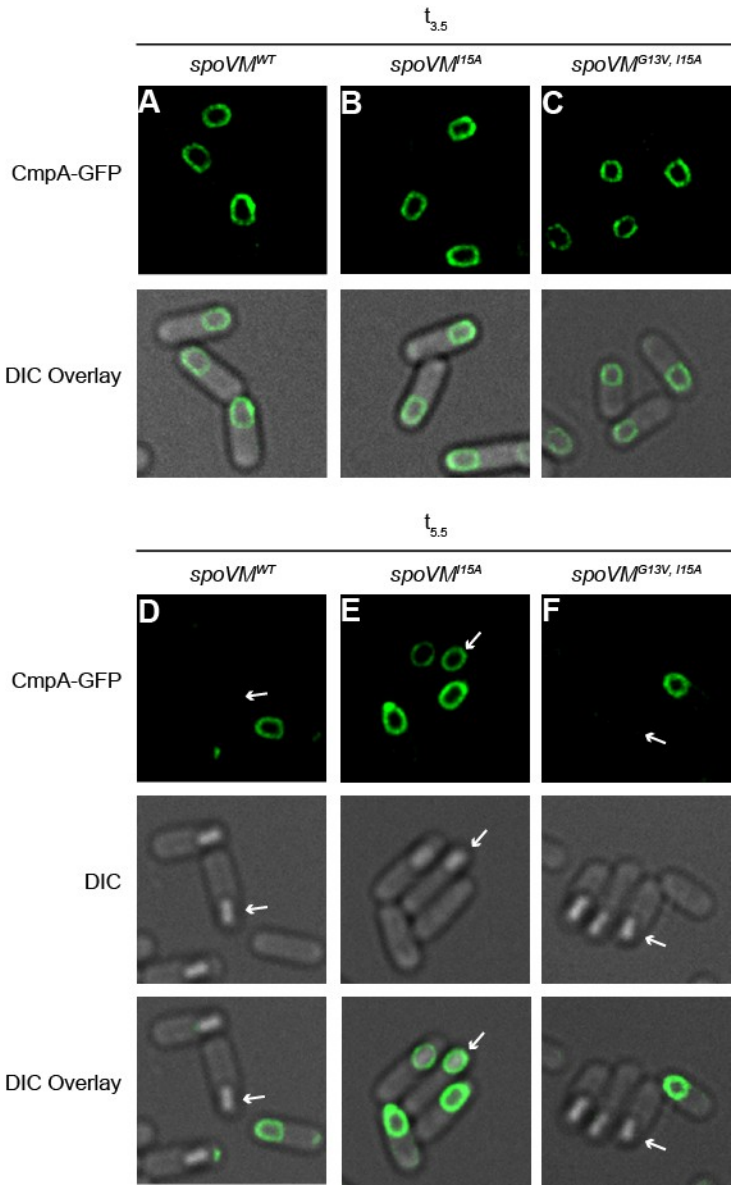

Table 4.1. Sporulation efficiencies of additional *spoVM*^{I15A} suppressors. Standard deviation from mean is reported in parentheses (n=3).

Strain[a]	*spoVM*	Suppressor	Sporulation Efficiency
A	WT	-	1
B	*spoVM*^{I15A}	-	1 x 10^{-6} (2 x 10^{-7})
C	*spoVM*^{I15A}	*spoVM* $^{G13V, I15A}$	0.2 (0.08)
D	*spoVM*^{I15A}	*ymfH*$^{\Delta 291-428}$	0.01 (1 x 10^{-3})
E	*spoVM*^{I15A}	*spoVID*$^{1-545}$	0.08 (0.01)

[a] Strain A: PY79; B: KR322; C: IT2; D: SE282; E: IT899. Genotypes are listed in Table 4.5.

YmfH

We also isolated an extragenic suppressor of the *spoVM*^{I15A} mutant and mapped it to the *ymfH* gene, which encodes a putative processing protease of unknown function. The original suppressor was a single nucleotide change which resulted in a C-terminal truncation of YmfH, and brought the sporulation efficiency from 1 x 10^{-6} to 0.01 relative to wild type (Table 4.1, Strain B and D). To determine whether the suppressor was causing a loss-of-function in YmfH we deleted the *ymfH* gene and tested whether it was also able to suppress the *spoVM*^{I15A} sporulation defect. Similar to the C-terminal truncation in YmfH the complete removal of YmfH also suppressed *spoVM*^{I15A} (Table 4.2, Strain H) indicating that the original suppressor was causing a loss of function.

Next, we wondered if the putative protease activity of YmfH was important for suppression. To test this, we constructed an *ymfH*^{E71AH72A} putative active site mutant and found that loss of putative protease activity was sufficient for suppression of the sporulation defect imposed by the *spoVM*^{I15A} mutant (Table 4.2; Strain J). Therefore, it appears that YmfH's putative proteolytic activity plays a role in helping to orchestrate coat and cortex assembly, however, the mechanism still remains unclear.

Table 4.2. Sporulation efficiencies of strains harboring *spoVM*^{I15A} with variations of *ymfH*. Standard deviation from mean is reported in parentheses (n=3).

Strain[a]	*spoVM*	*ymfH*	Sporulation Efficiency
F	WT	WT	1
G	WT	Δ	1 (0.076)
H	*spoVM*^{I15A}	Δ	0.01 (5 x 10^{-3})
I	*spoVM*^{I15A}	WT	1.8 X 10^{-4} (7 X 10^{-5})
J	*spoVM*^{I15A}	*ymfH*^{E71AH72A}	0.15 (0.09)

[a] Strain F: PY79; G: IT77; H: IT87; I: IT397; J: IT410. Genotypes are listed in Table 4.5.

SpoVID and YsxE

SpoVID is a coat protein that interacts with SpoIVA (Mullerova, Krajcikova, & Barak, 2009) and has been reported to be required for the encasement step of coat assembly (Wang et al., 2009). The deletion of *spoVID* was reported to have no effect on cortex assembly via examination by electron microscopy (Beall et al., 1993), however we found that deleting *spoVID* decreased heat resistance to 0.07 relative to wild type (Table 4.3, Strain M) suggesting there may be slight defects in cortex assembly. Our lab isolated a *spoVID* mutant that caused a C-terminal truncation causing only the first 545 amino acids to be translated that suppressed the sensor T *spoIVA*$^{T70-71A}$ mutant. Since deletion of *cmpA* also suppressed the *spoIVA*$^{T70-71A}$ mutant (Table 3.6, Strain AA), we wondered whether the truncation in SpoVID was acting similarly to a deletion of *cmpA*. To test this, we determined if the truncated SpoVID mutant was able to suppress the cortex-deficient *spoVM*^{I15A} mutant by measuring the sporulation efficiency and found that the *spoVID*$^{1-545}$ was able to suppress the *spoVM*^{I15A} mutation (Table 4.1, Strain E). The truncation in SpoVID appears to be a loss of function since deletion of *spoVID* was also able to suppress the *spoVM*^{I15A} mutant (Table 4.3, Strain N). As a result, we concluded that SpoVID may indeed be playing a similar roll to CmpA in inhibiting cortex assembly and

wondered whether suppression of *spoVM*^{I15A} was through stabilization of SpoIVA. Thus, we used fluorescence microscopy to observe the localization and persistence of GFP-SpoIVA in wild type and *spoVM*^{I15A} cells with or without the deletion of *spoVID* (Fig. 4.2). We found that similarly to the deletion of *cmpA* (Fig. 3.7H), deletion of *spoVID* in *spoVM*^{I15A} cells restored stability of GFP-SpoIVA in phase bright forespores (Fig. 4.2J). Interestingly, the deletion of *spoVID* caused GFP-SpoIVA localization to be less homogenously distributed around the forespore in both wild type (Fig.4.2C and I) and *spoVM*^{I15A} cells (Fig.4.2D and J), however, these results differ from the reported localization defects that were seen when looking at SpoIVA-GFP in the absence of *spoVID* where they saw a single cap on the mother cell side of the forespore (Wang et al., 2009).

Table 4.3. Sporulation efficiencies of strains harboring *spoVM*^{I15A} with or without deletion of *spoVID.* Standard deviation from mean is reported in parentheses (n=3).

Strain[a]	*spoVM*	*spoVID*	Sporulation Efficiency
K	WT	WT	1
L	*spoVM*^{I15A}	WT	1.8×10^{-5} (8×10^{-6})
M	WT	Δ	0.07 (0.02)
N	*spoVM*^{I15A}	Δ	0.01

[a] Strain K: PY79; L: IT854; M: AD394; N: IT885. Genotypes are listed in Table 4.5.

SpoVID exists in an operon with *ysxE*, which is a gene of unknown function that localizes to the inner spore coat (McKenney & Eichenberger, 2012). Bioinformatics analysis suggests that YsxE is an aminoglycoside kinase that may be responsible for phosphorylating a sugar. We wondered whether YsxE affects SpoVID's activity or role in SpoIVA degradation and observed the effect of deleting *ysxE* on GFP-SpoIVA stability. We found that similar to deletion of *cmpA* and *spoVID*, deletion of *ysxE* also prevented degradation of GFP-SpoIVA in phase

bright forespores of *spoVM*^{I15A} cells (Fig.4.2L). However, the mechanisms through which YsxE and SpoIVD are normally participating in SpoIVA degradation in *spoVM*^{I25A} cells are still unknown.

ClpY

Since the co-overexpression of *cmpA* and *clpX* caused a more drastic decrease in sporulation efficiency, which would allow for more stringent selection we decided to use this strain for selection of spontaneous suppressors. From this selection we identified a suppressor in the *clpY* gene (also called *codX*), which similarly to *clpX* encodes the ATPase subunit of the ClpYQ (also called CodXW) protease. ClpYQ in *B. subtilis* shares 52% amino acid identity with the *E.coli* HslUV protease and has been reported to act as an N-terminal serine protease (Kang et al., 2001). The suppressor was a change in the leucine at residue 210 to a glutamine. Based on molecular modeling the suppressor mutation appears to lie in the I domain of ClpY which is responsible for interacting with substrates (Krishnamoorthy et al., 2008). We then wondered whether *clpY* or *clpQ* were necessary for sporulation and found that deletion of *clpY* or *clpQ* had near wild type levels of sporulation efficiency (Table 4.4, Strains Q and R) indicating they are not required for sporulation. While the *clpY*^{L210Q} suppressor was identified as a suppressor of the *cmpA* and *clpX* overexpressing strain, we wanted to check if it also suppressed the *cmpA* overexpressing strain and found that it did (Table 4.4, Strain T). To determine whether the suppression was due to a loss in function of ClpYQ we individually deleted *clpY* and *clpQ* in the *cmpA* overexpressing strain and found that both had no effect on the *cmpA* overexpressing sporulation defect (Table 4.4, Strains U and V) suggesting the suppressor may not be a loss in function, but rather a change or gain in function.

Table 4.4. Sporulation efficiencies of *clpY* and *clpQ* mutants with or without *cmpA* overexpression. Standard deviation from mean is reported in parentheses (n=3). "++" indicates overexpression.

Strain[a]	*cmpA*	*clpY*	*clpQ*	Sporulation Efficiency
P	WT	-	-	1
Q	WT	Δ	-	0.35
R	WT	-	Δ	0.97
S	++	-	-	0.005 (0.01)
T	++	$clpY^{L210Q}$	-	0.22 (0.15)
U	++	Δ	-	0.002 (0.05)
V	++	-	Δ	0.009 (0.003)

[a] Strain P: PY79; Q: IT654; R: IT653; S: IT478; T: CSS7; U: IT662; V: IT660. Genotypes are listed in Table 4.5.

CONCLUSION

While the exact roles of YmfH, SpoVID and YsxE in spore envelope assembly remain unclear, we have established that their loss-of-function leads to suppression of the $spoVM^{I15A}$ sporulation defect, which indicates they normally have inhibitory roles on sporulation. In this fashion, they behave similarly to CmpA, and could be acting in the CmpA-dependent regulated cell death pathway to assist in the degradation of SpoIVA. This possibility seems to be likely in the case of SpoVID and YsxE since their deletions lead to SpoIVA stability. However, the effect of YmfH deletion on SpoIVA is currently unknown and it could be participating in a parallel pathway. Since proteolytic activity of YmfH is important for its inhibitory function, identifying its substrate(s) could help us understand its mechanism of action.

The mutation in ClpY does not appear to be a complete loss-of-function, but may be a change or gain-of-function. However, similar to YmfH, the substrate(s) of ClpY are unknown and its specific role in spore envelope assembly pathway remains a mystery. Since a change of

function in the ClpY suppressor mutant is possible, it is not entirely clear whether ClpY even acts in this pathway ordinarily. Both YmfH and ClpY do not have clear sporulation promoters and when deleted have no sporulation defect suggesting that they may not be sporulation-specific proteins. However, they may be playing analogous roles to other sporulation-specific proteins and the charcteriziation of the suppressor mutants further may still give us insight into the spore envelope assembly pathway.

Table 4.5. Strains used in this chapter.

Strain	Genotype	Source
PY79	Prototrophic derivative of *B. subtilis* 168	Youngman et al., 1984
IT478	*amyE::P$_{sigA}$-cmpA spec*	
KR322	Δ*spoVM::tet amyE::spoVM^{I15A} cat*	Ebmeier et al., 2012
IT2	Δ*spoVM::tet amyE::spoVM^{G13V,I15A} cat*	
SE282	Δ*spoVM::tet amyE::spoVM^{I15A} cat thrc::cmpA spec ymfH$^{\Delta 291-428}$*	
IT77	Δ*ymfH::kan*	
IT87	Δ*spoVM::tet amyE::spoVM^{I15A} cat* Δ*ymfH::kan*	
IT397	Δ*spoVM::tet amyE::P$_{hyperspank}$-ymfH spec thrC::spoVM^{I15A} erm* Δ*ymfH::kan*	
IT410	Δ*spoVM::tet amyE::P$_{hyperspank}$-ymfH^{E71AH72A} spec thrC::spoVM^{I15A} erm* Δ*ymfH::kan*	
IT654	Δ*clpY::erm*	
IT653	Δ*clpQ::erm*	
CSS7	*amyE::P$_{hyperspank}$-cmpA spec thrC::P$_{hyperspank}$-clpX erm clpY^{L210Q}*	
IT662	Δ*clpY::erm amyE::P$_{sigA}$-cmpA spec*	
IT660	Δ*clpQ::erm amyE::P$_{sigA}$-cmpA spec*	
SE381	Δ*spoVM::tet amyE::P$_{hyperspank}$-cmpA-gfp spec thrC::spoVM^{WT} erm*	Ebmeier et al., 2012
SE380	Δ*spoVM::tet amyE::P$_{hyperspank}$-cmpA-gfp spec thrC::spoVM^{I15A} erm*	Ebmeier et al., 2012
IT854	Δ*spoVM::tet thrC::spoVM^{I15A} spec*	
IT898	Δ*spoVM::tet thrC::spoVM^{WT} spec amyE::spoVID$^{1-545}$ cat* Δ*spoVID::kan*	
IT899	Δ*spoVM::tet thrC::spoVM^{I15A} spec amyE::spoVID$^{1-545}$ cat* Δ*spoVID::kan*	
AD394	Δ*spoVID::kan*	Driks et al.,

1994

IT885	*∆spoVM::tet amyE::spoVM^{I15A} cat ∆spoVID::kan*
KR165	*∆spoVM::tetR amyE::spoVM^{WT} cat thrC::gfp-spoIVA spec*
KRC77	*∆spoVM::tet amyE::spoVM^{I15A} cat thrC::gfp-spoIVA spec*
IT887	*∆spoVM::tet amyE::spoVM^{WT}cat thrC::gfp-spoIVA spec ∆spoVID::kan*
IT888	*∆spoVM::tet amyE::spoVM^{I15A} cat thrC::gfp-spoIVA spec ∆spoVID::kan*
IT932	*∆spoVM::tetR amyE::spoVM^{WT} cat thrC::gfp-spoIVA spec ∆ysxE::erm*
IT937	*∆spoVM::tet amyE::spoVM^{I15} cat thrC::gfp-spoIVA spec ∆ysxE::erm*
IT254	*∆spoVM::tet amyE::VM^{G13V,I15A} cat thrC::P$_{hyperspank}$-cmpA-gfp erm*

Figure 4.2. Degradation of GFP-SpoIVA in *spoVM*^{15A} cells is inhibited by the deletion of *spoVID* and *ysxE*. Localization and persistence of GFP-SpoIVA at $t_{3.5}$ (A-F) or $t_{5.5}$ (G-L) after induction of sporulation in *spoVM*^{WT} (A, C, E, G, I, K) or *spoVM*^{I15A} (B, D, F, H, J, L) cells with a deletion of *spoVID* (C, D, I, J), a deletion of *ysxE* (E, F, K, L) or no deletion (A, B, G, H). Arrows indicate phase bright forespores.

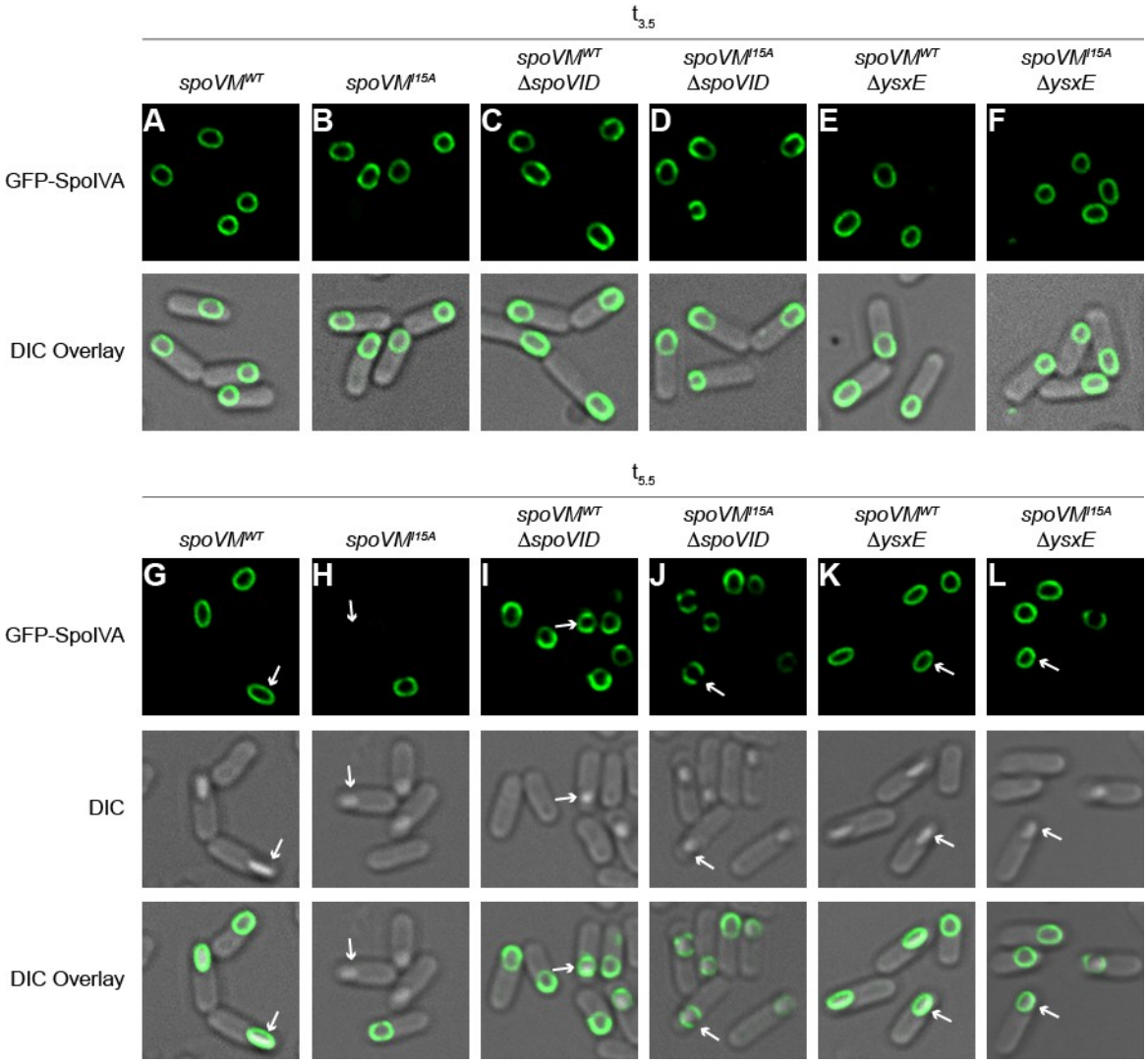

Chapter 5

Concluding Remarks

At the onset of our research, little was known about the unique roles that SpoVM and SpoIVA play in orchestrating the coordinated assembly of the coat and cortex. Thus our goal was to further elucidate the mechanisms through which SpoVM and SpoIVA coordinate the assemblies of these two spatially separated macromolecular structures. Our initial approach was to utilize a *spoVM*^{I15A} mutant that was defective in cortex, but not coat assembly to specifically investigate the role that SpoVM plays in cortex assembly. Through the selection of spontaneous suppressors that restored heat resistance and cortex assembly we identified a previously un-annotated small gene, which we named *cortex morphogenetic protein A* (*cmpA*). We found that *cmpA* encoded a small protein of only 37-amino acids with no conserved motifs to give us insight into its biological function. In characterizing *cmpA,* we found that it was expressed during sporulation under the mother cell-specific transcription factors σ^E and SpoIIID. When we tagged CmpA with GFP we saw that it localized to the forespore surface as would be expected from a protein involved in coordinating coat and cortex assembly. Overexpression of *cmpA* caused defects in sporulation and deletion of *cmpA* restored cortex formation in the *spoVM*^{I15A} mutant indicating CmpA was playing an inhibitory role during sporulation.

Together our data suggested a model where CmpA participates in a quality control pathway for spore envelope assembly. We proposed that SpoVM and SpoIVA localize to the outer forespore membrane during engulfment and once they properly initiate spore envelope assembly a signal is sent to degrade CmpA. However, the basis of this signal and what is responsible for degrading CmpA remain a mystery. We hypothesize that the signal to degrade CmpA may be a structural change in SpoVM and SpoIVA and that this structural change is unable to occur in cortex-deficient SpoVM and SpoIVA mutants. The isolation of the *spoVM*^{G13V,I15A} intragenic suppressor that restored CmpA degradation in the *spoVM*^{I15A} mutant is consistent with the idea that the structure of SpoVM is important for signaling, however the mechanism through which this structural change may be conveying a signal is still unknown.

In instances when initiation of spore envelope assembly is unable to occur properly, CmpA is unable to be degraded and we propose it acts as switch to activate a regulated cell death pathway. In this pathway, CmpA acts as an adaptor to deliver SpoIVA to ClpXP for degradation. CmpA interaction with ClpX is independent of SpoIVA while SpoIVA interaction with ClpX is dependent on CmpA consistent with an adaptor function. Suppressor mutations affecting assembly of the CmpA-ClpX-SpoIVA complex all restored stability of SpoIVA and restored sporulation efficiency indicating that the degradation of SpoIVA via complex formation is normally responsible for the defect in sporulation. While both CmpA and ClpXP are necessary for the degradation of SpoIVA, we found that they are not sufficient. Interestingly, we noted that SpoIVA was degraded only in cells that had reached the phase bright forespore state, which is indicative of forespore dehydration. This is the same stage at which CmpA abnormally persists in the cortex-deficient *spoVM*^{I15A} mutant and suggested that the transition to the phase bright state was required for activation of CmpA-dependent degradation of SpoIVA. We then found that activation of the late-acting mother cell-specific sigma factor, σ^K, prevented degradation of SpoIVA indicating that unknown factor(s) under the σ^K regulon are required for degradation of SpoIVA. Additionally, prevention of σ^K activation also prevented degradation of CmpA in wild type cells suggesting that unknown factor(s) under σ^K are also required for degradation of CmpA during proper spore envelope assembly. Thus, we propose that the activation of σ^K is the point at which the cell evaluates the assembly state of the spore envelope to determine whether CmpA should be degraded or whether it should persist and activate degradation of SpoIVA. We also found that *spoVID* and *ysxE*, which reside in an operon together, are required for SpoIVA degradation. SpoVID has been reported to interact with SpoIVA (Mullerova et al., 2009) and is important for the encasement step of coat assembly (Wang et al., 2009). The function of YsxE is unknown, but bioinformatics analysis suggests it may be a kinase. Since SpoVID interacts with SpoIVA we wondered whether it was required for assembly of the CmpA-ClpX-SpoIVA complex,

but found that deleting *spoVID* had no effect on complex formation. In conclusion, in addition to CmpA and ClpX, unknown factor(s) under σ^K control as well as *spoVID* and *ysxE* are required for degradation of SpoIVA. There may be additional undiscovered factors that are also necessary for degradation of SpoIVA.

SpoIVA is a morphogenetic protein that uses ATP hydrolysis to polymerize into static filaments that serve as a basement layer atop which other coat proteins are deposited. While ordinarily the peptidoglycan of cell walls acts to maintain a cell's size and shape, in the absence of a properly assembled cortex, SpoIVA may help to maintain the forespore's stability. We found that in instances when SpoIVA was degraded, the cells eventually underwent cell lysis and we propose that this is a mechanism through which cells defective in spore envelope assembly are selectively removed from the population.

In the absence of *cmpA* cells with mutations in *spoVM* and *spoIVA* are able to complete the sporulation program at a higher frequency, but the end result was the maintenance of cells that lack a robust ability to sporulate properly in the population. In nutrient rich conditions that do not require sporulation, the rapid accumulation of mutations in sporulating genes can occur and lead to loss of the ability to sporulate. However, sporulation is a last resort survival mechanism that allows *B. subtilis* to survive harsh environmental conditions. Therefore, maintaining the fidelity of the sporulation program is essential for the *B. subtilis'* long-term survival in fluctuating environments. While natural selection may help select for *B. subtilis* that are able to maintain robust sporulation programs, we believe a more active selection is necessary since non-sporulating subpopulations that have accumulated mutations in sporulation genes can easily take over the population.

In the environment, populations of bacteria capable of sporulation utilize a bet-hedging strategy wherein only a subpopulation of the cells undergoes sporulation. Therefore, any subpopulation that is unable to sporulate can continue to grow vegetatively as long as it is able to survive. In this fashion, these non-sporulating mutants may easily outgrow cells that are able

to sporulate if there is no environmental pressure present at any given time. Thus, we propose active selection for cells that have a robust sporulation program that is able to properly assemble the spore envelope is necessary for the long-term maintenance of the sporulation program in the bacterial species.

Despite the discovery of the CmpA-dependent regulated cell death pathway that ensures proper spore envelope assembly during sporulation, there are still many parts of the pathway that remain a mystery. Whether the mechanism that signals proper coat assembly is really a structural change is unclear. How proper coat assembly transmits a signal to degrade CmpA and the identity of the protease responsible for degrading CmpA also remain a mystery. While we have identified factors that are required for SpoIVA degradation, we have not yet found all factors sufficient for degradation. Additionally, the roles that the additional *spoVM*^{I15A} suppressors play in spore envelope assembly are unclear. Perhaps SpoVM and SpoIVA play additional roles in cortex assembly that have yet to be identified.

Nonetheless, we have identified a novel pathway that we believe supports the concept of altruistic cell death in single-celled organisms. Additionally, it has revealed that small proteins, which have been conspicuously overlooked in the past, can play fundamental roles during developmental processes. Both SpoVM and CmpA are sproteins of less than 50 amino acids that are key players in the CmpA-dependent regulated cell death pathway. To our knowledge, CmpA is the smallest protease adaptor identified suggesting that there may be other important sprotein adaptors that have yet to be discovered. In developing novel antibiotics, one might consider engineering sproteins similar to CmpA that may activate cell death pathways in pathogenic bacteria.

References

Abanes-De Mello, A., Sun, Y. L., Aung, S., & Pogliano, K. (2002). A cytoskeleton-like role for the bacterial cell wall during engulfment of the Bacillus subtilis forespore. *Genes Dev, 16*(24), 3253-3264.

Atrih, A., & Foster, S. J. (1999). The role of peptidoglycan structure and structural dynamics during endospore dormancy and germination. *Antonie Van Leeuwenhoek, 75*(4), 299-307.

Atrih, A., & Foster, S. J. (2001). Analysis of the role of bacterial endospore cortex structure in resistance properties and demonstration of its conservation amongst species. *J Appl Microbiol, 91*(2), 364-372.

Baker, M. D., & Neiditch, M. B. (2011). Structural basis of response regulator inhibition by a bacterial anti-activator protein. *PLoS Biol, 9*(12), e1001226. doi: 10.1371/journal.pbio.1001226

Baker, T. A., & Sauer, R. T. (2012). ClpXP, an ATP-powered unfolding and protein-degradation machine. *Biochim Biophys Acta, 1823*(1), 15-28. doi: 10.1016/j.bbamcr.2011.06.007

Battesti, A., & Gottesman, S. (2013). Roles of adaptor proteins in regulation of bacterial proteolysis. *Curr Opin Microbiol, 16*(2), 140-147. doi: 10.1016/j.mib.2013.01.002

Beall, B., Driks, A., Losick, R., & Moran, C. P., Jr. (1993). Cloning and characterization of a gene required for assembly of the Bacillus subtilis spore coat. *J Bacteriol, 175*(6), 1705-1716.

Beaman, T. C., & Gerhardt, P. (1986). Heat resistance of bacterial spores correlated with protoplast dehydration, mineralization, and thermal adaptation. *Appl Environ Microbiol, 52*(6), 1242-1246.

Becker, E. C., & Pogliano, K. (2007). Cell-specific SpoIIIE assembly and DNA translocation polarity are dictated by chromosome orientation. *Mol Microbiol, 66*(5), 1066-1079.

Ben-Yehuda, S., Fujita, M., Liu, X. S., Gorbatyuk, B., Skoko, D., Yan, J., . . . Losick, R. (2005). Defining a centromere-like element in Bacillus subtilis by Identifying the binding sites for the chromosome-anchoring protein RacA. *Mol Cell, 17*(6), 773-782.

Ben-Yehuda, S., Rudner, D. Z., & Losick, R. (2003). RacA, a bacterial protein that anchors chromosomes to the cell poles. *Science, 299*(5606), 532-536.

Bender, G. R., & Marquis, R. E. (1985). Spore heat resistance and specific mineralization. *Appl Environ Microbiol, 50*(6), 1414-1421.

Blaylock, B., Jiang, X., Rubio, A., Moran, C. P., Jr., & Pogliano, K. (2004). Zipper-like interaction between proteins in adjacent daughter cells mediates protein localization. *Genes Dev, 18*(23), 2916-2928.

Boonstra, M., de Jong, I. G., Scholefield, G., Murray, H., Kuipers, O. P., & Veening, J. W. (2013). Spo0A regulates chromosome copy number during sporulation by directly binding to the origin of replication in Bacillus subtilis. *Mol Microbiol, 87*(4), 925-938.

Bos, J., Yakhnina, A. A., & Gitai, Z. (2012). BapE DNA endonuclease induces an apoptotic-like response to DNA damage in *Caulobacter*. *Proc Natl Acad Sci U S A, 109*(44), 18096-18101. doi: 10.1073/pnas.1213332109

Broder, D. H., & Pogliano, K. (2006). Forespore engulfment mediated by a ratchet-like mechanism. *Cell, 126*(5), 917-928.

Burbulys, D., Trach, K. A., & Hoch, J. A. (1991). Initiation of sporulation in B. subtilis is controlled by a multicomponent phosphorelay. *Cell, 64*(3), 545-552.

Burke, B. (2001). Lamins and apoptosis: a two-way street? *J Cell Biol, 153*(3), F5-7.

Burkholder, W. F., Kurtser, I., & Grossman, A. D. (2001). Replication initiation proteins regulate a developmental checkpoint in Bacillus subtilis. *Cell, 104*(2), 269-279.

Burton, B., & Dubnau, D. (2010). Membrane-associated DNA transport machines. *Cold Spring Harb Perspect Biol, 2*(7), a000406.

Burton, B. M., Marquis, K. A., Sullivan, N. L., Rapoport, T. A., & Rudner, D. Z. (2007). The ATPase SpoIIIE transports DNA across fused septal membranes during sporulation in Bacillus subtilis. *Cell, 131*(7), 1301-1312.

Camp, A. H., & Losick, R. (2009). A feeding tube model for activation of a cell-specific transcription factor during sporulation in Bacillus subtilis. *Genes Dev, 23*(8), 1014-1024.

Campo, N., & Rudner, D. Z. (2006). A branched pathway governing the activation of a developmental transcription factor by regulated intramembrane proteolysis. *Mol Cell, 23*(1), 25-35.

Cano, R. J., & Borucki, M. K. (1995). Revival and identification of bacterial spores in 25- to 40-million-year-old Dominican amber. *Science, 268*(5213), 1060-1064.

Carniol, K., Ben-Yehuda, S., King, N., & Losick, R. (2005). Genetic dissection of the sporulation protein SpoIIE and its role in asymmetric division in Bacillus subtilis. *J Bacteriol, 187*(10), 3511-3520.

Castaing, J. P., Lee, S., Anantharaman, V., Ravilious, G. E., Aravind, L., & Ramamurthi, K. S. (2014). An autoinhibitory conformation of the *Bacillus subtilis* spore coat protein SpoIVA prevents its premature ATP-independent aggregation. *FEMS Microbiol Lett, 358*(2), 145-153. doi: 10.1111/1574-6968.12452

Castaing, J. P., Nagy, A., Anantharaman, V., Aravind, L., & Ramamurthi, K. S. (2013). ATP hydrolysis by a domain related to translation factor GTPases drives polymerization of a static bacterial morphogenetic protein. *Proc Natl Acad Sci U S A, 110*(2), E151-160.

Catalano, F. A., Meador-Parton, J., Popham, D. L., & Driks, A. (2001). Amino acids in the Bacillus subtilis morphogenetic protein SpoIVA with roles in spore coat and cortex formation. *J Bacteriol, 183*(5), 1645-1654.

Chada, V. G., Sanstad, E. A., Wang, R., & Driks, A. (2003). Morphogenesis of bacillus spore surfaces. *J Bacteriol, 185*(21), 6255-6261.

Chai, Y., Kolter, R., & Losick, R. (2011). Reversal of an epigenetic switch governing cell chaining in Bacillus subtilis by protein instability. *Mol Microbiol, 78*(1), 218-229.

Chu, F., Kearns, D. B., McLoon, A., Chai, Y., Kolter, R., & Losick, R. (2008). A novel regulatory protein governing biofilm formation in Bacillus subtilis. *Mol Microbiol, 68*(5), 1117-1127.

Cohn, F. (1877). Untersuchungen über bacterien. IV. Beiträge zur biologie der Bacillen. *Beiträge zur biologie der Pflanzen, 7*, 249-276.

Coote, J. G. (1972). Sporulation in Bacillus subtilis. Characterization of oligosporogenous mutants and comparison of their phenotypes with those of asporogenous mutants. *J Gen Microbiol, 71*(1), 1-15.

Costa, T., Isidro, A. L., Moran, C. P., Jr., & Henriques, A. O. (2006). Interaction between coat morphogenetic proteins SafA and SpoVID. *J Bacteriol, 188*(22), 7731-7741.

Cunningham, K. A., & Burkholder, W. F. (2009). The histidine kinase inhibitor Sda binds near the site of autophosphorylation and may sterically hinder autophosphorylation and phosphotransfer to Spo0F. *Mol Microbiol, 71*(3), 659-677.

Daniel, R. A., Drake, S., Buchanan, C. E., Scholle, R., & Errington, J. (1994). The Bacillus subtilis spoVD gene encodes a mother-cell-specific penicillin-binding protein required for spore morphogenesis. *J Mol Biol, 235*(1), 209-220.

Date, A., Pasini, P., & Daunert, S. (2010). Fluorescent and bioluminescent cell-based sensors: strategies for their preservation. *Adv Biochem Eng Biotechnol, 117*, 57-75.

Deves, M., & Bourrat, F. (2012). Transcriptional mechanisms of developmental cell cycle arrest: problems and models. *Semin Cell Dev Biol, 23*(3), 290-297. doi: 10.1016/j.semcdb.2012.03.003

Diez, V., Schujman, G. E., Gueiros-Filho, F. J., & de Mendoza, D. (2012). Vectorial signalling mechanism required for cell-cell communication during sporulation in Bacillus subtilis. *Mol Microbiol, 83*(2), 261-274.

Doan, T., Coleman, J., Marquis, K. A., Meeske, A. J., Burton, B. M., Karatekin, E., & Rudner, D. Z. (2013). FisB mediates membrane fission during sporulation in Bacillus subtilis. *Genes Dev*.

Doan, T., Marquis, K. A., & Rudner, D. Z. (2005). Subcellular localization of a sporulation membrane protein is achieved through a network of interactions along and across the septum. *Mol Microbiol, 55*(6), 1767-1781.

Doan, T., Morlot, C., Meisner, J., Serrano, M., Henriques, A. O., Moran, C. P., Jr., & Rudner, D. Z. (2009). Novel secretion apparatus maintains spore integrity and developmental gene expression in Bacillus subtilis. *PLoS Genet, 5*(7), e1000566.

Driks, A. (2002). Maximum shields: the assembly and function of the bacterial spore coat. *Trends Microbiol, 10*(6), 251-254.

Driks, A. (2004). The bacillus spore coat. *Phytopathology, 94*(11), 1249-1251.

Driks, A., Roels, S., Beall, B., Moran, C. P., Jr., & Losick, R. (1994). Subcellular localization of proteins involved in the assembly of the spore coat of Bacillus subtilis. *Genes Dev, 8*(2), 234-244.

Duncan, L., Alper, S., Arigoni, F., Losick, R., & Stragier, P. (1995). Activation of cell-specific transcription by a serine phosphatase at the site of asymmetric division. *Science, 270*(5236), 641-644.

Dworkin, J., & Losick, R. (2001). Differential gene expression governed by chromosomal spatial asymmetry. *Cell, 107*(3), 339-346.

Dworkin, J., & Losick, R. (2005). Developmental commitment in a bacterium. *Cell, 121*(3), 401-409.

Dwyer, D. J., Camacho, D. M., Kohanski, M. A., Callura, J. M., & Collins, J. J. (2012). Antibiotic-induced bacterial cell death exhibits physiological and biochemical hallmarks of apoptosis. *Mol Cell, 46*(5), 561-572. doi: 10.1016/j.molcel.2012.04.027

Ebmeier, S. E., Tan, I. S., Clapham, K. R., & Ramamurthi, K. S. (2012). Small proteins link coat and cortex assembly during sporulation in Bacillus subtilis. *Mol Microbiol, 84*(4), 682-696.

Eichenberger, P., Fujita, M., Jensen, S. T., Conlon, E. M., Rudner, D. Z., Wang, S. T., . . . Losick, R. (2004). The program of gene transcription for a single differentiating cell type during sporulation in Bacillus subtilis. *PLoS Biol, 2*(10), e328.

Ellermeier, C. D., Hobbs, E. C., Gonzalez-Pastor, J. E., & Losick, R. (2006). A three-protein signaling pathway governing immunity to a bacterial cannibalism toxin. *Cell, 124*(3), 549-559.

Erental, A., Sharon, I., & Engelberg-Kulka, H. (2012). Two programmed cell death systems in *Escherichia coli*: an apoptotic-like death is inhibited by the mazEF-mediated death pathway. *PLoS Biol, 10*(3), e1001281. doi: 10.1371/journal.pbio.1001281

Erlendsson, L. S., Moller, M., & Hederstedt, L. (2004). Bacillus subtilis StoA Is a thiol-disulfide oxidoreductase important for spore cortex synthesis. *J Bacteriol, 186*(18), 6230-6238.

Errington, J. (2003). Regulation of endospore formation in Bacillus subtilis. *Nat Rev Microbiol, 1*(2), 117-126.

Eswaramoorthy, P., Dinh, J., Duan, D., Igoshin, O. A., & Fujita, M. (2010). Single-cell measurement of the levels and distributions of the phosphorelay components in a population of sporulating Bacillus subtilis cells. *Microbiology, 156*(Pt 8), 2294-2304.

Eswaramoorthy, P., Duan, D., Dinh, J., Dravis, A., Devi, S. N., & Fujita, M. (2010). The threshold level of the sensor histidine kinase KinA governs entry into sporulation in Bacillus subtilis. *J Bacteriol, 192*(15), 3870-3882.

Eswaramoorthy, P., Winter, P. W., Wawrzusin, P., York, A. G., Shroff, H., & Ramamurthi, K. S. (2014). Asymmetric division and differential gene expression during a bacterial developmental program requires DivIVA. *PLoS Genet, 10*(8), e1004526. doi: 10.1371/journal.pgen.1004526

Fay, A., & Dworkin, J. (2009). Bacillus subtilis homologs of MviN (MurJ), the putative Escherichia coli lipid II flippase, are not essential for growth. *J Bacteriol, 191*(19), 6020-6028.

Fay, A., Meyer, P., & Dworkin, J. (2010). Interactions between late-acting proteins required for peptidoglycan synthesis during sporulation. *J Mol Biol, 399*(4), 547-561.

Ferguson, C. C., Camp, A. H., & Losick, R. (2007). gerT, a newly discovered germination gene under the control of the sporulation transcription factor sigmaK in Bacillus subtilis. *J Bacteriol, 189*(21), 7681-7689.

Fiche, J. B., Cattoni, D. I., Diekmann, N., Langerak, J. M., Clerte, C., Royer, C. A., . . . Nollmann, M. (2013). Recruitment, Assembly, and Molecular Architecture of the SpoIIIE DNA Pump Revealed by Superresolution Microscopy. *PLoS Biol, 11*(5), e1001557.

Frandsen, N., Barak, I., Karmazyn-Campelli, C., & Stragier, P. (1999). Transient gene asymmetry during sporulation and establishment of cell specificity in Bacillus subtilis. *Genes Dev, 13*(4), 394-399.

Fujita, M., Gonzalez-Pastor, J. E., & Losick, R. (2005). High- and low-threshold genes in the Spo0A regulon of Bacillus subtilis. *J Bacteriol, 187*(4), 1357-1368.

Fujita, M., & Losick, R. (2002). An investigation into the compartmentalization of the sporulation transcription factor sigmaE in Bacillus subtilis. *Mol Microbiol, 43*(1), 27-38.

Fujita, M., & Losick, R. (2005). Evidence that entry into sporulation in Bacillus subtilis is governed by a gradual increase in the level and activity of the master regulator Spo0A. *Genes Dev, 19*(18), 2236-2244.

Gallego del Sol, F., & Marina, A. (2013). Structural basis of Rap phosphatase inhibition by Phr peptides. *PLoS Biol, 11*(3), e1001511.

Galluzzi, L., Vitale, I., Abrams, J. M., Alnemri, E. S., Baehrecke, E. H., Blagosklonny, M. V., . . . Kroemer, G. (2012). Molecular definitions of cell death subroutines: recommendations of the Nomenclature Committee on Cell Death 2012. *Cell Death Differ, 19*(1), 107-120. doi: 10.1038/cdd.2011.96

Gartner, A., Boag, P. R., & Blackwell, T. K. (2008). Germline survival and apoptosis. *WormBook*, 1-20. doi: 10.1895/wormbook.1.145.1

Gilmore, M. E., Bandyopadhyay, D., Dean, A. M., Linnstaedt, S. D., & Popham, D. L. (2004). Production of muramic delta-lactam in Bacillus subtilis spore peptidoglycan. *J Bacteriol, 186*(1), 80-89.

Gonzalez-Pastor, J. E., Hobbs, E. C., & Losick, R. (2003). Cannibalism by sporulating bacteria. *Science, 301*(5632), 510-513.

Gottesman, S. (1996). Proteases and their targets in *Escherichia coli*. *Annu Rev Genet, 30*, 465-506. doi: 10.1146/annurev.genet.30.1.465

Gottesman, S., Clark, W. P., de Crecy-Lagard, V., & Maurizi, M. R. (1993). ClpX, an alternative subunit for the ATP-dependent Clp protease of *Escherichia coli*. Sequence and in vivo activities. *J Biol Chem, 268*(30), 22618-22626.

Gould, G. W., & Dring, G. J. (1975). Heat resistance of bacterial endospores and concept of an expanded osmoregulatory cortex. *Nature, 258*(5534), 402-405.

Gould, G. W., & Hitchins, A. D. (1963). Sensitization of Bacterial Spores to Lysozyme and to Hydrogen Peroxide with Agents Which Rupture Disulphide Bonds. *J Gen Microbiol, 33*, 413-423.

Guberman, J. M., Fay, A., Dworkin, J., Wingreen, N. S., & Gitai, Z. (2008). PSICIC: noise and asymmetry in bacterial division revealed by computational image analysis at sub-pixel resolution. *PLoS Comput Biol, 4*(11), e1000233.

Guerout-Fleury, A. M., Frandsen, N., & Stragier, P. (1996). Plasmids for ectopic integration in Bacillus subtilis. *Gene, 180*(1-2), 57-61.

Hacker, G. (2013). Is there, and should there be, apoptosis in bacteria? *Microbes Infect, 15*(8-9), 640-644. doi: 10.1016/j.micinf.2013.05.005

Hagen, C. A., Hawrylewicz, E. J., & Ehrlich, R. (1964). Survival of Microorganisms in a Simulated Martian Environment. I. Bacillus Subtilis Var. Globigii. *Appl Microbiol, 12*, 215-218.

Hamon, M. A., & Lazazzera, B. A. (2001). The sporulation transcription factor Spo0A is required for biofilm development in Bacillus subtilis. *Mol Microbiol, 42*(5), 1199-1209.

Hartwell, L. H., & Weinert, T. A. (1989). Checkpoints: controls that ensure the order of cell cycle events. *Science, 246*(4930), 629-634.

Heffron, J. D., Orsburn, B., & Popham, D. L. (2009). Roles of germination-specific lytic enzymes CwlJ and SleB in *Bacillus anthracis*. *J Bacteriol, 191*(7), 2237-2247. doi: 10.1128/JB.01598-08

Henriques, A. O., & Moran, C. P., Jr. (2007). Structure, assembly, and function of the spore surface layers. *Annu Rev Microbiol, 61*, 555-588.

Higgins, D., & Dworkin, J. (2012). Recent progress in *Bacillus subtilis* sporulation. *FEMS Microbiol Rev, 36*(1), 131-148. doi: 10.1111/j.1574-6976.2011.00310.x

Hinc, K., Isticato, R., Dembek, M., Karczewska, J., Iwanicki, A., Peszynska-Sularz, G., . . . Ricca, E. (2010). Expression and display of UreA of Helicobacter acinonychis on the surface of Bacillus subtilis spores. *Microb Cell Fact, 9*, 2.

Hobbs, E. C., Fontaine, F., Yin, X., & Storz, G. (2011). An expanding universe of small proteins. *Curr Opin Microbiol, 14*(2), 167-173.

Hofmeister, A. E., Londono-Vallejo, A., Harry, E., Stragier, P., & Losick, R. (1995). Extracellular signal protein triggering the proteolytic activation of a developmental transcription factor in B. subtilis. *Cell, 83*(2), 219-226.

Holtje, J. V. (1998). Growth of the stress-bearing and shape-maintaining murein sacculus of *Escherichia coli*. *Microbiol Mol Biol Rev, 62*(1), 181-203.

Ikeda, M., Sato, T., Wachi, M., Jung, H. K., Ishino, F., Kobayashi, Y., & Matsuhashi, M. (1989). Structural similarity among Escherichia coli FtsW and RodA proteins and Bacillus subtilis SpoVE protein, which function in cell division, cell elongation, and spore formation, respectively. *J Bacteriol, 171*(11), 6375-6378.

Imae, Y., & Strominger, J. L. (1976a). Cortex content of asporogenous mutants of Bacillus subtilis. *J Bacteriol, 126*(2), 914-918.

Imae, Y., & Strominger, J. L. (1976b). Relationship between cortex content and properties of *Bacillus sphaericus* spores. *J Bacteriol, 126*(2), 907-913.

Imamura, D., Kuwana, R., Takamatsu, H., & Watabe, K. (2011). Proteins involved in formation of the outermost layer of Bacillus subtilis spores. *J Bacteriol, 193*(16), 4075-4080.

Imamura, D., Zhou, R., Feig, M., & Kroos, L. (2008). Evidence that the Bacillus subtilis SpoIIGA protein is a novel type of signal-transducing aspartic protease. *J Biol Chem, 283*(22), 15287-15299.

Ishikawa, S., Yamane, K., & Sekiguchi, J. (1998). Regulation and characterization of a newly deduced cell wall hydrolase gene (cwlJ) which affects germination of Bacillus subtilis spores. *J Bacteriol, 180*(6), 1375-1380.

Isticato, R., Cangiano, G., Tran, H. T., Ciabattini, A., Medaglini, D., Oggioni, M. R., . . . Ricca, E. (2001). Surface display of recombinant proteins on Bacillus subtilis spores. *J Bacteriol, 183*(21), 6294-6301.

Jacotot, H., & Virat, B. (1954). La longevite des spores de *B. antbracis* (premier vaccin de Pasteur). *Annales de l'Institut Pasteur, 87*, 215-217.

Janssen, F. W., Lund, A. J., & Anderson, L. E. (1958). Colorimetric assay for dipicolinic acid in bacterial spores. *Science, 127*(3288), 26-27.

Jonas, R. M., Weaver, E. A., Kenney, T. J., Moran, C. P., Jr., & Haldenwang, W. G. (1988). The Bacillus subtilis spoIIG operon encodes both sigma E and a gene necessary for sigma E activation. *J Bacteriol, 170*(2), 507-511.

Kang, M. S., Lim, B. K., Seong, I. S., Seol, J. H., Tanahashi, N., Tanaka, K., & Chung, C. H. (2001). The ATP-dependent CodWX (HslVU) protease in Bacillus subtilis is an N-terminal serine protease. *Embo J, 20*(4), 734-742. doi: 10.1093/emboj/20.4.734

Kearns, D. B., Chu, F., Branda, S. S., Kolter, R., & Losick, R. (2005). A master regulator for biofilm formation by Bacillus subtilis. *Mol Microbiol, 55*(3), 739-749.

Keaton, M. A., & Lew, D. J. (2006). Eavesdropping on the cytoskeleton: progress and controversy in the yeast morphogenesis checkpoint. *Curr Opin Microbiol, 9*(6), 540-546.

Kenney, T. J., & Moran, C. P., Jr. (1987). Organization and regulation of an operon that encodes a sporulation-essential sigma factor in Bacillus subtilis. *J Bacteriol, 169*(7), 3329-3339.

Kim, H., Hahn, M., Grabowski, P., McPherson, D. C., Otte, M. M., Wang, R., . . . Driks, A. (2006). The Bacillus subtilis spore coat protein interaction network. *Mol Microbiol, 59*(2), 487-502.

Kim, Y. I., Levchenko, I., Fraczkowska, K., Woodruff, R. V., Sauer, R. T., & Baker, T. A. (2001). Molecular determinants of complex formation between Clp/Hsp100 ATPases and the ClpP peptidase. *Nat Struct Biol, 8*(3), 230-233. doi: 10.1038/84967

Klobutcher, L. A., Ragkousi, K., & Setlow, P. (2006). The Bacillus subtilis spore coat provides "eat resistance" during phagocytic predation by the protozoan Tetrahymena thermophila. *Proc Natl Acad Sci U S A, 103*(1), 165-170.

Koshikawa, T., Beaman, T. C., Pankratz, H. S., Nakashio, S., Corner, T. R., & Gerhardt, P. (1984). Resistance, germination, and permeability correlates of Bacillus megaterium spores successively divested of integument layers. *J Bacteriol, 159*(2), 624-632.

Krishnamoorthy, N., Gajendrarao, P., Eom, S. H., Kwon, Y. J., Cheong, G. W., & Lee, K. W. (2008). Molecular modeling study of CodX reveals importance of N-terminal and C-terminal domain in the CodWX complex structure of Bacillus subtilis. *J Mol Graph Model, 27*(1), 1-12. doi: 10.1016/j.jmgm.2008.01.009

Kunkel, B., Kroos, L., Poth, H., Youngman, P., & Losick, R. (1989). Temporal and spatial control of the mother-cell regulatory gene spoIIID of Bacillus subtilis. *Genes Dev, 3*(11), 1735-1744.

Kunkel, B., Losick, R., & Stragier, P. (1990). The *Bacillus subtilis* gene for the development transcription factor sigma K is generated by excision of a dispensable DNA element containing a sporulation recombinase gene. *Genes Dev, 4*(4), 525-535.

Laaberki, M. H., & Dworkin, J. (2008). Role of spore coat proteins in the resistance of Bacillus subtilis spores to Caenorhabditis elegans predation. *J Bacteriol, 190*(18), 6197-6203.

LeDeaux, J. R., Yu, N., & Grossman, A. D. (1995). Different roles for KinA, KinB, and KinC in the initiation of sporulation in Bacillus subtilis. *J Bacteriol, 177*(3), 861-863.

Leggett, M. J., McDonnell, G., Denyer, S. P., Setlow, P., & Maillard, J. Y. (2012). Bacterial spore structures and their protective role in biocide resistance. *J Appl Microbiol, 113*(3), 485-498.

Leipe, D. D., Wolf, Y. I., Koonin, E. V., & Aravind, L. (2002). Classification and evolution of P-loop GTPases and related ATPases. *J Mol Biol, 317*(1), 41-72.

Lenarcic, R., Halbedel, S., Visser, L., Shaw, M., Wu, L. J., Errington, J., . . . Hamoen, L. W. (2009). Localisation of DivIVA by targeting to negatively curved membranes. *Embo J, 28*(15), 2272-2282.

Levdikov, V. M., Blagova, E. V., McFeat, A., Fogg, M. J., Wilson, K. S., & Wilkinson, A. J. (2012). Structure of components of an intercellular channel complex in sporulating Bacillus subtilis. *Proc Natl Acad Sci U S A, 109*(14), 5441-5445.

Levin, P. A., Fan, N., Ricca, E., Driks, A., Losick, R., & Cutting, S. (1993). An unusually small gene required for sporulation by Bacillus subtilis. *Mol Microbiol, 9*(4), 761-771.

Levine, J. H., Fontes, M. E., Dworkin, J., & Elowitz, M. B. (2012). Pulsed feedback defers cellular differentiation. *PLoS Biol, 10*(1), e1001252.

Lewis, J. C., Snell, N. S., & Burr, H. K. (1960). Water Permeability of Bacterial Spores and the Concept of a Contractile Cortex. *Science, 132*(3426), 544-545.

Liu, J., Cosby, W. M., & Zuber, P. (1999). Role of Ion and ClpX in the post-translational regulation of a sigma subunit of RNA polymerase required for cellular differentiation in *Bacillus subtilis*. *Mol Microbiol, 33*(2), 415-428.

Liu, W. T., Yang, Y. L., Xu, Y., Lamsa, A., Haste, N. M., Yang, J. Y., . . . Dorrestein, P. C. (2010). Imaging mass spectrometry of intraspecies metabolic exchange revealed the cannibalistic factors of Bacillus subtilis. *Proc Natl Acad Sci U S A, 107*(37), 16286-16290.

Liu, Y., Carlsson Moller, M., Petersen, L., Soderberg, C. A., & Hederstedt, L. (2010). Penicillin-binding protein SpoVD disulphide is a target for StoA in Bacillus subtilis forespores. *Mol Microbiol, 75*(1), 46-60.

Lopez, D., Vlamakis, H., Losick, R., & Kolter, R. (2009). Cannibalism enhances biofilm development in Bacillus subtilis. *Mol Microbiol, 74*(3), 609-618.

Lu, S., Cutting, S., & Kroos, L. (1995). Sporulation protein SpoIVFB from Bacillus subtilis enhances processing of the sigma factor precursor Pro-sigma K in the absence of other sporulation gene products. *J Bacteriol, 177*(4), 1082-1085.

Mallidis, C. G., & Scholefield, J. (1987). Relation of the heat resistance of bacterial spores to chemical composition and structure. II. Relation to cortex and structure. *J Appl Bacteriol, 63*(3), 207-215.

Marquis, R. E., & Bender, G. R. (1985). Mineralization and heat resistance of bacterial spores. *J Bacteriol, 161*(2), 789-791.

Maughan, H., Masel, J., Birky, C. W., Jr., & Nicholson, W. L. (2007). The roles of mutation accumulation and selection in loss of sporulation in experimental populations of *Bacillus subtilis*. *Genetics, 177*(2), 937-948. doi: 10.1534/genetics.107.075663

Mauriello, E. M., Duc le, H., Isticato, R., Cangiano, G., Hong, H. A., De Felice, M., . . . Cutting, S. M. (2004). Display of heterologous antigens on the Bacillus subtilis spore coat using CotC as a fusion partner. *Vaccine, 22*(9-10), 1177-1187.

McKenney, P. T., Driks, A., & Eichenberger, P. (2013). The Bacillus subtilis endospore: assembly and functions of the multilayered coat. *Nat Rev Microbiol, 11*(1), 33-44.

McKenney, P. T., Driks, A., Eskandarian, H. A., Grabowski, P., Guberman, J., Wang, K. H., . . . Eichenberger, P. (2010). A distance-weighted interaction map reveals a previously uncharacterized layer of the Bacillus subtilis spore coat. *Curr Biol, 20*(10), 934-938.

McKenney, P. T., & Eichenberger, P. (2012). Dynamics of spore coat morphogenesis in Bacillus subtilis. *Mol Microbiol, 83*(2), 245-260.

McPherson, D. C., Driks, A., & Popham, D. L. (2001). Two class A high-molecular-weight penicillin-binding proteins of Bacillus subtilis play redundant roles in sporulation. *J Bacteriol, 183*(20), 6046-6053. doi: 10.1128/jb.183.20.6046-6053.2001

Meador-Parton, J., & Popham, D. L. (2000). Structural analysis of Bacillus subtilis spore peptidoglycan during sporulation. *J Bacteriol, 182*(16), 4491-4499.

Meisner, J., Maehigashi, T., Andre, I., Dunham, C. M., & Moran, C. P., Jr. (2012). Structure of the basal components of a bacterial transporter. *Proc Natl Acad Sci U S A, 109*(14), 5446-5451.

Meisner, J., Wang, X., Serrano, M., Henriques, A. O., & Moran, C. P., Jr. (2008). A channel connecting the mother cell and forespore during bacterial endospore formation. *Proc Natl Acad Sci U S A, 105*(39), 15100-15105.

Melly, E., Genest, P. C., Gilmore, M. E., Little, S., Popham, D. L., Driks, A., & Setlow, P. (2002). Analysis of the properties of spores of Bacillus subtilis prepared at different temperatures. *J Appl Microbiol, 92*(6), 1105-1115.

Meyer, P., Gutierrez, J., Pogliano, K., & Dworkin, J. (2010). Cell wall synthesis is necessary for membrane dynamics during sporulation of Bacillus subtilis. *Mol Microbiol, 76*(4), 956-970.

Middleton, R., & Hofmeister, A. (2004). New shuttle vectors for ectopic insertion of genes into Bacillus subtilis. *Plasmid, 51*(3), 238-245. doi: 10.1016/j.plasmid.2004.01.006

Mitri, S., Xavier, J. B., & Foster, K. R. (2011). Social evolution in multispecies biofilms. *Proc Natl Acad Sci U S A, 108 Suppl 2*, 10839-10846.

Moeller, R., Schuerger, A. C., Reitz, G., & Nicholson, W. L. (2012). Protective role of spore structural components in determining Bacillus subtilis spore resistance to simulated mars surface conditions. *Appl Environ Microbiol, 78*(24), 8849-8853.

Mohammadi, T., van Dam, V., Sijbrandi, R., Vernet, T., Zapun, A., Bouhss, A., . . . Breukink, E (2011). Identification of FtsW as a transporter of lipid-linked cell wall precursors across the membrane. *Embo J, 30*(8), 1425-1432.

Mohammadi, T., van Dam, V., Sijbrandi, R., Vernet, T., Zapun, A., Bouhss, A., . . . Breukink, E. (2011). Identification of FtsW as a transporter of lipid-linked cell wall precursors across the membrane. *Embo J, 30*(8), 1425-1432.

Molle, V., Fujita, M., Jensen, S. T., Eichenberger, P., Gonzalez-Pastor, J. E., Liu, J. S., & Losick, R. (2003). The Spo0A regulon of Bacillus subtilis. *Mol Microbiol, 50*(5), 1683-1701.

Mueller, J. P., & Sonenshein, A. L. (1992). Role of the Bacillus subtilis gsiA gene in regulation of early sporulation gene expression. *J Bacteriol, 174*(13), 4374-4383.

Mullerova, D., Krajcikova, D., & Barak, I. (2009). Interactions between Bacillus subtilis early spore coat morphogenetic proteins. *FEMS Microbiol Lett, 299*(1), 74-85. doi: 10.1111/j.1574-6968.2009.01737.x

Musacchio, A., & Salmon, E. D. (2007). The spindle-assembly checkpoint in space and time. *Nat Rev Mol Cell Biol, 8*(5), 379-393.

Narula, J., Devi, S. N., Fujita, M., & Igoshin, O. A. (2012). Ultrasensitivity of the Bacillus subtilis sporulation decision. *Proc Natl Acad Sci U S A, 109*(50), E3513-3522.

Nicholson, W. L., Schuerger, A. C., & Race, M. S. (2009). Migrating microbes and planetary protection. *Trends Microbiol, 17*(9), 389-392.

Nicholson, W. L., & Setlow, P. (1990). Sporulation, Germination, and Outgrowth. In C. R. Harwood & S. Cutting (Eds.), *Molecular Biological Methods for Bacillus* (pp. 391-450). New York, NY: John Wiley & Sons.

Nicholson, W. L., & Setlow, P. (1990). *Sporulation, germination, and outgrowth*. New York: John Wiley & Sons.

Ou, L. T., & Marquis, R. E. (1970). Electromechanical interactions in cell walls of gram-positive cocci. *J Bacteriol, 101*(1), 92-101.

Paidhungat, M., Setlow, B., Driks, A., & Setlow, P. (2000). Characterization of spores of *Bacillus subtilis* which lack dipicolinic acid. *J Bacteriol, 182*(19), 5505-5512.

Parashar, V., Jeffrey, P. D., & Neiditch, M. B. (2013). Conformational change-induced repeat domain expansion regulates Rap phosphatase quorum-sensing signal receptors. *PLoS Biol, 11*(3), e1001512. doi: 10.1371/journal.pbio.1001512

Paredes-Sabja, D., Setlow, P., & Sarker, M. R. (2011). Germination of spores of Bacillales and Clostridiales species: mechanisms and proteins involved. *Trends Microbiol, 19*(2), 85-94.

Pedersen, L. B., Ragkousi, K., Cammett, T. J., Melly, E., Sekowska, A., Schopick, E., . . . Setlow, P. (2000). Characterization of ywhE, which encodes a putative high-molecular-weight class A penicillin-binding protein in Bacillus subtilis. *Gene, 246*(1-2), 187-196.

Pedrido, M. E., de Ona, P., Ramirez, W., Lenini, C., Goni, A., & Grau, R. (2013). Spo0A links de novo fatty acid synthesis to sporulation and biofilm development in Bacillus subtilis. *Mol Microbiol, 87*(2), 348-367.

Perego, M., Hanstein, C., Welsh, K. M., Djavakhishvili, T., Glaser, P., & Hoch, J. A. (1994). Multiple protein-aspartate phosphatases provide a mechanism for the integration of diverse signals in the control of development in B. subtilis. *Cell, 79*(6), 1047-1055.

Perez Morales, T. G., Ho, T. D., Liu, W. T., Dorrestein, P. C., & Ellermeier, C. D. (2013). Production of the Cannibalism Toxin SDP Is a Multistep Process That Requires SdpA and SdpB. *J Bacteriol, 195*(14), 3244-3251.

Piggot, P. J., & Coote, J. G. (1976). Genetic aspects of bacterial endospore formation. *Bacteriol Rev, 40*(4), 908-962.

Piggot, P. J., & Hilbert, D. W. (2004). Sporulation of Bacillus subtilis. *Curr Opin Microbiol, 7*(6), 579-586.

Plomp, M., Carroll, A. M., Setlow, P., & Malkin, A. J. (2014). Architecture and assembly of the *Bacillus subtilis* spore coat. *PLoS One, 9*(9), e108560. doi: 10.1371/journal.pone.0108560

Popham, D. L., Gilmore, M. E., & Setlow, P. (1999). Roles of low-molecular-weight penicillin-binding proteins in Bacillus subtilis spore peptidoglycan synthesis and spore properties. *J Bacteriol, 181*(1), 126-132.

Popham, D. L., Helin, J., Costello, C. E., & Setlow, P. (1996a). Analysis of the peptidoglycan structure of Bacillus subtilis endospores. *J Bacteriol, 178*(22), 6451-6458.

Popham, D. L., Helin, J., Costello, C. E., & Setlow, P. (1996b). Muramic lactam in peptidoglycan of Bacillus subtilis spores is required for spore outgrowth but not for spore dehydration or heat resistance. *Proc Natl Acad Sci U S A, 93*(26), 15405-15410.

Popham, D. L., Illades-Aguiar, B., & Setlow, P. (1995). The Bacillus subtilis dacB gene, encoding penicillin-binding protein 5*, is part of a three-gene operon required for proper spore cortex synthesis and spore core dehydration. *J Bacteriol, 177*(16), 4721-4729.

Popham, D. L., & Setlow, P. (1993a). Cloning, nucleotide sequence, and regulation of the Bacillus subtilis pbpF gene, which codes for a putative class A high-molecular-weight penicillin-binding protein. *J Bacteriol, 175*(15), 4870-4876.

Popham, D. L., & Setlow, P. (1993b). The cortical peptidoglycan from spores of Bacillus megaterium and Bacillus subtilis is not highly cross-linked. *J Bacteriol, 175*(9), 2767-2769.

Popham, D. L., & Stragier, P. (1991). Cloning, characterization, and expression of the spoVB gene of Bacillus subtilis. *J Bacteriol, 173*(24), 7942-7949.

Price, K. D., & Losick, R. (1999). A four-dimensional view of assembly of a morphogenetic protein during sporulation in Bacillus subtilis. *J Bacteriol, 181*(3), 781-790.

Ptacin, J. L., Nollmann, M., Becker, E. C., Cozzarelli, N. R., Pogliano, K., & Bustamante, C. (2008). Sequence-directed DNA export guides chromosome translocation during sporulation in Bacillus subtilis. *Nat Struct Mol Biol, 15*(5), 485-493.

Rahn-Lee, L., Merrikh, H., Grossman, A. D., & Losick, R. (2011). The sporulation protein SirA inhibits the binding of DnaA to the origin of replication by contacting a patch of clustered amino acids. *J Bacteriol, 193*(6), 1302-1307.

Ramamurthi, K. S., Clapham, K. R., & Losick, R. (2006). Peptide anchoring spore coat assembly to the outer forespore membrane in Bacillus subtilis. *Mol Microbiol, 62*(6), 1547-1557.

Ramamurthi, K. S., Lecuyer, S., Stone, H. A., & Losick, R. (2009). Geometric cue for protein localization in a bacterium. *Science, 323*(5919), 1354-1357.

Ramamurthi, K. S., & Losick, R. (2008). ATP-driven self-assembly of a morphogenetic protein in Bacillus subtilis. *Mol Cell, 31*(3), 406-414.

Ramamurthi, K. S., & Losick, R. (2009). Negative membrane curvature as a cue for subcellular localization of a bacterial protein. *Proc Natl Acad Sci U S A, 106*(32), 13541-13545.

Rao, C. V., Glekas, G. D., & Ordal, G. W. (2008). The three adaptation systems of Bacillus subtilis chemotaxis. *Trends Microbiol, 16*(10), 480-487.

Rawson, D. M., Willmer, A. J., & Turner, A. P. (1989). Whole-cell biosensors for environmental monitoring. *Biosensors, 4*(5), 299-311.

Real, G., Fay, A., Eldar, A., Pinto, S. M., Henriques, A. O., & Dworkin, J. (2008). Determinants for the subcellular localization and function of a nonessential SEDS protein. *J Bacteriol, 190*(1), 363-376.

Regan, G., Itaya, M., & Piggot, P. J. (2012). Coupling of sigmaG activation to completion of engulfment during sporulation of Bacillus subtilis survives large perturbations to DNA translocation and replication. *J Bacteriol, 194*(22), 6264-6271.

Resnekov, O., & Losick, R. (1998). Negative regulation of the proteolytic activation of a developmental transcription factor in Bacillus subtilis. *Proc Natl Acad Sci U S A, 95*(6), 3162-3167.

Richman, J. M., & Handrigan, G. R. (2011). Reptilian tooth development. *Genesis, 49*(4), 247-260.

Roels, S., Driks, A., & Losick, R. (1992). Characterization of spoIVA, a sporulation gene involved in coat morphogenesis in Bacillus subtilis. *J Bacteriol, 174*(2), 575-585.

Rudner, D. Z., Pan, Q., & Losick, R. M. (2002). Evidence that subcellular localization of a bacterial membrane protein is achieved by diffusion and capture. *Proc Natl Acad Sci U S A, 99*(13), 8701-8706.

Ruiz, N. (2008). Bioinformatics identification of MurJ (MviN) as the peptidoglycan lipid II flippase in Escherichia coli. *Proc Natl Acad Sci U S A, 105*(40), 15553-15557.

Ryter, A. (1965). [Morphologic Study of the Sporulation of Bacillus Subtilis]. *Ann Inst Pasteur (Paris), 108*, 40-60.

Ryter, A., Schaeffer, P., & Ionesco, H. (1966). [Cytologic classification, by their blockage stage, of sporulation mutants of Bacillus subtilis Marburg]. *Ann Inst Pasteur (Paris), 110*(3), 305-315.

Sasai, Y. (2013). Cytosystems dynamics in self-organization of tissue architecture. *Nature, 493*(7432), 318-326.

Sastalla, I., Rosovitz, M. J., & Leppla, S. H. (2010). Accidental selection and intentional restoration of sporulation-deficient *Bacillus anthracis* mutants. *Appl Environ Microbiol, 76*(18), 6318-6321. doi: 10.1128/AEM.00950-10

Schaeffer, P., Ionesco, H., Ryter, A., & Balassa, G. (1963). La sporulation de *Bacillus subtilis*: etude gendtique et physiologique *Mechanismes de regulation des activites cellulaires chez les microorganisms* (Vol. 124, pp. 553-563). Paris.

Schirmer, E. C., Glover, J. R., Singer, M. A., & Lindquist, S. (1996). HSP100/Clp proteins: a common mechanism explains diverse functions. *Trends Biochem Sci, 21*(8), 289-296.

Schmalisch, M., Maiques, E., Nikolov, L., Camp, A. H., Chevreux, B., Muffler, A., . . . Losick, R. (2010). Small genes under sporulation control in the Bacillus subtilis genome. *J Bacteriol, 192*(20), 5402-5412.

Setlow, B., Atluri, S., Kitchel, R., Koziol-Dube, K., & Setlow, P. (2006). Role of dipicolinic acid in resistance and stability of spores of *Bacillus subtilis* with or without DNA-protective alpha/beta-type small acid-soluble proteins. *J Bacteriol, 188*(11), 3740-3747. doi: 10.1128/JB.00212-06

Setlow, B., & Setlow, P. (1987). Thymine-containing dimers as well as spore photoproducts are found in ultraviolet-irradiated Bacillus subtilis spores that lack small acid-soluble proteins. *Proc Natl Acad Sci U S A, 84*(2), 421-423.

Setlow, B., & Setlow, P. (1993). Binding of small, acid-soluble spore proteins to DNA plays a significant role in the resistance of Bacillus subtilis spores to hydrogen peroxide. *Appl Environ Microbiol, 59*(10), 3418-3423.

Setlow, P. (2006). Spores of Bacillus subtilis: their resistance to and killing by radiation, heat and chemicals. *J Appl Microbiol, 101*(3), 514-525.

Setlow, P. (2007). I will survive: DNA protection in bacterial spores. *Trends Microbiol, 15*(4), 172-180.

Sharp, M. D., & Pogliano, K. (1999). An in vivo membrane fusion assay implicates SpoIIIE in the final stages of engulfment during Bacillus subtilis sporulation. *Proc Natl Acad Sci U S A, 96*(25), 14553-14558.

Sharp, M. D., & Pogliano, K. (2002). Role of cell-specific SpoIIIE assembly in polarity of DNA transfer. *Science, 295*(5552), 137-139.

Siebring, J., Elema, M. J., Drubi Vega, F., Kovacs, A. T., Haccou, P., & Kuipers, O. P. (2014). Repeated triggering of sporulation in *Bacillus subtilis* selects against a protein that affects the timing of cell division. *ISME J, 8*(1), 77-87. doi: 10.1038/ismej.2013.128

Slepecky, R., & Foster, J. W. (1959). Alterations in metal content of spores of Bacillus megaterium and the effect on some spore properties. *J Bacteriol, 78*(1), 117-123.

Smith, T. J., & Foster, S. J. (1995). Characterization of the involvement of two compensatory autolysins in mother cell lysis during sporulation of *Bacillus subtilis* 168. *J Bacteriol, 177*(13), 3855-3862.

Sonenshein, A. L. (2000). Control of sporulation initiation in *Bacillus subtilis*. *Curr Opin Microbiol, 3*(6), 561-566.

Sowell, M. O., & Buchanan, C. E. (1983). Changes in penicillin-binding proteins during sporulation of Bacillus subtilis. *J Bacteriol, 153*(3), 1331-1337.

Steinmetz, M., & Richter, R. (1994). Easy cloning of mini-Tn10 insertions from the Bacillus subtilis chromosome. *J Bacteriol, 176*(6), 1761-1763.

Sterlini, J. M., & Mandelstam, J. (1969). Commitment to sporulation in Bacillus subtilis and its relationship to development of actinomycin resistance. *Biochem J, 113*(1), 29-37.

Stragier, P., Bonamy, C., & Karmazyn-Campelli, C. (1988). Processing of a sporulation sigma factor in Bacillus subtilis: how morphological structure could control gene expression. *Cell, 52*(5), 697-704.

Stragier, P., & Losick, R. (1996). Molecular genetics of sporulation in Bacillus subtilis. *Annu Rev Genet, 30*, 297-241.

Takamatsu, H., Kodama, T., Nakayama, T., & Watabe, K. (1999). Characterization of the yrbA gene of Bacillus subtilis, involved in resistance and germination of spores. *J Bacteriol, 181*(16), 4986-4994.

Tan, I. S., & Ramamurthi, K. S. (2014). Spore formation in *Bacillus subtilis*. *Environ Microbiol Rep, 6*(3), 212-225. doi: 10.1111/1758-2229.12130

Tipper, D. J., & Linnett, P. E. (1976). Distribution of peptidoglycan synthetase activities between sporangia and forespores in sporulating cells of Bacillus sphaericus. *J Bacteriol, 126*(1), 213-221.

Tocheva, E. I., Lopez-Garrido, J., Hughes, H. V., Fredlund, J., Kuru, E., Vannieuwenhze, M. S., . . . Jensen, G. J. (2013). Peptidoglycan transformations during Bacillus subtilis sporulation. *Mol Microbiol, 88*(4), 673-686.

van Ooij, C., & Losick, R. (2003). Subcellular localization of a small sporulation protein in Bacillus subtilis. *J Bacteriol, 185*(4), 1391-1398.

Vasudevan, P., Weaver, A., Reichert, E. D., Linnstaedt, S. D., & Popham, D. L. (2007). Spore cortex formation in Bacillus subtilis is regulated by accumulation of peptidoglycan precursors under the control of sigma K. *Mol Microbiol, 65*(6), 1582-1594.

Veening, J. W., Murray, H., & Errington, J. (2009). A mechanism for cell cycle regulation of sporulation initiation in Bacillus subtilis. *Genes Dev, 23*(16), 1959-1970.

Veening, J. W., Stewart, E. J., Berngruber, T. W., Taddei, F., Kuipers, O. P., & Hamoen, L. W. (2008). Bet-hedging and epigenetic inheritance in bacterial cell development. *Proc Natl Acad Sci U S A, 105*(11), 4393-4398.

Vishnoi, M., Narula, J., Devi, S. N., Dao, H. A., Igoshin, O. A., & Fujita, M. (2013). Triggering sporulation in Bacillus subtilis with artificial two-component systems reveals the importance of proper Spo0A activation dynamics. *Mol Microbiol, 90*(1), 181-194.

Vlamakis, H., Chai, Y., Beauregard, P., Losick, R., & Kolter, R. (2013). Sticking together: building a biofilm the Bacillus subtilis way. *Nat Rev Microbiol, 11*(3), 157-168.

Vreeland, R. H., Rosenzweig, W. D., & Powers, D. W. (2000). Isolation of a 250 million-year-old halotolerant bacterium from a primary salt crystal. *Nature, 407*(6806), 897-900.

Wach, A. (1996). PCR-synthesis of marker cassettes with long flanking homology regions for gene disruptions in S. cerevisiae. *Yeast, 12*(3), 259-265.

Wang, K. H., Isidro, A. L., Domingues, L., Eskandarian, H. A., McKenney, P. T., Drew, K., . . . Eichenberger, P. (2009). The coat morphogenetic protein SpoVID is necessary for spore encasement in Bacillus subtilis. *Mol Microbiol, 74*(3), 634-649.

Warth, A. D. (1978). Molecular structure of the bacterial spore. *Adv Microb Physiol, 17*, 1-45.

Warth, A. D., & Strominger, J. L. (1972). Structure of the peptidoglycan from spores of Bacillus subtilis. *Biochemistry, 11*(8), 1389-1396.

Webb, C. D., Decatur, A., Teleman, A., & Losick, R. (1995). Use of green fluorescent protein for visualization of cell-specific gene expression and subcellular protein localization during sporulation in Bacillus subtilis. *J Bacteriol, 177*(20), 5906-5911.

Wilson, G. A., & Bott, K. F. (1968). Nutritional factors influencing the development of competence in the Bacillus subtilis transformation system. *J Bacteriol, 95*(4), 1439-1449.

Wojtkowiak, D., Georgopoulos, C., & Zylicz, M. (1993). Isolation and characterization of ClpX, a new ATP-dependent specificity component of the Clp protease of *Escherichia coli*. *J Biol Chem, 268*(30), 22609-22617.

Wojtyra, U. A., Thibault, G., Tuite, A., & Houry, W. A. (2003). The N-terminal zinc binding domain of ClpX is a dimerization domain that modulates the chaperone function. *J Biol Chem, 278*(49), 48981-48990. doi: 10.1074/jbc.M307825200

Wu, L. J., & Errington, J. (1994). Bacillus subtilis SpoIIIE protein required for DNA segregation during asymmetric cell division. *Science, 264*(5158), 572-575.

Wu, L. J., & Errington, J. (1998). Use of asymmetric cell division and spoIIIE mutants to probe chromosome orientation and organization in Bacillus subtilis. *Mol Microbiol, 27*(4), 777-786.

Wu, R., Gu, M., Wilton, R., Babnigg, G., Kim, Y., Pokkuluri, P. R., . . . Schiffer, M. (2013). Insight into the sporulation phosphorelay: crystal structure of the sensor domain of Bacillus subtilis histidine kinase, KinD. *Protein Sci, 22*(5), 564-576.

Youngman, P., Perkins, J. B., & Losick, R. (1984). Construction of a cloning site near one end of Tn917 into which foreign DNA may be inserted without affecting transposition in Bacillus subtilis or expression of the transposon-borne erm gene. *Plasmid, 12*(1), 1-9.

Zheng, L. B., Donovan, W. P., Fitz-James, P. C., & Losick, R. (1988). Gene encoding a morphogenic protein required in the assembly of the outer coat of the Bacillus subtilis endospore. *Genes Dev, 2*(8), 1047-1054.

Zhou, Y., Gottesman, S., Hoskins, J. R., Maurizi, M. R., & Wickner, S. (2001). The RssB response regulator directly targets sigma(S) for degradation by ClpXP. *Genes Dev, 15*(5), 627-637. doi: 10.1101/gad.864401

Curriculum Vitae

Irene S. Tan

37 Convent Dr. Bethesda, MD 20814 | tan.irene.s@gmail.com

Education

The Johns Hopkins University
NIH-JHU Graduate Partnerships Program
Ph.D., Biology, (expected spring 2015)

University of California, Berkeley
B.S., Microbial Biology, 2009

Research Experience

Pre-Doctoral Fellow, Laboratory of Dr. Kumaran Ramamurthi (June 2011-present)
National Institutes of Health, Bethesda, MD

Research Associate, Laboratory of Dr. Deepak Srivastava (November 2009-May 2010)
Gladstone Institute of Cardiovascular Disease, San Francisco, CA

Biology Intern, HCV group (June 2009-October 2009)
Gilead Sciences, Foster City, CA

Undergraduate Researcher, Laboratory of Dr. Deborah Dean (June 2007- June 2008)
Children's Hospital Oakland Research Institute, Oakland, CA

Undergraduate Researcher, Laboratory of Dr. Cherie Briggs (January 2007-May 2007)
University of California, Berkeley, CA

Teaching Experience

Teaching Assistant, Cell biology Lab
The Johns Hopkins University, Baltimore, MD (January 2011-May 2011)

Teaching Assistant, Biochemistry Lab
The Johns Hopkins University, Baltimore, MD (August 2010-December 2010)

Private Tutor, Computer Science
Private Home, Saratoga, CA (August 2004-June 2005)

Publications

Tan IS, Weiss CA, Popham DL, Ramamurthi KS (in review). Regulated cell death through proteolysis of a morphogenetic protein selectively removes unfit cells from a population of differentiating bacteria.

Gill RL, Castaing JP, Hsin J, **Tan IS**, Wang X, Huang KC, Ramamurthi KS (2015). Structural and mechanistic basis for the geometric cue-driven subcellular localization of a bacterial protein. *Proceedings of the National Academy of Sciences.*

Tan IS, Ramamurthi KS (2014). Spore formation in *Bacillus subtilis*. *Environmental Microbiology Reports.*

Tan IS, Ramamurthi KS (2013). Membrane remodeling: FisB will do in a pinch. *Current Biology.*

Keller KE, **Tan IS**, Lee YS (2012). SAICAR stimulates pyruvate kinase isoform M2 and promotes cancer cell survival in glucose-limited conditions. *Science.*

Ebmeier SE*, **Tan IS***, Clapham KR, Ramamurthi KS (2012). Small proteins link coat and cortex assembly during sporulation in *Bacillus subtilis*. *Molecular Microbioogy*.
*These authors contributed equally to the work.

Selected Presentations

Poster Presentation: Small Proteins Orchestrate Coat and Cortex Assembly during Sporulation in *Bacillus subtilis*
ASM (American Society for Microbiology) conference, Boston, MA (May 2014)

Oral Presentation: Coordinated Assembly of the Coat and Cortex during Sporulation in *Bacillus subtilis*
NY/BIG (Bacillus Interest Group) conference, New York City, NY (May 2013)

Awards

NIH Graduate Student Research Award (2012)

JOHNS HOPKINS
UNIVERSITY
PROGRAM IN CELL, MOLECULAR,
DEVELOPMENTAL BIOLOGY & BIOPHYSICS

THESIS DEFENSE FORM

Irene Tan
Name of Student

has successfully completed the Final Examination on 5/13/15
Date

Signatures of Examination Committee

Chair: